

Identification of novel *Salmonella*
susceptibility loci using ENU chemical
mutagenesis

Kyoko Emily Yuki

March 2016

Department of Human Genetics,
McGill University, Montreal, Quebec, Canada

A thesis submitted to McGill University in partial fulfillment of the requirements of the degree
of Doctor of Philosophy.

©Kyoko Emily Yuki, 2016

TABLE OF CONTENTS

Abstract	5
Résumé	7
List of Figures.....	9
List of Tables.....	11
Acknowledgements.....	12
Preface and Author Contributions	14
Abbreviations	17
Chapter 1: General Introduction	20
<i>Salmonella</i> : The Bacterium	20
<i>Salmonella</i> Infection and Classification	20
<i>Salmonella</i> Infection in the Human Population	21
Enteric (Typhoid and Paratyphoid) Fever:	21
Chronic carriage	23
Gastroenteritis	24
Invasive NTS (iNTS).....	24
Use of Vaccination	25
Pathogenesis of <i>Salmonella</i> Disease	26
Route of infection:	26
Impact of Host Genetics	31
Immune response to infection.....	31
Iron Metabolism in Host Defense	37
Regulation of Iron Metabolism.....	37

Anemia of inflammation.....	39
Pathogen Acquisition of Iron.....	40
Mouse models.....	41
Models of <i>Salmonella</i> Infection.....	41
Typhoid:	41
Intestinal:	42
Chronic carriage:	43
Genetic approaches.....	44
Congenics/Collaborative Cross	44
Chemical Mutagenesis.....	45
Gene Identification	47
Thesis rationale, hypothesis & objectives:.....	48
Rationale.....	48
Hypothesis	49
Objectives	49
Bridging Statement Chapter 1 to Chapter 2.....	50
Chapter 2: Mouse ENU Mutagenesis Screen for the Discovery of Novel <i>Salmonella</i>	
Susceptibility Genes	51
Abstract:	52
Introduction:.....	53
Materials & Methods:.....	55
Results:	57
Discussion:	60
Acknowledgements:	64

Figures and Figure Legends:	65
Bridging Statement from Chapter 2 to Chapter 3	79
Chapter 3: Suppression of Hcpidin Expression and Iron Overload Mediate <i>Salmonella</i>	
Susceptibility in Ankyrin1 ENU Induced Mutant.....	80
Abstract:	81
Introduction:.....	82
Materials & Methods:.....	84
Results:	87
Discussion:	94
Acknowledgements:	100
Figures and Figure Legends	101
Bridging Statement From Chapter 3 and Chapter 4.....	124
Mutation in FAM49B Causes Susceptibility to <i>Salmonella</i> Infection.....	125
Abstract.....	126
Introduction:.....	127
Materials & Methods:.....	129
Results:	134
Discussion:	140
Acknowledgements:	143
Figures and Figure Legends:	144
Chapter 5: General Discussion	168
Chapter 2: Discovery of Novel Genes in <i>Salmonella</i> Susceptibility.....	168
Chapter 3: Importance of Iron Metabolism in <i>Salmonella</i> Infection	171
Chapter 4: Phenotypic Characterization of FAM49B	173

Perspective: 175
References:..... 177

ABSTRACT

Salmonella infections in humans are responsible for two major clinical diseases, typhoid fever and salmonellosis, a self-limiting gastroenteritis. *Salmonella* infections are transmitted by a fecal-oral route through contaminated food and water and are endemic in areas of poor water sanitation. The severity and outcome of infection depends on a variety of factors including a complex interplay between host genetics, environment and the bacteria. The laboratory mouse has been used with success to study the pathogenesis of *Salmonella* infection. In the mouse, *Salmonella* Typhimurium infection results in a systemic disease with clinical manifestations resembling those found in humans with typhoid fever. We report in the current thesis the use of a forward genetic approach within the framework of a large recessive *N*-ethyl-*N*-nitrosourea (ENU) screen for susceptibility to infectious diseases, to identify novel *Salmonella* susceptibility genes. We report the screening of over 1223 G3 progeny (80 G1 pedigrees) and the identification of four pedigrees named *Ity14* (*Immunity to Typhimurium locus 14*), *Ity15*, *Ity19* and *Ity21* showing increased susceptibility to infection. The genes responsible for the mutant phenotypes were identified using a combination of genetic mapping and whole exome sequencing, leading to the discovery of 3 genes associated with resistance to *Salmonella* infection: *Stat4* (*Ity14*), *Fam49b* (*Ity15*) and *Cnp* (*Ity19*). In addition, we characterized two loci identified through ENU mutagenesis: *Ity15* and *Ity16*. *Ity16* was mapped to chromosome 8. A nonsense mutation was identified in exon 33 of the *Ank1* (ankyrin 1) gene. This gene is known to play an important role in the formation and stabilization of the red cell cytoskeleton. The mutation identified in *Ank1* results in abrogation of ANK1 protein expression and causes severe hemolytic anemia in mice. The anemia is accompanied by decreased hepcidin expression, and iron overload in liver and kidneys. This study illustrates that the regulation of hepcidin and iron balance are crucial in the host response to *Salmonella* infection in the *Ank1* mutant. We also determined that a splice mutation in *Fam49b*, a gene with no prior known function, underlies the susceptibility of the *Ity15* locus. Abrogation of FAM49B resulted in uncontrolled *Salmonella* replication and septic shock. We show that FAM49B localizes with proteins of the host cytoskeleton and may have a role in the intersection of the cytoskeleton and the bacteria.

Altogether, our results provide new insights into the genetics controlling the complex host response to *Salmonella* infection and have led to the identification of additional novel host resistance mechanisms.

RÉSUMÉ

Les salmonelles sont responsables de diverses maladies allant de la simple gastroentérite aux formes plus graves telles que la fièvre typhoïde. Les infections à *Salmonella* empruntent généralement la voie digestive et posent un problème de santé publique dans des régions du monde où il y a peu d'accès à l'eau potable. La sensibilité de l'hôte dans la réponse à l'infection peut s'expliquer par plusieurs facteurs localisés à l'interface de l'interaction hôte (gènes de prédisposition), pathogène (dose infectante, virulence) et environnement. L'utilisation du modèle murin par approche génétique a permis de mieux comprendre la physiopathologie des infections à salmonelles. Chez la souris, les salmonelles provoquent une maladie systémique accompagnée de symptômes semblables à ceux de la fièvre typhoïde chez l'homme. Nous avons utilisé une approche de mutagenèse chimique (non dirigée et au hasard) utilisant du *N*-éthyl-*N*-nitroso-urée (ENU) dans le but d'obtenir des mutants sensibles à l'infection à salmonelles. Nous avons effectué un crible de mutations récessives chez 1223 G3 provenant de 80 lignées G1. Cette approche nous a permis d'identifier 4 lignées mutantes (*Ity14*, *Immunity to Typhimurium locus 14*, *Ity15*, *Ity19* et *Ity21*) qui présentaient une susceptibilité accrue à l'infection à salmonelles. Le repérage et l'identification des mutations impliquées se sont faits par cartographie génétique et séquençage haut débit d'exomes. Les gènes porteurs de mutation ont été identifiés pour *Ity14* (signal transducer and activator of transcription 4, *Stat4*), *Ity15* (family with sequence homology 49 member b, *Fam49b*) et *Ity19* (2',3'-cyclic nucleotide 3' phosphodiesterase, *Cnp*). Nous avons aussi caractérisé, tant du point phénotypique que mécanistique, deux loci (*Ity15* et *Ity16*) identifiés lors du crible ENU. *Ity16* a été localisé sur le chromosome 8 et une mutation non-sens dans l'exon 33 du gène *Ank1* (ankyrin 1) a été identifiée. ANK1 joue un rôle important dans la formation et la stabilité du cytosquelette des globules rouges. La mutation ENU identifiée résulte en une absence complète de l'expression de la protéine ANK1 causant une anémie hémolytique sévère. Cette anémie s'accompagne d'une diminution de l'expression de l'hepcidine, une hormone qui régule l'homéostasie du fer, et d'une surcharge en fer tissulaire. Cette étude aura permis de démontrer l'importance de la régulation de l'hepcidine et du métabolisme du fer dans la réponse de l'hôte à l'infection à

salmonelles. Finalement, nous avons découvert qu'une mutation dans le site d'épissage de l'intron 9-10 du gène *Fam49b* était responsable de la susceptibilité des souris *Ity15*. Le gène *Fam49b* est très peu connu et l'absence de la protéine FAM49B résulte en une prolifération accrue des bactéries dans les organes cibles menant au choc septique. Nous avons démontré que FAM49B se retrouve en proximité de protéines du cytosquelette et pourrait avoir un rôle à jouer dans l'interaction de celui-ci avec les bactéries. Cette étude aura donc permis d'accroître les connaissances sur la pathogénie des infections à *Salmonella* Typhimurium.

LIST OF FIGURES

<u>CHAPTER 1: GENERAL INTRODUCTION.....</u>	<u>20</u>
Figure 1: Global burden of Typhoid Fever	23
Figure 2: Differences between <i>Salmonella</i> Typhimurium and <i>Salmonella</i> Typhi in establishing infection	27
Figure 3: SPI1 effectors and its impact on host actin cytoskeleton.....	29
Figure 4: Regulation of iron metabolism	38
Figure 5: Survival curve of laboratory strains of mice	42
<u>CHAPTER 2: MOUSE ENU MUTAGENESIS SCREEN FOR THE DISCOVERY OF NOVEL <i>SALMONELLA</i> SUSCEPTIBILITY GENES.....</u>	<u>52</u>
Figure 1: ENU mutagenesis breeding schemes.....	65
Figure 2: Survival analysis of <i>Salmonella</i> -susceptible pedigrees identified in mutagenesis screen	67
Figure 3: Mapping strategies used to identify <i>Ity14</i> and <i>Ity15</i>	69
Figure 4: Mapping strategies used to identify <i>Ity19</i> and <i>Ity21</i>	71
Figure 5: Efficiency of breeding schemes to identify deviant pedigrees.....	73
<u>CHAPTER 3: SUPPRESSION OF HEPCIDIN EXPRESSION AND IRON OVERLOAD MEDIATE <i>SALMONELLA</i> SUSCEPTIBILITY OF ANKYRIN1 ENU INDUCED MUTANT</u>	<u>81</u>
Figure 1: Identification and mapping of the <i>Ity16</i> pedigree.....	101
Figure 2: <i>Ity16</i> mutant mice present massive splenomegaly, moderate increase in kidneys and heart weights and bilirubinemia.....	103
Figure 3: <i>Ity16</i> mutant mice carry mutation within the <i>Ank1</i> gene	105
Figure 4: Bacterial load in spleen, liver and kidney after infection with <i>Salmonella</i> Typhimurium in <i>Ity16</i> mutant, heterozygous and wild type mice	107
Figure 5: <i>Ity16</i> mutant mice present elevated blood urea nitrogen (BUN), alanine transaminase (ALT) and asparatate transaminase (AST) during <i>Salmonella</i> infection	109
Figure 6: Tissue expression of genes involved in iron metabolism in 7 week old <i>Ank1</i> ^{+/+} wild type and <i>Ank1</i> ^{Ity16/Ity16} mutant mice.....	111
Figure 7: Cytokine profiles in 7 week-old <i>Ank1</i> ^{+/+} wild type and <i>Ank1</i> ^{Ity16/Ity16} mutant mice during infection with <i>Salmonella</i> Typhimurium.....	113
Figure 8: Characterization of <i>Ank1</i> ^{+/Ity16} heterozygous mice	115
Supplemental Figure 1: Histopathologic examination of the spleen, liver and kidney of 7 week old <i>Ank1</i> ^{+/+} wild type, <i>Ank1</i> ^{+/Ity16} heterozygous, and <i>Ank1</i> ^{Ity16/Ity16} mutant mice before infection (day 0)	118

Supplemental Figure 2: Progression of lesions in kidney and liver 2 days after <i>Salmonella</i> infection of <i>Ank1^{+/+}</i> wild type, <i>Ank1^{+/Ity16}</i> heterozygous, and <i>Ank1^{Ity16/Ity16}</i> mutant mice aged 7 and 24 weeks using hematoxylin & eosin staining.....	120
Supplemental Figure 3: Prussian blue staining of liver and kidney of 7 week old <i>Ank1^{+/+}</i> wild type and <i>Ank1^{+/Ity16}</i> heterozygous mice at day 2 and day 6 post infection with <i>Salmonella</i> Typhimurium.....	122
CHAPTER 4: MUTATION IN FAM49B CAUSES SUSCEPTIBILITY TO SALMONELLA INFECTION	126
Figure 1: Validation and mapping of the <i>Ity15</i> pedigree.....	144
Figure 2: A mutation in <i>Fam49b</i> confers susceptibility to <i>Salmonella</i> infection in the <i>Ity15</i> pedigree	146
Figure 3: Loss of FAM49B results in early <i>Salmonella</i> dissemination and septic shock.....	148
Figure 4: FAM49B is expressed within the cytoplasm of immune cells and is regulated by LPS and type I IFN	150
Figure 5: Global transcriptional profile of <i>Ity15^{m/m}</i> mice.....	152
Supplemental Figure 1: Expression of <i>Gsdmc4</i> in the <i>Ity15</i> pedigree.....	158
Supplemental Figure 2: Loss of FAM49B results in <i>Salmonella</i> dissemination and early intestinal pathology	160
Supplemental Figure 3: <i>Ity15^{m/m}</i> mice display severe histopathological changes during infection	162
Supplemental Figure 4: <i>Ity15</i> mutant mice are resistance to infection with <i>Listeria monocytogenes</i>	164
Supplemental Figure 5: <i>Fam49b</i> mRNA expression in <i>Ity15^{+/+}</i> and <i>Ity15^{m/m}</i> mice.....	166

LIST OF TABLES

<u>CHAPTER 2: MOUSE ENU MUTAGENESIS SCREEN FOR THE DISCOVERY OF NOVEL <i>SALMONELLA</i> SUSCEPTIBILITY GENES.....</u>	<u>52</u>
Table 1: Summary of ENU mutagenesis screen for susceptibility to <i>Salmonella</i> Typhimurium infection.....	75
Table 2: Mutations identified by exome sequencing in 3 samples from the <i>Ity19</i> pedigree.....	76
Table 3: Mutations identified by exome sequencing in 3 samples from the <i>Ity21</i> pedigree.....	77
<u>CHAPTER 3: SUPPRESSION OF HEPCIDIN EXPRESSION AND IRON OVERLOAD MEDIATE <i>SALMONELLA</i> SUSCEPTIBILITY OF ANKYRIN1 ENU INDUCED MUTANT.....</u>	<u>81</u>
Table 1: RBC hematological parameters.....	117
<u>CHAPTER 4: MUTATION IN FAM49B CAUSES SUSCEPTIBILITY TO SALMONELLA INFECTION</u>	<u>126</u>
Table 1: Hematological parameters of <i>Ity15^{+/+}</i> , <i>Ity15^{+/m}</i> and <i>Ity15^{m/m}</i> before and during infection.....	154
Table 2: ENU induced mutations identified by exome sequencing in the <i>Ity15</i> pedigree.....	155
Table 3: GO terms associated with genes differentially regulated at day 0 and day 4 post infection.....	156
Table 4: FAM49B proximity interactors identified by BioID.....	157

ACKNOWLEDGEMENTS

I would like to begin by thanking my supervisor, Dr. Danielle Malo, for her endless support, patience and guidance throughout the years spent in her laboratory. Thank you for giving me an opportunity to work on the projects described in this thesis and for creating such a warm atmosphere that made working in your lab a wonderful experience.

Thank you to my supervisory committee: Dr. Salman Qureshi and Dr. Silvia Vidal for their time and advice throughout the years.

I am especially grateful to have worked with my fellow ENU team members Dr. Shauna Dauphinee and Megan Eva. Their friendship and discussions were invaluable during the many hours we spent together infecting, monitoring the mice and analyzing all the data. I would also like to thank Dr. Etienne Richer for his insight while we undertook the ENU screen. To Sean Beatty, for all of his help analyzing data with R and the adventures we had during conferences. To Line Lariviere for taking me under her wing when I first started and her countless contributions to various projects throughout the years. And to the members of the Malo lab, past and present, not yet mentioned Mimi Chen, Marie Chevenon, Stuart Foster, Melissa Herman, Rabia Khan, Mayss Naccache, Caitlin Prendergast, and Jessica Tjong: thank you for your friendship in making the lab a home away from home.

There have been an enormous number of mice generated through the ENU screen and the subsequent phenotypic characterization of the pedigrees. The work presented in this thesis would not have been possible without our incredible animal technicians. So thank you to: Genevieve Perreault, Vanessa Guay, Cynthia Villeda-Herrera, Leigh Piercey-Brunet and especially to Nadia Prud'homme and Patricia D'Arcy for their work in the breeding, maintenance and infecting of the ENU colony.

I would like to thank my friends. You asked if you would make it into the acknowledgements, well here you are. Thank you for all laughs, diversions and encouragement. Last but not least, to my family: My parents and brother for all their encouragement, enthusiasm and Skype calls throughout the years. To Justin, thank you for being my rock and my sounding board. You give me the strength and motivation to do my utmost each and every day.

PREFACE AND AUTHOR CONTRIBUTIONS

This thesis consists of 5 chapters: a literature review, 3 full length manuscripts and a general discussion. One manuscript has been published and the other two will be submitted shortly. A statement has been included in order to bridge the materials presented in each chapter. I, Kyoko E. Yuki, under the supervision of Dr. Danielle Malo, have designed, performed, analyzed the experiments and written the manuscripts described below unless otherwise indicated. The co-authors listed below have contributed as follows:

Mouse ENU Mutagenesis Screen for the Discovery of Novel *Salmonella* Susceptibility Genes

Kyoko E. Yuki, Megan M. Eva, Shauna M. Dauphinee, Lou Beaulieu-Laroche, Robert Eveleigh, Guillaume Bourque, Jeremy A. Schwartzentruber, Jacek Majewski, Silvia M. Vidal, Danielle Malo

The generation of G0 males was done by Nadia Prud'homme and Patricia D'Arcy. Infection, monitoring and identification of mutant pedigrees were done with the technical assistance of Megan Eva and Dr. Shauna Dauphinee. Lou Beaulieu-Laroche helped with the validation of *Ity19* and *Ity21* candidate genes by Sanger sequencing. Analysis of exome sequencing data was performed by Dr. Jeremy Schwartzentruber and Robert Everleigh under the supervision of Dr. Jacek Majewski and Dr. Guillaume Bourque respectively. Dr. Silvia Vidal provided the G0 mice for the screen. I was responsible for the rational, experimental design and performance, data analysis as well as the writing of the manuscript.

Suppression of Hpcidin expression and iron overload mediate *Salmonella* susceptibility in *Ankyrin1* ENU induced mutant

Kyoko E. Yuki, Megan M. Eva, Etienne Richer, Dudley Chung, Marilene Paquet, Mathieu Cellier, Francois Canonne-Hergaux, Sophie Vaultont, Silvia M. Vidal, Danielle Malo

Megan Eva identified the *Ity16* pedigree in her ENU *Salmonella* screen on a DBA/2 background. Dr. Etienne Richer provided survival data of the Hamp KO mice following infection. Dudley Chung helped identify the mutation in *Ank1* by Sanger sequencing. Dr. Marilene Paquet

provided pathological analysis of the spleen, liver and kidneys. Dr. Mathieu Cellier provided the Δ TonB *Salmonella* mutant. Dr. Francois Canonne-Hergaux and Dr. Sophie Vulont provided the *Hamp* KO mouse. Dr. Silvia Vidal provided the G0 mouse for ENU mutagenesis. Nadia Prud'homme was instrumental in the maintenance of the animal colony and assisted in all infections and necropsies. I was responsible for the rational, experimental design and performance, data analysis as well as the writing of the manuscript.

Mutation in *Fam49b* causes susceptibility to *Salmonella* infection

Kyoko E. Yuki, Megan M. Eva, Jessica Tjong, Jarred Chicoine, Gregory Caignard, Jeremy Schwartzentruber, Jacek Majewski, Mathieu Cellier, Pierre-Olivier Vidalain, Rob Sladek, Silvia M. Vidal, Danielle Malo

Megan Eva provided technical assistance with the early primary phenotyping of the *Ity15* pedigree. Jessica Tjong was an undergraduate honors student who performed the BMDM stimulation work under my supervision. Dr. Jarred Chicoine with Dr. Rob Sladek provided reagents and analytical assistance for cloning *Fam49b* to perform the BioID assay. Dr. Gregory Caignard and Dr. Pierre-Olivier Vidalain provided reagents and technical assistance for the Gateway cloning of *Fam49b*. Dr. Jeremy Schwartzentruber under the supervision of Dr. Jacek Majewski analyzed the exome sequencing data. Dr. Mathieu Cellier provided help with the proteomic analysis. Dr. Silvia Vidal provided the animals for ENU mutagenesis. In addition, Nadia Prud'homme and Patricia D'Arcy were responsible for the maintenance of the animal colony and assisted in infections. I was responsible for the rational, experimental design and performance, data analysis as well as the writing of the manuscript.

In addition I was involved in varying degrees to the publication of the following papers:

I was involved in a study with Dr. Etienne Richer, a postdoctoral fellow in our laboratory, in his study looking at the role of *Usp18* in *Salmonella* typhlitis.

Richer, E., Yuki, KE., Dauphinee, SM., Lariviere, L., Paquet, M., Malo, D. Impact of Usp18 and IFN signaling in Salmonella induced typhlitis. (2011) Genes and Immunity 12, 531-543.

As part of our ENU screen, we identified a number of mutants. I was part of studies led by Ph.D candidate Megan Eva and postdoctoral fellow Dr. Shauna Dauphinee investigating the involvement of STAT4 on susceptibility to Salmonella infection and characterizing two ENU mutants with skeletal deformities:

Eva, MM., Yuki, KE., Dauphinee, SM., Schwartzentruber, JA., Pyzik, M., Paquet, M., Lathrop, M. Majewski, J., Vidal, SM., Malo, D. Altered IFN γ -Mediated Immunity and Transcriptional Expression Patterns in N-Ethyl-N-Nitrosourea-Induced STAT4 Mutants Confer Susceptibility to Acute Typhoid-like Disease. (2014). *Journal of Immunology* 192:259-270.

Dauphinee, SM., Eva, MM., Yuki, KE., Herman, M., Vidal, SM., Malo, D. Characterization of Two ENU-Induced Mutations Affecting Mouse Skeletal Morphology. (2013) *G3* 3(10):1753-8.

I collaborated with former Ph.D candidate Rabia Khan on two papers elucidating the complex genetic architecture underlying the *Ity3* locus found in the wild-derived MOLF/Ei mouse strain:

Khan, RT., Yuki, KE., Malo, D. Fine-mapping and Phenotypic Analysis of the Ity3 Salmonella Susceptibility Locus Identify a Complex Genetic Structure (2014) *PLoS One* 9(1): e88009

Khan, RT., Chevenon, M., Yuki, KE., Malo, D. Genetic dissection of the Ity3 locus identifies a role for Ncf2co-expression modules and suggests Selp as a candidate gene underlying the Ity3.2 locus. (2014) *Front. Immunol.* 5:375

I was also involved in a study led by Ph.D candidate Sean Beatty identifying candidate genes underlying the *Ity5* *Salmonella* susceptibility locus:

Beatty, SC., Yuki, KE., Eva, MM., Dauphinee, S., Lariviere, L., Vidal, SM., Malo, D. Survival analysis and microarray profiling identify Cd40 as a candidate for the Salmonella susceptibility locus, Ity5. (2016) *Genes and Immunity* 17, 19-29.

Lastly, I collaborated in a study led by postdoctoral fellow Dr. Olivier Papapietro from the laboratory of Dr. Samantha Gruenheid regarding the role of *Rspo2* in mediating susceptibility to fatal infectious diarrhea:

Papapietro, O., Teatero, S., Thanabalasuriar, A., Yuki, KE., Diez, E., Zhu, L., Kang, E., Dhillon, S., Muise, AM., Durocher, Y., Marcinkiewicz, MM., Malo, D., Gruenheid, S. R-spondin 2 signalling mediates susceptibility to fatal infectious diarrhea. (2013) *Nature Communications* 4:1898

ABBREVIATIONS

129	129Sv
ALT	alanine transaminase
Ank1	ankyrin 1
Anxa2	annexin 2
AP-1	activating protein 1
Arp2/3	actin related protein 2/3 complex
AST	aspartate transaminase
B6	C57Bl/6
BMPR	bone morphogenetic protein receptor
BUN	blood urea nitrogen
CC	collaborative cross
CD	cluster of differentiation
CFU	colony forming units
CGD	chronic granulomatous disease
CNP	2',3'-Cyclic-nucleotide 3'-phosphodiesterase
DBA/2	DBA/2J
DC	dendritic cell
EEA1	early endosome antigen 1
ENU	N-ethyl-N-nitrosourea
EPO	erythropoietin
ERAAP	endoplasmic reticulum aminopeptidase associated with antigen presentation
ERFE	erythroferrone
Fam49b	family with sequence homology 49 member b
Fpn	ferroportin
G0	generation 0
G1	generation 1
G2	generation 2
G3	generation 3
GAP	GTPase activating protein
GDF15	growth differentiation factor 15
GEF	guanine exchange factor
GWAS	genome wide association study
HAMP	hepcidin 1
Hbb	hemoglobin subunit beta
HJV	hemojuvelin
HLA	human leukocyte antigen

Hmox1	heme oxygenase 1
IBD	identical by descent
IFN	interferon
IL	interleukin
iNOS	inducible nitric oxide synthase
iNTS	invasive non-typhoidal Salmonella
i.p.	intraperitoneal
<i>Ity</i>	<i>Immunity to Typhimurium</i>
<i>i.v.</i>	<i>intravenous</i>
JAK	Janus kinase
Kb	kilobase
KO	knockout
LAMP	lysosomal associated membrane protein
Lcn2	lipocalin 2
LPS	lipopolysaccharide
Ltf	lactoferrin
M	Microfold
M6PR	mannose-6-phosphate receptor
MAPK	mitogen-activated protein kinase
Mb	mega base pair
MDR	multi-drug resistant
MHC	major histocompatibility complex
MLN	mesenteric lymph node
MOI	multiplicity of infection
mTOR	mammalian target of rapamycin
MSMD	Mendelian susceptibility to mycobacterial disease
NADPH	nicotinamide adenine dinucleotide phosphate
NK	natural killer
NF-κB	nuclear factor κB
NLR	NOD like receptor
NLRC4	NLR family CARD domain containing protein 4
NOD	nucleotide oligomerization domain
Nramp1	natural resistance-associated macrophage protein 1
NTS	non-typhoidal Salmonella
PAMP	pathogen associated molecular pattern
PARK2	Parkin RBR E3 Ubiquitin Protein Ligase
p.i.	post infection
Pklr	pyruvate kinase liver and RBC

PMN	polymorphonuclear leukocytes
PRR	pathogen recognition receptor
QTL	quantitative trait locus
Rag1	recombination activation gene
RBC	red blood cell
RCS	recombinant congenic strain
RES	reticuloendothelial system
RI	recombinant inbred
RNS	reactive nitrogen species
ROS	reactive oxygen species
S1	129S1/SvlmJ
SCV	<i>Salmonella</i> containing vacuole
SGEF	SH3 containing GEF
Sif	<i>Salmonella</i> induced filaments
Slc11a1	solute carrier family 11 member a1
Slc40a1	solute carrier family 40 member a1
SMAD	mothers against DPP homolog
SNP	single nucleotide polymorphism
SPI	Salmonella pathogenicity island
STAT	signal transducer and activator of transcription
Subsp.	subspecies
T3SS	type 3 secretion system
TFR	transferrin
TFRC	transferrin receptor
TLR	toll like receptor
TNF	tumor necrosis factor
TWSG1	twisted gastrulation BMP signaling modulator 1
Usp18	ubiquitin specific peptidase 18
VAP	Vacuole-associated Actin Polymerization
WASP	Wiskott-Aldrich syndrome protein
WAVE	WASP-family verprolin homologous protein
WHO	World Health Organization
Wt	wild-type
X1	129X1/SvJ

CHAPTER 1: GENERAL INTRODUCTION

Infectious diseases were responsible for approximately 15 million deaths in 2010. Deaths due to infectious diseases are projected to stay at this level until 2050 [1]. Despite advances in treatment and prevention and a better understanding of the pathogenesis of disease, annual mortality due to typhoid fever has increased 39% from 1990 to 2010 [2]. In addition, *Salmonella enterica* is responsible for an estimated 1 million deaths annually, making it a significant cause of mortality worldwide.

SALMONELLA: THE BACTERIUM

SALMONELLA INFECTION AND CLASSIFICATION

One of the earliest mentions of a typhoid-like disease is made by Hippocrates who noted a seasonal incidence of a fever characterized by diarrhea, watery stool, bilious vomiting, red rashes and abdominal pain and swelling. In 1880 the discovery of *Bacillus typhosus* (now called *Salmonella Typhi*) separately by Eberth, Klebs and Koch made typhoid fever one of the first diseases with a known causative agent [3]. Even before the isolation of the causative bacteria, William Budd demonstrated the importance of human carriers in the transmission of *Salmonella* disease [4, 5]. In 1896, Achard and Bensaude first reported cases of a disease similar to typhoid which we now know as paratyphoid fever. The name *Salmonella* was not used until 1900 when the bacteria was named in honor of Dr. Daniel E. Salmon whose student Theobald Smith isolated *Salmonella choleraesuis* in 1885 from the intestines of pigs that had developed hog cholera.

The genus *Salmonella* consists of a group of rod-shaped Gram-negative bacteria that are found ubiquitously. The genus can be subdivided into two species: *Salmonella enterica* and *bongori*. *Salmonella enterica* is further subdivided into 6 subspecies: *arizonae*, *diarizonae*, *enterica*, *houtenae*, *indica* and *salamae*. *Salmonella bongori* contains 22 serovars whereas *Salmonella enterica* contains over 2500 serovars combining to a total of over 2600 serovars [6]. Serovars are classified based on O (lipopolysaccharide (LPS)), H (flagellar), and K (capsular) antigens as proposed by the Kauffman-White classification scheme [7], however serovars in the *Salmonella*

enterica enterica subspecies are given names usually based on the location of isolation such as *Salmonella enterica* subsp. *enterica* serovar Dublin or the disease that they cause such as *Salmonella enterica* subsp. *enterica* serovar Typhimurium (subsequently *Salmonella* Typhimurium). *Salmonella* serovars can be host restricted and infect a single host such as *Salmonella* Typhi (humans) and *Salmonella* Gallinarum (chickens) or zoonotic with the ability to infect multiple hosts such as *Salmonella* Typhimurium and *Salmonella* Enteritidis. The serovars most commonly associated with disease manifestation in humans fall within *Salmonella enterica* subsp. *enterica*.

SALMONELLA INFECTION IN THE HUMAN POPULATION

Salmonella enterica species are typically transmitted by the fecal – oral route and can cause a broad spectrum of diseases from asymptomatic carriage to the more severe enteric fever. The disease manifestation largely depends on the serovar, infectious dose, host genetics, as well as the immunocompetence of the host and the composition of the gut flora. There are four main clinical outcomes that can result following *Salmonella* infection in humans.

ENTERIC (TYPHOID AND PARATYPHOID) FEVER:

Enteric fever consisting of typhoid and paratyphoid fever is a potentially fatal multi-organ disease. Typhoid fever is caused by the human restricted *Salmonella* Typhi whereas paratyphoid fever is caused by the human restricted *Salmonella* Paratyphoid A, B, C and *Salmonella* Sendai. Annually, it is estimated that there are 21 million new cases and 200,000 deaths associated with typhoid fever [8, 9]. There is also an additional 5.4 million cases of paratyphoid fever caused predominantly by Paratyphoid A [9]. *Salmonella* is typically spread through contaminated food and water therefore lack of access to clean water and proper sanitation is an important risk factor in the development of enteric fever. Consequently, enteric fever in the developed world is considered a traveler's disease, but in developing nations enteric fever is still a major problem.

Symptoms of typhoid fever typically start following an incubation period of about 14 days and lasting about 3 weeks if left untreated. Clinical features include: sustained fever, fatigue,

stomach pain, poor appetite, rosy spots, and hepatosplenomegaly. Mortality following enteric fever is 20% when left untreated but decreases to less than 1% when treated with antibiotics [10, 11]. Antimicrobial therapy using first line drugs such as ampicillin, chloramphenicol, and trimethoprim-sulfamethoxazole were initially used to treat acute typhoid fever. However the emergence of multidrug resistance has necessitated alternative treatment options including fluoroquinolones, third generation cephalosporins and azithromycin [12].

Paratyphoid fever results in a milder disease with symptoms starting following an incubation period of 1-10 days. Paratyphoid fever is also associated with lower mortality and lower chronic carriage rates [13]. The incidence of paratyphoid fever has been increasing in Asia, accounting for up to 50% of enteric fever cases [9]. It is thought that the increasing incidence of paratyphoid fever could be due to the increasing use of the typhoid vaccine.

There are much fewer GWAS (genome wide association studies) in humans for infectious diseases compared to other common chronic human diseases. Limitations to using this method include the necessity of large sample sizes, selection of controls can be difficult due to limited information on pathogen exposure, and the confounding source of genetic variation due to the pathogen [14]. Despite these limitations, four loci have been identified for outcome to enteric fever: HLA (Human Leukocyte Antigen) class II and class III as well as the TNF (Tumor Necrosis Factor) region and an E3 ubiquitin ligase PARK2 (Parkin) [15-19].

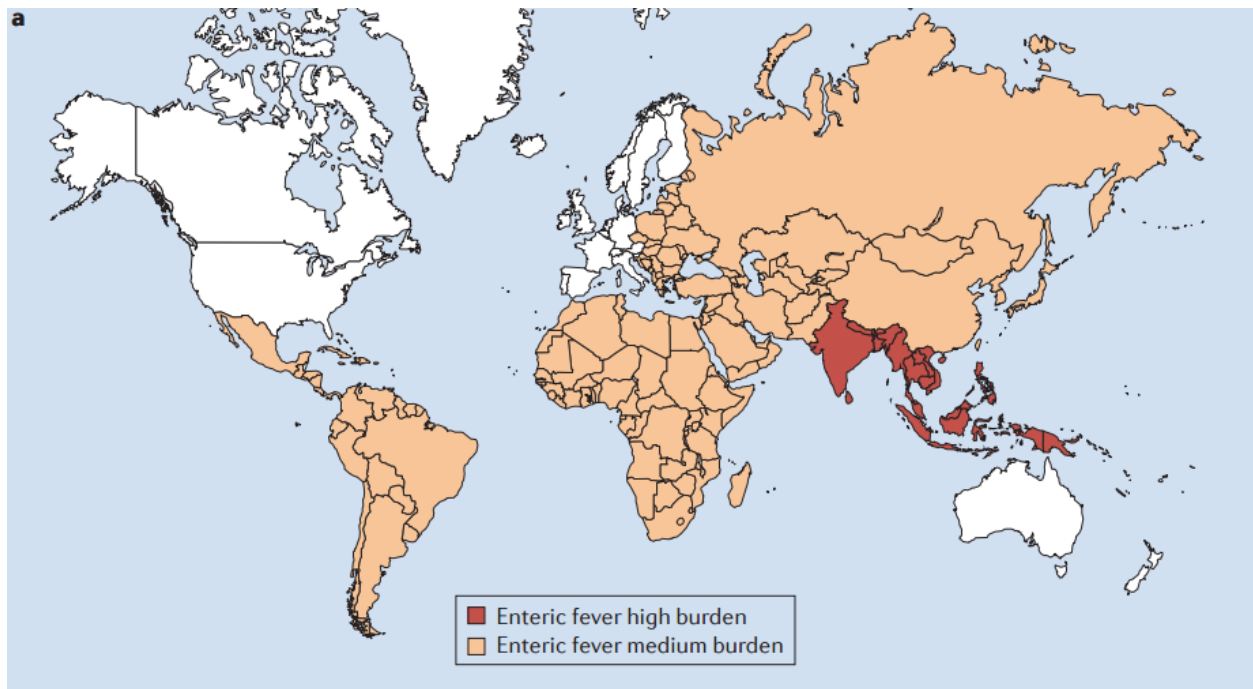


FIGURE 1: GLOBAL BURDEN OF TYPHOID FEVER

Taken from Gilchrist JJ et al Nat. Rev. Immunol. 2015. Global distribution of enteric fever, including both typhoid and paratyphoid fever. High burden is defined as greater than 100 cases per 100,000 people per year and medium burden is defined as 10-100 cases per 100,000 people per year.

CHRONIC CARRIAGE

Most people after being infected with *Salmonella* Typhi or Paratyphi will shed bacteria from their stool and sometimes urine for days to weeks following recovery from acute infection. However 2-5% of patients will continue to shed *Salmonella* for a year or longer termed chronic carriage. Chronic carriage following typhoid and paratyphoid fever is a key feature of bacterial persistence within the population as there is no known environmental reservoir for *Salmonella* Typhi or *Salmonella* Paratyphi [20, 21]. The mechanism leading to the establishment of the carrier state is poorly understood however mouse studies indicate that biofilm formation in the gallbladder and biliary tract may be important [22, 23]. Human studies of gallbladder injury show an increased correlation with carrier status. In endemic populations there is also a presence of a subset of people who are healthy carriers and have shown no previous sign of disease [23]. The risk of becoming a chronic carrier increases with age. It has been seen that

less than 1% of people under 20 years old become carriers whereas over 10% of people over 50 become carriers. In addition women are twice as likely to become a carrier as men [24]. Treatment of the chronic carrier state can be done with antibiotics however compared to treatment of acute typhoid fever treatment requires larger doses over a longer period of time.

GASTROENTERITIS

Gastroenteritis is caused by non-typhoidal *Salmonella* (NTS) serovars resulting in an estimated 93.8 million cases and 155,000 deaths a year worldwide but occurring mainly in immunocompetent patients in industrialized nations [25]. The serovars most commonly isolated from patients are *Salmonella* Typhimurium, Enteritidis and Heidelberg. However there has been an increase in recent years in which new serovars are frequently being isolated from fresh fruit and vegetables. This is thought to be due to the rapid growth of global trade in food products and the accompanying changes in food consumption which was exemplified recently by the outbreak of *Salmonella* Poona caused by contaminated imported cucumbers in the United States [6]. The serovars causing gastroenteritis are zoonotic and able to infect a broad range of hosts like chicken, pigs, and cows as well as fruits and vegetables which are then consumed by and infect humans. There has also been an increase in the incidence of gastroenteritis associated with exposure to exotic pets especially reptiles. Exposure to reptiles account for 6% of all sporadic *Salmonella* infections while 11% of all infections in persons under 21 years old can be attributed to contact with reptiles or amphibians [26]. Symptoms tend to start after an incubation period of 6 to 12 hours and typically last less than 10 days. The clinical features of NTS gastroenteritis are self-limiting acute gastroenteritis, water diarrhea, nausea, vomiting, abdominal pain and fever. Treatment of gastroenteritis involves replacement of fluids and electrolytes, and control of nausea, vomiting and pain. Antibiotic treatment is used only in severe cases.

INVASIVE NTS (INTS)

Non typhoidal *Salmonella* infections in immunocompromised individuals may result in an invasive bloodstream disease occurring mainly in sub-Saharan Africa. There is a bimodal

distribution in the incidence of cases where young children between 6-36 months and adults in their 3rd and 4th decades are at the highest risk. In addition, comorbidities such as HIV, malaria and malnutrition increase the risk of developing iNTS. Other risk factors such as sickle cell anemia, Chronic Granulomatous Disease (CGD), genetic deficiencies in the IFN γ and IL-12/23 pathways also increase the risk of recurrent iNTS disease [27, 28]. In 2010, there was an estimated 3.4 million cases with approximately 680,000 deaths mainly in children occurring mainly in Africa [29, 30]. Symptoms of iNTS closely resemble those of enteric fever with a number of symptoms that are non-specific to the disease. Most cases of iNTS results from infection with either *Salmonella* Typhimurium (65.2%) or *Salmonella* Enteritidis (33.1%), but especially with the ST313 strain of *Salmonella* Typhimurium [31]. In addition, there seems to be a seasonal incidence of iNTS cases which probably coincides with the increased incidence of malaria and malnutrition during the rainy season [32]. The case fatality for iNTS is an estimated 20-25% [33, 34]. Similar to typhoid fever, there has been an increase in the incidence of multidrug resistant (MDR) strains of *Salmonella* causing iNTS [31]. Therefore, treatment for iNTS typically requires 2-6 weeks of 3rd generation cephalosporins and fluoroquinolones [35]. These MDR strains of *Salmonella* are distinct from the *Salmonella* strains causing gastroenteritis in developed nations.

USE OF VACCINATION

Vaccine development against typhoid fever was first attempted by Fraenkel in 1893 using subcutaneous injection of killed cultured [36]. Although Pfeiffer and Kolle developed an inoculation against typhoid in 1896, the first effective vaccine against typhoid fever was developed in 1896 by Dr. Almroth Wright which consisted of heat killed whole cell bacteria. The first large scale inoculation was done for the British Army in India in 1898 where it was observed that the vaccinated soldiers experienced a reduction in the number of cases compared to unvaccinated soldiers [37]. By 1911 the United States had also started vaccinating their military against typhoid. Two vaccines are currently available for the prevention of enteric fever caused by *Salmonella* Typhi. The first is based on the live attenuated mutated strain of *Salmonella* Typhi Ty21a and is an oral vaccine and the second is a

vaccine based on the Vi polysaccharide capsule. Despite the availability of a vaccine, it is mainly used by travelers from developed countries and not by the people in endemic areas who would benefit the most. In addition, the use of vaccination has not been shown to improve the rate of chronic carriage. There is also no vaccine available for *Salmonella* Paratyphi A despite there being an increasing incidence of this disease. There is no vaccine available for the prevention of gastroenteritis.

PATHOGENESIS OF *SALMONELLA* DISEASE

ROUTE OF INFECTION:

The establishment of systemic infection begins with the ingestion of food or water contaminated with *Salmonella*. The acidic pH of the stomach is capable of destroying most bacteria however a small proportion can survive due to acid tolerance mechanisms allowing survival and subsequent colonization of the small intestine [38, 39]. *Salmonella* preferentially traverses the gut barrier through invasion of M (Microfold) cells in Peyer's patches [40]. *Salmonella* Typhi produces very little intestinal inflammation, very little neutrophilic infiltration and very little intestinal replication which enables the bacteria to spread to systemic sites by travelling through the blood stream [41-43]. Once *Salmonella* has disseminated to systemic sites of the secondary lymphoid system the bacteria replicates in the spleen, liver and mesenteric lymph node (MLN) within specialized vacuoles. Colonization of the gallbladder and subsequent shedding is an important part of dissemination as humans are the only known reservoir for *Salmonella* Typhi.

Non-typhoidal serovars such as *Salmonella* Typhimurium after invading enterocytes and M cells in Peyer's patches are engulfed by macrophages and dendritic cells (DCs) where it replicates. Following engulfment, *Salmonella* induces caspase-1 mediated cell death resulting in the production of IL-1 β and IL-18 and subsequent recruitment of neutrophils. Due to the inflammation and massive neutrophil infiltrate, *Salmonella* Typhimurium is limited to the intestine and does not typically disseminate past the MLN.

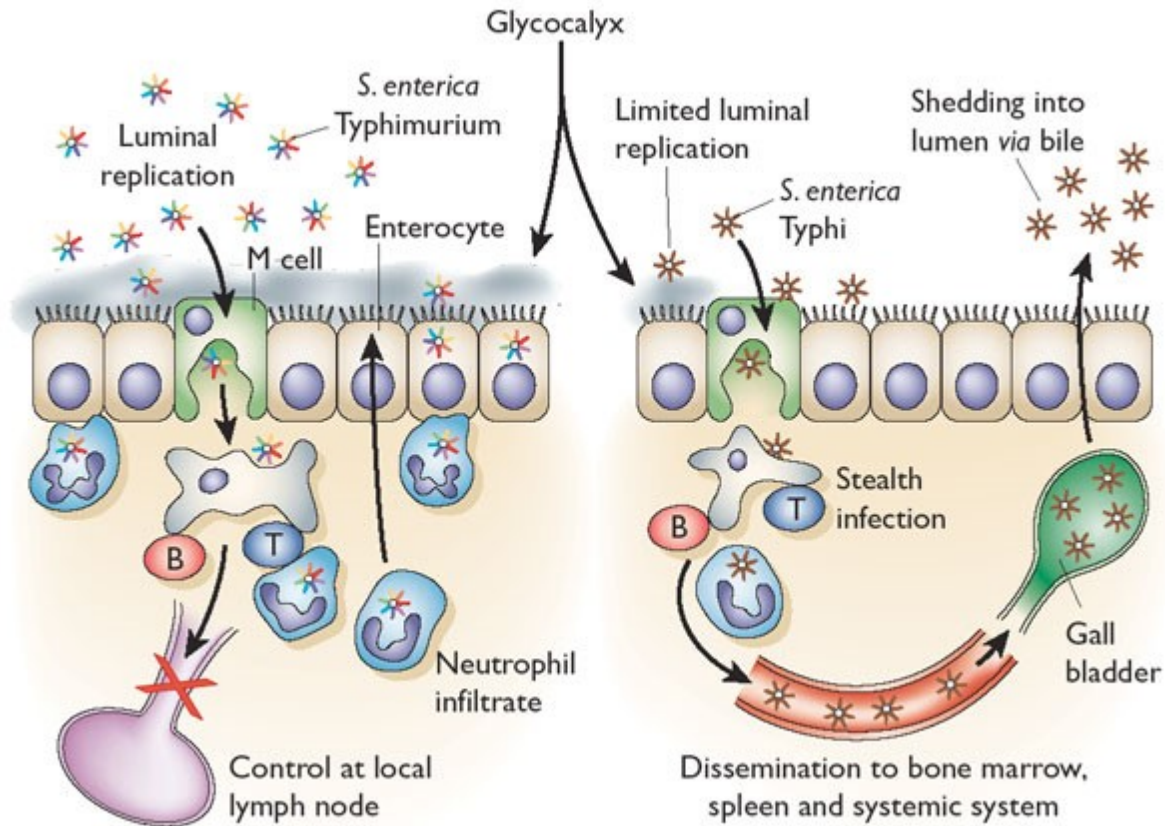


FIGURE 2: DIFFERENCES BETWEEN *SALMONELLA* TYPHIMURIUM AND *SALMONELLA* TYPHI IN ESTABLISHING INFECTION

Taken from Young et al Nat. Immunol 2002. This schematic highlights differences between infection routes of *Salmonella Typhimurium* (left) and *Salmonella Typhi* (right). T=T cell, B=B cell

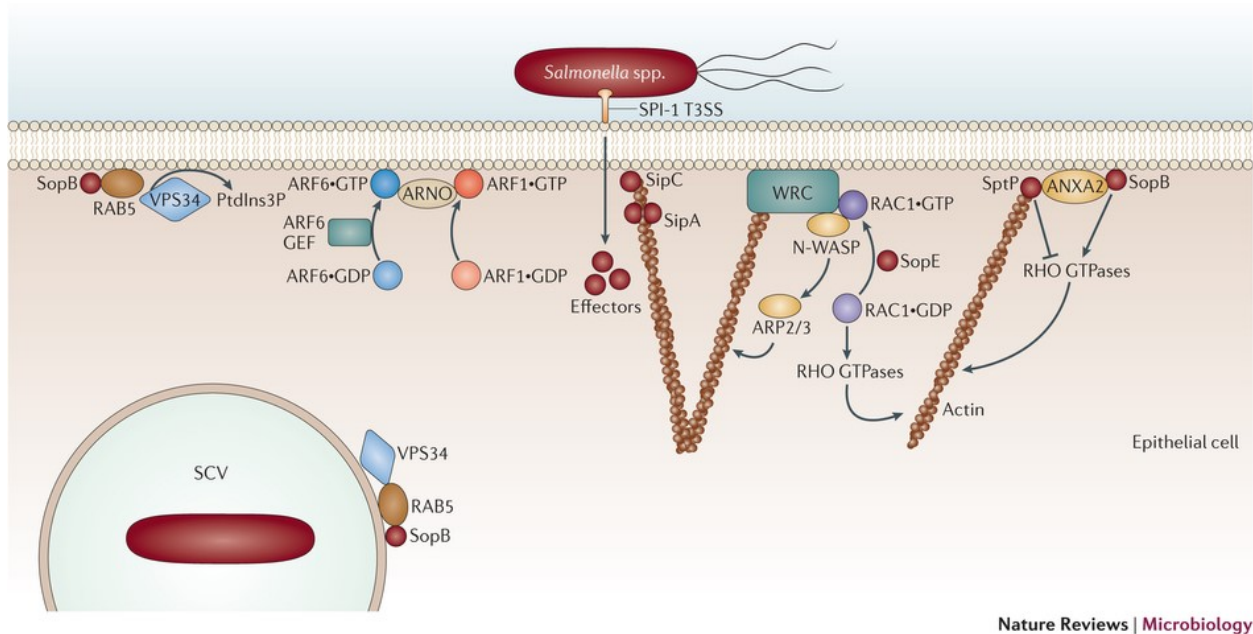
SALMONELLA VIRULENCE:

Salmonella Typhi shares approximately 90% of its genome with other *Salmonella* serovars [44, 45]. The genome of *Salmonella* encodes *Salmonella* Pathogenicity Islands (SPIs) which are important for virulence and survival. To date 21 SPIs have been identified [46]. The two most well studied SPIs are SPI-1 and SPI-2. SPI-1 and SPI-2 both encode a type 3 secretion system (T3SS): a complex composed of a motor, a needle complex and a translocon through which secreted effectors are delivered into host cells [47]. Traditionally SPI-1 has been thought to be important for bacterial entry into host cells whereas SPI-2 has been thought to be important for

intracellular survival and replication [48, 49]. However recent studies have shown significant overlap in SPI-1 and SPI-2 effectors in intestinal disease and intracellular replication [50-52].

Invasion (SPI-1 mediated)

SPI-1 is a 40 kb locus that is conserved across all *Salmonella* serovars. Upon ingestion of *Salmonella* by the host, *Salmonella* invades M cells and enterocytes using SPI-1 genes and SPI-1 encoded effectors. SipA and SipC directly control and localize actin polymerization at the site of bacterial attachment. SipC is important for nucleating the assembly of actin filaments. This leads to the rapid growth from barbed ends [53]. SipC has similar function to the ARP2/3 complex of the host. SipA promotes actin filament formation by reducing the monomer concentration required for filament assembly [54]. In addition, the formation of actin networks is mediated by host Rho GTPases RAC1 and CDC42 following activation by SPI-1 effectors SopB, SopE, and SopE2. The activation of RAC1 and CDC42 results in activation of N-WASP and the WAVE-ARP2/3 complex to trigger actin remodeling such as membrane ruffles and filopodia. This is important for bacteria mediated endocytosis to allow invasion of *Salmonella* into cells. SopB is an inositol phosphatase and can indirectly activate Rho GTPases, acting in particular on RHOG by activating its GEF (guanine exchange factor): SGEF [55]. In addition, SopB recruits annexin A2 (ANXA2) which acts as a platform for actin rearrangements [56]. The actin remodeling initiated by *Salmonella* SPI-1 effectors is transient. The process is reversed by 2- 3 hours p.i. using bacterial effector SptP which is GTPase activating protein (GAP) towards RAC1 and CDC42 [57]. In addition, the gene InvA is a structural component of the T3SS needle complex for SPI-1 [58]. More recently, SPI-1 has been shown to be important for the activation of the immune system. SPI-1 induces inflammation through the induction of IL-8 production and the activation of MAPK and NF- κ B. This results in the activation of caspase 1 leading to the production of pro IL-1b and IL-18 and the subsequent recruitment of PMNs [43, 59, 60].



Nature Reviews | Microbiology

FIGURE 3: SPI1 EFFECTORS AND ITS IMPACT ON HOST ACTIN CYTOSKELETON

Taken from LaRock et al Nat. Rev. Microbiol. 2015. SPI1 effectors (red circle) can manipulate proteins that regulate the host cytoskeleton in order to facilitate invasion and replication.

As noted earlier, there are a few differences in the mechanism used by *Salmonella* Typhi and *Salmonella* Typhimurium during invasion, namely the lack of inflammation seen in the intestine during *Salmonella* Typhi infection. *Salmonella* Typhi expresses SPI-7 which is not expressed by NTS serovars. One mechanism by which *Salmonella* Typhi evades detection is through its expression of the Vi polysaccharide which does not contain hydroxyl groups such that it cannot be detected by the complement cascade. This has several effects: 1) inhibiting phagocytosis by neutrophils, and 2) limiting recruitment of neutrophils to the site of infection [61-63]. In addition, SPI-7 expresses the TviA regulatory protein which has dual functions as a positive regulator of capsule biosynthesis and a negative regulator of genes encoding flagella and SPI-1 [64]. Repression of flagellar genes by TviA is associated with increased dissemination to the spleen [65, 66]. In addition, TviA inhibits inflammation by inhibiting RAC1 dependent NF-κB activation [67].

Formation of the *Salmonella* containing vacuole (SCV)

Following invasion, *Salmonella* resides within a specialized compartment called the SCV which protects the bacteria from host killing mechanisms and establishes an intracellular replication niche. The biogenesis of the SCV involves sequential interactions with the endocytic pathway and can be simplified into three steps: early (<30 min), intermediate (30 min – 5 hrs) and late (>5 hrs). This process is coordinated by both SPI-1 and SPI-2 effectors. The early SCV is enriched in early endosomal markers such as EEA1 (early endosome antigen 1), RAB5 and TFRC (transferrin receptor). It quickly transitions into an intermediate SCV with the replacement of the early endosomal markers with late endosomal markers such as LAMP (lysosomal associated membrane protein) and vATPase which closely resembles phagosome biogenesis and results in the acidification of the SCV [68]. The intermediate SCV is positioned at a juxtannuclear position. However unlike phagosome biogenesis, the SCV does not express cathepsin D, cathepsin L or mannose-6-phosphate receptor (M6PR). During the late stage of SCV biogenesis, *Salmonella* induced filaments (Sifs) begin to form and bacterial replication initiates. Another characteristic of the late SCV is the formation of an F-actin mesh network called Vacuole-associated Actin Polymerization (VAP), which is associated with the integrity of the SCV membrane [69]. Throughout the maturation process, the SCV avoids the delivery of NADPH oxidase or iNOS (inducible nitric oxide synthase) in order to minimize exposure of *Salmonella* to harmful reactive oxygen and nitrogen intermediates.

Replication and survival (SPI-2 mediated)

SPI-2 is also a 40 kb locus that consists of two distinct regions: one region is found in both *enterica* and *bongori* species and is dispensable for systemic virulence; the second region is present only within the *enterica* species and is essential for systemic pathogenesis [70]. SPI-2 functions by translocating effectors across the membrane of the SCV of infected cells. The expression of SPI-2 and its effectors is induced in response to acidification of the SCV [71, 72]. The SsaR gene encodes a part of the conserved SPI-2 apparatus component and is important for secretion of SPI-2 effectors. SPI-2 effector proteins include SifA, SseJ, SseF, and SseG are involved in the maintenance of the SCV membrane and the localization of the SCV to a

juxtannuclear region within the cell [73-75]. SPI-2 also prevents the recruitment of NADPH oxidase and iNOS to the SCV [76, 77] which protects *Salmonella* from damage by ROS (reactive oxygen species) and RNS (reactive nitrogen species).

IMPACT OF HOST GENETICS

IMMUNE RESPONSE TO INFECTION

PHASES OF INFECTION

The use of the mouse model of typhoid fever has greatly furthered our understanding of the immune response to infection. It has become generally accepted that infection can be subdivided into 4 distinct phases: 1) bacterial clearance from the blood; 2) exponential bacterial growth 3) host mediated suppression of bacterial replication; 4) resolution of infection [78].

Phase 1: clearance from the blood

Following invasion of the intestine, *Salmonella* is transported from the gastrointestinal tract to the bloodstream through the MLN where it is found as extracellular bacteria or associated with CD18+ phagocytic cells [79]. During the first phase of infection, *Salmonella* is rapidly cleared from the blood via the complement cascade and macrophages.

The recognition of the O-antigen on *Salmonella* LPS by complement component C3b activates the alternative pathway of the complement system. Complement has a number of important roles in infection. The fixation of C3b on the bacterial surface is a process called opsonization which enhances phagocytosis by neutrophils. At the same time, C5 convertase generates C5a which is a potent chemoattractant for neutrophils towards bacteria and also acts to enhance cytokine responses by stimulating TLR4 (toll-like receptor 4) [80, 81]. Finally members of the complement cascade (C5b, C6, C7, C8 and C9) can form a membrane attack complex that can kill pathogens by forming pores in their cell membrane [82].

Phase 2: bacterial growth

After being cleared from the blood, *Salmonella* is mainly found within secondary lymphoid tissues like spleen and liver where it resides within resident macrophages, PMNs and DCs. *Salmonella* undergoes a period of replication within the SCV. Bacterial killing by phagocytes is

an important factor during this phase to control bacterial growth. This is mediated by the production of ROS and, to a lesser extent, RNS by NADPH oxidase and iNOS. In addition SLC11A1 is important for controlling bacterial replication.

Slc11a1: SLC11A1 (formerly NRAMP1) is a divalent metal ion transporter (especially Fe^{2+} , Mg^{2+} , and Mn^{2+}) expressed within the late endosomal and phagolysosomal membranes of macrophages, DCs and neutrophils and is important for controlling the exponential growth of *Salmonella* in tissues [83-88]. SLC11A1 has been associated with decreased IL-10 expression as well as increased activity of pro-inflammatory immune pathways ultimately resulting in increased ROS and RNS production [89-92]. Certain inbred strains of mice such as C57BL/6 (B6) and BALB/C have a mutation in *Slc11a1* making them hyper susceptible to *Salmonella* infection resulting in overwhelming bacteremia. The expression of the *Slc11a1*^{susceptible} allele in B6 mice shows decreased expression of late endosomal markers such as M6PR and EEA1 on the SCV which led to decreased phagosome maturation and decreased microbicidal activity [93, 94]. Despite the strong impact of the *Slc11a1*^{susceptible} allele in mice, no association has been found between *Slc11a1* and typhoid susceptibility in humans but has been associated with susceptibility to leprosy and tuberculosis [95]. SLC11A1 has also been shown to have a role in macrophage iron homeostasis as shown by decreased cytoplasmic iron levels, enhanced cellular iron export and limiting iron availability to intracellular bacteria [96-98]. It has also been shown to have a role recycling iron in macrophages following erythrophagocytosis [99].

Reactive intermediates – (ROS/RNS and NADPH oxidase/iNOS): Reactive intermediates produced by phagocytes are important for controlling the growth of *Salmonella*. ROS is generated by the enzyme NADPH oxidase expressed on PMNs and phagocytes. Mice lacking the gp91 subunit of NADPH oxidase show increased susceptibility to *Salmonella* with increased bacterial load in the spleen and liver [100]. ROS can promote *Salmonella* elimination by a number of mechanisms including direct oxidative damage, promoting autophagy and inflammasome activation, affecting neutrophil recruitment and affecting iron availability [101]. RNS is produced by phagocytes through the expression of NOS2. NOS2 is expressed by a variety of cells including intestinal epithelial cells, macrophages and neutrophils and is induced by IFN γ [102]. NOS2 functions to convert L-arginine to NO (nitric oxide) that inhibits enzymes essential

for bacterial respiration and replication [103]. Mice lacking NOS2, although able to control early replication of *Salmonella*, are unable to control bacterial growth later during infection and ultimately succumb to infection suggesting that RNS is important in the control of bacterial replication late during infection [100].

Phase 3: host mediated suppression of bacterial growth

Here, the suppression of bacterial growth coincides with hepatosplenomegaly and the migration of bone marrow derived inflammatory cells and requires the action of several immunological mediators. The bacteriostatic role of RNS is crucial along with the induction of multiple cytokines which are essential for the control of bacterial growth. These include pro-inflammatory cytokines such as TNF α , IFN γ , IL-1, and IL-6 as well as anti-inflammatory cytokines such as IL-4 and IL-10.

Cell Death Mechanisms: During infection, *Salmonella* interacts with a variety of host cells and often induces cell death through a variety of cell death mechanisms. Cell death is used by the host to eliminate pathogens as part of the host defense system whereas pathogens have evolved numerous methods to evade cell death mechanisms in order to proliferate and disseminate within the host.

Apoptosis: Apoptosis plays a crucial role in immune response or cellular damage by disease or harmful agents [104]. Studies have shown that apoptosis of intestinal epithelial cells occurs only after prolonged exposure to *Salmonella* and requires SPI-2 effectors which suggests that the bacteria can suppress cell death in the early stages of infection [105, 106].

Necroptosis: Necroptosis is a form of cell death that is similar to necrosis which is characterized by cell and organelle swelling, rapid membrane rupture and inflammation. *Salmonella* has been shown to suppress the activation of caspase-8 and induce autocrine secretion of type I IFNs to drive necroptosis of macrophages [107]. It is thought that *Salmonella* induces necroptosis in macrophages to promote invasion and persistence.

Pyroptosis: Pyroptosis is an important host defense mechanism to inhibit intracellular bacterial growth through the proteolytic cleavage of pro-IL-1 β and pro-IL-18 and subsequent secretion of IL-1 β and IL-18. During *Salmonella* infection, NLRC4 (NLR Family, CARD Domain Containing 4) inflammasome recognizes cytosolic flagellin to trigger activation of caspase-1. More recently,

caspase-11 was found to directly bind cytoplasmic LPS to activate a non-canonical inflammasome and trigger pyroptosis [108]. *Salmonella* can evade inflammasome detection by repressing the expression of a SPI-1 rod component and flagella and switching to the expression of SPI-2 effectors which are not detected by NLRC4 [109]. However for *Salmonella*, induction of macrophage cell death through this pathway is thought to be important for dissemination and pathogenesis.

Autophagy: During infection, damaged SCVs and cytosolic bacteria can be targeted for autophagic degradation through the recruitment of adaptor proteins, LC3, p62 and NDP52. Autophagy protects the cytosol from bacterial colonization [110]. Autophagy of the SCV influences the elimination of pathogens, control of pro-inflammatory signaling, antigen presentation and the adaptive immune response. KO of autophagy genes such as ATG5 and ATG6L1 in intestinal epithelial cells show increased susceptibility to *Salmonella* infection [111, 112].

Cytokine response – IFN γ , IL-12, TNF α , IL-6, IL-10: Secretion of pro- and anti-inflammatory cytokines are important for regulating host response to infection and results in immune activation, chemotaxis, microbicidal activity and proliferation. The production of pro-inflammatory cytokines such as IL-12, IFN γ , TNF α and IL-6 occur as a result of TLR signaling. IL-12 production by phagocytes results in the production of IFN γ , mainly from NK cells, and Th1 polarization which is essential for the early response against *Salmonella* infection [113, 114]. In mice lacking IL-12, macrophages are unable to control bacterial replication [115]. In humans, patients deficient in the IL-12/IL-23 or IFN γ pathways are predisposed to MSMD and/or iNTS [27, 116]. However reports of an association between IL-12/IL-23 and IFN γ signaling pathways and enteric fever have been limited to situations in which MSMD has been comorbidity [117, 118]. IFN γ is also essential for inducing the production of ROS.

TNF α is produced mainly by macrophages. TNF α and TNF receptor KO mice show increased susceptibility to *Salmonella* infection with increased dissemination of bacteria to spleen and liver [119, 120]. TNF α has many functions that work in concert with IFN γ [121]. IL-6 is a cytokine with a broad range of functions encompassing expansion and activation of T cell, differentiation of B cells, regulation of the acute phase response and hematopoiesis [122].

IL-10 is an anti-inflammatory cytokine produced following TLR and Dectin signaling. IL-10 can be produced by many immune cells including macrophages, DCs, T cells and B cells and is vital for regulating the development of the immune response [123]. IL-10 indirectly regulates T cell responses by inhibiting cytokine/chemokine production and antigen presentation by monocytes and macrophages [124, 125]. IL-10 deficiency results in increased susceptibility to endotoxic shock [126, 127]. In sub-Saharan Africa, co-infection with malaria is a risk factor for developing iNTS. In a mouse model of co-infection, it has been shown that infection with malaria results in increased production of IL-10. In this context IL-10 is responsible for increased susceptibility to non-typhoidal *Salmonella* by suppressing the ability of macrophages and neutrophils to respond to infection [128]. IL-10 is important for the prevention of excess tissue damage therefore the timing of IL-10 expression is important for the resolution of infection.

Innate sensing of bacteria: Recognition of bacteria is an important facet of the immune system. There exist a number of evolutionarily conserved receptors to detect bacterial ligands. These include TLRs which recognize extracellular ligands and Nod like receptors (NLRs) which recognize intracellular danger signals. The TLRs are a large family of PRRs (pathogen recognition receptors) involved in the recognition of specific microbial molecules. Each TLR recognizes a distinct PAMP (pathogen associated molecular pattern) derived from bacteria, viruses, mycobacteria, fungi and parasites including lipoproteins (TLR1, -2, -6), LPS (TLR4), double-stranded RNA (TLR3), flagellin (TLR5), single-stranded RNA (TLR7, -8) and DNA (TLR9). Upon recognition of their respective PAMP, they elicit a conserved inflammatory pathway that results in the activation of transcription factors like NF- κ B, AP-1 and IFN response factors and the production of pro-inflammatory cytokines.

TLR4 is important in the recognition of LPS. Certain inbred strains, especially C3H/HeJ, demonstrated hyporesponsiveness to LPS, a glycolipid which constitutes a major component of the outer membrane of Gram-negative bacteria [129]. C3H/HeJ mice could tolerate LPS doses that were 20-40 times higher than that of wild type mice [129]. Despite the ability of C3H/HeJ mice to tolerate high doses of LPS, these mice are highly susceptible to *Salmonella* infection [130]. A point mutation was identified in the gene *Tlr4* in C3H/HeJ mice [131, 132]. This

mutation affected cytokine secretion by macrophages in response to LPS as well as the proliferation of splenic B cells [131]. The role of TLR4 in innate immunity was confirmed using *Tlr4* KO mice [133]. In humans, two SNPs in *TLR4* have been associated with susceptibility to infections with Gram-negative bacteria and septic shock [134, 135].

TLR5 is another receptor important for the recognition of *Salmonella*. Starting in the late 1990s, flagellin from *Salmonella* Typhi was reported to induce cytokine release from human monocytes and impaired antigen presentation by human macrophages [136-138]. It was later discovered that flagellin activated TLR5 [139]. Recognition of flagella by TLR5 promotes *Salmonella* infection and its systemic spread [140].

Phase 4: resolution of infection

Effective control and eradication of bacteria is dependent on the adaptive immune response. T cells and B cells are important in the clearance of bacteria from the RES (reticuloendothelial system). In addition the MHC (major histocompatibility complex) in mice has also been shown to play a major role in the extent of bacterial clearance [141].

T cell mediated immunity: athymic and alpha/beta T cell deficient mice have increased late susceptibility to infection [142, 143]. Immune response is mediated in part by CD4+ T cells but also, to a lesser extent, CD8+ T cells [144]. The MHC in particular has been shown to be important for T cell mediated immunity in the amount of *Salmonella* antigen presented. In mice, susceptibility to infection has been linked to different H2 haplotypes [141]. In humans two alleles of the HLA-DRB1 locus have been shown to be important. Particularly the HLA-DRB1 *04:05 allele has been shown to be protective in the Vietnamese population whereas the HLA-DRB1 *12 allele has been shown to be associated with susceptibility in the Vietnamese and Javanese populations [15, 17].

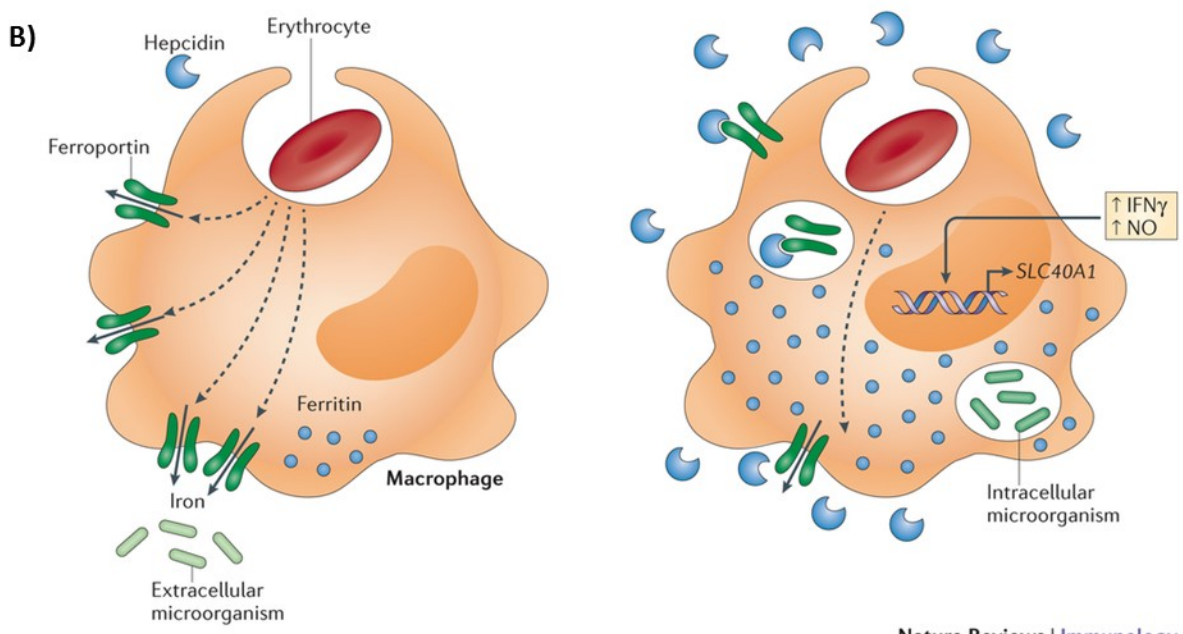
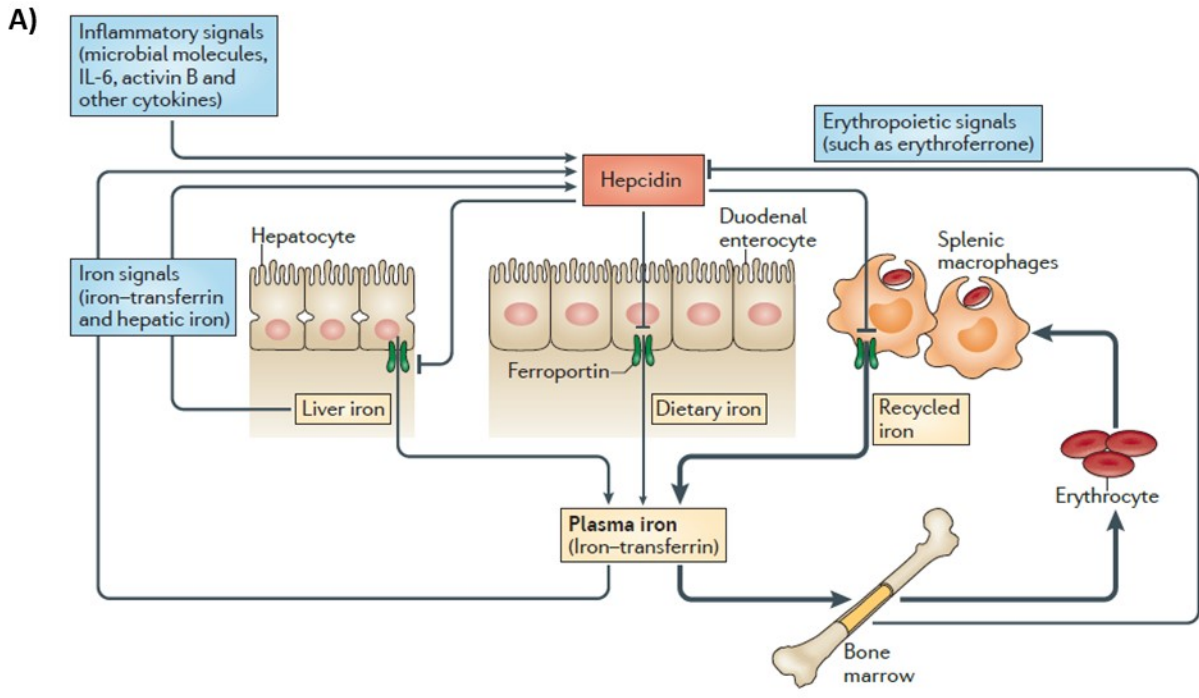
B cells have also been shown to be important for acquired immune responses as demonstrated by the susceptibility of B cell deficient mice to secondary *Salmonella* infection following vaccination [145].

IRON METABOLISM IN HOST DEFENSE

REGULATION OF IRON METABOLISM

Within the host, the vast majority of iron is maintained in the plasma and is stored in hepatocytes, as well as splenic and hepatic macrophages. Over 50% of total iron in the body is bound by hemoglobin in RBCs. In humans, approximately 1-2 mg of iron is absorbed from the diet to replace the small amount of iron that is lost from bleeding and shedding of intestinal and skin cells. The rest of the iron comes from the recycling of senescent RBCs by erythrophagocytosis by macrophages. The metabolism of iron in the body is regulated by the liver hormone hepcidin (HAMP). In turn, HAMP inhibits the expression of the sole iron exporter ferroportin (FPN also known as SLC40A1), which is expressed on the surface of macrophages, thereby resulting in a decrease of iron influx into the plasma [146]. The effect of increased HAMP expression is an increase of iron in macrophages and subsequent decrease in plasma iron concentration. The expression of HAMP is tightly regulated by a number of environmental cues such as infection and inflammation, iron status of the host and the erythropoietic demands of the host [147].

Erythroid regulation of HAMP until recently was thought to be regulated by twisted gastrulation 1 (TWSG1) and/or growth differentiation factor 15 (GDF15). It has since been shown to also be regulated by erythroferrone (ERFE). ERFE is a hormone that is rapidly produced by erythroid precursors in response to erythropoietin (EPO) via STAT5 signaling during stress erythropoiesis. ERFE then acts directly in the liver to decrease HAMP transcription [148]. In addition, the regulation of HAMP expression during inflammation is regulated by the cytokine IL-6 through JAK and STAT3 signaling. The expression of FPN is systemically regulated by HAMP; however macrophage heme and iron content can regulate FPN expression within individual cells [149, 150].



Nature Reviews | Immunology

FIGURE 4: REGULATION OF IRON METABOLISM

Taken from Ganz & Nemeth Nat. Rev. Immunol. 2015. The different ways iron metabolism and HAMP can be regulated is shown at the systemic **(A)** and cellular **(B)** level.

ANEMIA OF INFLAMMATION

Anemia of inflammation, previously called anemia of chronic disease, occurs as a result of various etiologies: infection, autoimmune disease, and chronic disease [151]. Clinically, the anemia tends to be normocytic and normochromic but can become microcytic and hypochromic following chronic disease [152]. Anemia of inflammation results from HAMP induced hypoferrremia and cytokine mediated suppression of erythropoiesis and decreased erythrocyte survival with very little reticulocytosis [151, 153]. Decreased erythrocyte survival is thought to be due to activation of macrophages that prematurely remove aging RBCs from the blood stream [154, 155]. Upregulation of HAMP by IL-6 and subsequent downregulation of FPN results in retention of iron in macrophages, hepatocytes and intestinal enterocytes such that there is less iron delivered to plasma TFR. Other molecules can also sequester iron independently of HAMP such as lactoferrin (LTF), lipocalin 2 (LCN2), haptoglobin, hemopexin, SLC11A1, and TFRC. The expression of all but TFRC increase during infection [147].

Iron is an essential nutrient for both the host and the bacteria. The host response to *Salmonella* infection is dependent on the iron status of the host. Anemia of inflammation is one mechanism in which the host reduces the availability of iron to the bacteria. It is thought that inducing hypoferrremia in the host could increase the capacity for TFR to bind iron thereby limiting the generation of non-TFR bound iron that could be used by pathogens. This has a secondary benefit in that non-TFR bound iron can increase tissue injury due to extracellular production of ROS or can be taken up by cell types causing iron overload and increase secondary ROS [147]. In mice, iron overload induced by an iron rich diet or repeated injections of iron results in increased susceptibility to *Salmonella* infection [156, 157]. Mice with genetic deficiencies in *Hemoglobin subunit beta (Hbb)* or *Pyruvate kinase liver and red blood cell (Pklr)* resulting in iron overload also confer susceptibility to *Salmonella* infection [156, 158].

Conversely, iron depletion through an iron deficient diet results in resistance to *Salmonella* infection [159].

Pklr: PKLR is a liver and RBC-specific pyruvate kinase, an essential enzyme for RBC glycolysis.

Deficiency in this gene results in constitutive hemolytic anemia with reticulocytosis and splenomegaly [160]. Mice deficient in *Pklr* show decreased erythropoietic response in the face

of increased clearance of ageing RBCs. As a result of the rapid turnover of RBCs, there is iron accumulation in Kupffer cells and hepatocytes of the liver. Increased susceptibility to *Salmonella* infection in these mice is attributed to critical levels of hemolytic anemia which may affect macrophage function due to erythrophagocytosis and iron overload which may favor bacterial replication [156].

PATHOGEN ACQUISITION OF IRON

Iron is important for bacterial growth and replication as it functions as a cofactor for many biosynthetic pathways. Increased iron availability promotes *Salmonella* adhesion to and invasion of intestinal epithelial cells [161]. Although the host has many mechanisms to withhold iron from bacteria, *Salmonella* has developed counter-mechanisms to acquire iron from the host through the use of siderophores (also called siderochromes). Siderophores are small, high affinity iron chelating compounds that allow bacteria to compete for iron bound to TFR and LTF [162]. One example of a siderophore expressed by *Salmonella* is enterochelin which is a strong chelator of ferric iron found in many bacteria. However, the host expresses LCN2 secreted by neutrophil granules to bind siderophores like enterochelin to disrupt bacterial iron acquisition [163]. However, *Salmonella* also produces a unique siderophore called salmochelin, a glycosylated version of enterochelin, which is unable to be bound by LCN2 thereby evading the host's defense mechanism [164]. *Salmonella* acquires iron through ferric and ferrous iron, as well as from heme and TFR [164, 165]. Following acquisition of iron, the transport across the membrane requires either TonB dependent uptake systems to transport siderophores or ferrous iron transporter FeoAB [166, 167]. The gene TonB is part of a transport complex with ExbB and ExbD that gives energy to the outer membrane so that it can transport iron bound siderophores across the membrane [168]. TonB is required for cellular uptake of a variety of substrates besides Fe(iii) siderophores including heme proteins and siderophilins such as TFR and LTF.

MOUSE MODELS

The mouse model has been extensively used in the study of *Salmonella* infection for the following reasons. First, there already exist inbred strains of mice that are naturally susceptible to *Salmonella* infection including B6 (*Slc11a1*), and C3H/HeJ (*Tlr4*) as well as naturally resistant to infection including 129S1 [132, 169, 170]. Second, with the availability of the whole mouse and human genome sequences, we have seen that there exist a number of genome similarities between mouse and humans. Analysis of the two genomes shows that 80% of human genes have a 1:1 ortholog in the mouse genome [171]. Third, numerous technologies exist that facilitate genetic manipulation in order to generate models to mimic human disease which would not be ethical in humans.

MODELS OF *SALMONELLA* INFECTION

There are a number of mouse models to better understand the mechanisms underlying typhoid fever, gastroenteritis and chronic carriage.

TYPHOID:

Other than humans, chimpanzees are the only known natural host for *Salmonella* Typhi. There are a number of ethical and cost related issues with using chimps as a model for typhoid fever. *Salmonella* Typhimurium and Enteritidis are natural pathogens of mice and are frequently isolated from rodent reservoirs [172]. *Salmonella* Typhimurium was first discovered by Loeffler in 1892 as the causative agent of disease in mice. Orskov and Moltke in 1929 first described the course of *Salmonella* Typhimurium infection in mice and its resemblance to typhoid fever in humans.

Infection with typhoidal agent *Salmonella* Typhi does not typically cause disease in the mouse so most studies will model typhoid fever by infecting inbred mice strains with the zoonotic *Salmonella* Typhimurium. Inbred strains of mice show varying degrees of susceptibility. Three strains of inbred mice are of particular interest to us: the 129 family of mice are highly resistant

to infection, B6 mice are highly susceptible and the DBA/2 strain displays intermediate resistance when infected with 1000 CFUs of *Salmonella* Typhimurium *i.v.* [173, 174].

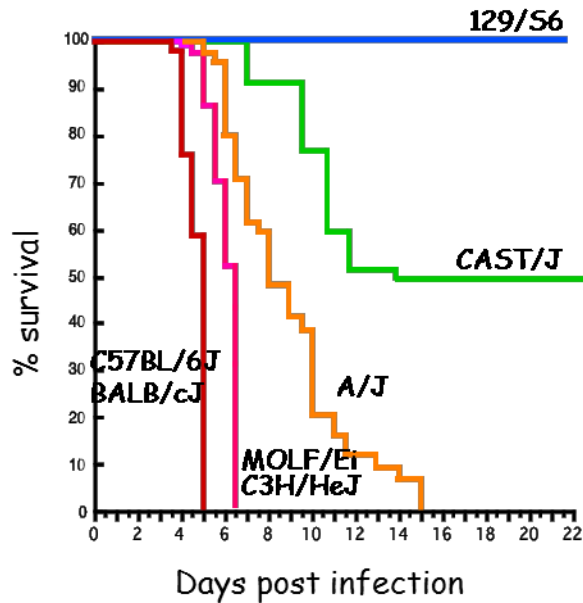


FIGURE 5: SURVIVAL CURVE OF LABORATORY STRAINS OF MICE

Taken from Roy & Malo Genes & Immunity 2002. Infection with 1,000 CFUs of *Salmonella* Typhimurium results in varying degrees of susceptibility in the seven strains of laboratory strains of mice tested. B6 and BALB/C strains of mice are highly susceptible while the 129S6 strain is highly resistant.

Recent studies have developed mouse models which uses *Salmonella* Typhi as the infectious agent. There are a number of humanized mouse models that can be infected with *Salmonella* Typhi: *Rag2^{-/-}Il2rg^{-/-}* mice engrafted with either human fetal liver cells or CD34+ human blood stem cells, or *Scid/Il12r^{null}* mice grafted with human hematopoietic stem cells [175, 176].

INTESTINAL:

Under normal circumstances, oral infection with *Salmonella* Typhimurium does not result in intestinal pathology in mice due to colonization resistance, in which the microbe-host interactions maintain intestinal immune homeostasis. However, pretreatment with

streptomycin greatly enhances the susceptibility of mice to oral *Salmonella* infection and allows greater intestinal colonization [177-179]. With this model, *Salmonella* can efficiently colonize the large intestine and trigger severe inflammation of the cecum and colon which closely resembles the intestinal inflammation as observed in human enterocolitis [180]. Inflammation in the streptomycin model is marked by the infiltration of PMNs, epithelial edema, loss of goblet cells and crypt abscesses [179]. Ultimately susceptible mice infected with *Salmonella* Typhimurium will die of systemic disease as bacteria disseminate to secondary lymphoid organs [179]. Mice infected with the less virulent *Salmonella* Enteritidis allows for the study of B6 mice past day 5 [181]. These studies have identified the importance of host genes such as *Slc11a1*, *Tlr5* and *Usp18* (ubiquitin specific peptidase 18), as well as bacterial effectors SPI1 and SPI2 [179, 181-184].

CHRONIC CARRIAGE:

Previous studies have shown that wild type mice infected with attenuated mutant *Salmonella* can carry bacteria for as late as two months after infection [185]. Although these studies have provided a useful basic understanding of chronic carriage, it does not use wild type bacteria. There are three mouse models currently in use to study chronic carriage of *Salmonella*. The first uses resistant 129 mice infected *per os* with 10^8 CFUs of *Salmonella* Typhimurium. Early during infection 129 mice will show signs of acute infection, however as time progresses they become asymptomatic. It has been shown that 129 mice sequester bacteria in macrophages of the RES organs for up to a year post infection [22]. The second method feeds mice a lithogenic diet consisting of 1% cholesterol and 0.5% cholic acid to induce formation of gallstones. Infection with *Salmonella* Typhimurium following the development of gallstones results in a 3 log increase in fecal shedding as well as an increase in colonization of gallbladder tissue and bile [23]. Studies using this model has shown that the formation of biofilms on gallstones mediate the carrier state [23, 186]. The third method, developed in our lab, uses *Salmonella* Enteritidis injected *i.v.* in B6 and 129S6 mice. In this model, we find that carrying a non-functional SLC11A1, as in B6 mice, is beneficial for clearance of bacteria whereas 129S6, carrying a functional SLC11A1, does not clear bacteria [187].

GENETIC APPROACHES

There are two basic approaches to identify gene function. The reverse genetics approach (also known as a gene-driven approach) starts with a known gene and determines whether aberrant expression of the gene causes a phenotype. These include using KO mice, transgenic mice, and gene silencing. There is a large KO initiative called the International Knockout Mouse Consortium (IKMC) encompassing 4 major consortiums (KOMP, EuCOMM, NorCOMM, TIGM) around the world generating KOs of every known gene [188-190]. A limitation to the gene-driven approach is that prior knowledge of the gene is necessary. As of 2014, less than 50% of the known mouse genes have some sort of functional annotation [191-193]. In addition, genes causing embryonic lethality would need to be studied using a different approach. In contrast, forward genetics is an approach to identify the genes responsible for a phenotype. There are a number of mouse models available for this approach including inbred and wild-derived strains of mice, congenic mice, and chemically induced mutants.

CONGENICS/COLLABORATIVE CROSS

With a few exceptions such as the mutation in *Slc11a1* in B6 mice or the mutation in *Tlr4* in C3H/HeJ mice, susceptibility to infection is inherited as a complex trait. There are a number of tools available to study this complex inheritance including the generation of congenic mice, recombinant congenic strains (RCS) and the Collaborative Cross (CC) mice. Traditionally when two inbred strains of mice showed contrasting phenotypes, these strains would be crossed to create congenic mice. The resulting mixed genomic background can be dissected to identify quantitative trait loci (QTL) responsible for your phenotype of interest. These loci can then be refined to genes and sequence level differences. However large sample sizes and extensive genotyping per sample is required to detect and identify a QTL [194]. RCS mice are generated by crossing two phenotypically different strains of mice and sequentially backcrossing to one parental strain twice and then inbred. The genome of a RCS contains approximately 87.5% of the background strain and 12.5% of the donor strain. The RCS using A/J and B6 strains have been successfully used to identify a number of loci involved in susceptibility

to *Salmonella* infection on chromosomes 7, 14 and 15 and has also identified a number of candidate genes: *Pklr* and *Cd40* [156, 195, 196].

In an effort to maximally represent the genetic diversity present in inbred strains of mice, a global initiative began to generate congenic strains made by crossing 8 founder strains (5 inbred and 3 wild-derived strains) of mice to generate a large panel of recombinant inbred strains collectively called the CC [197]. Due to the extensive genotyping using the diversity array, using the CC makes it possible to identify genetic loci to a high degree of resolution compared to other techniques like congenic mice [197, 198]. The CC strains have been successfully used to model the spectrum of symptoms found in Ebola infection as well as identified a number of QTLs for affecting susceptibility to *Klebsiella*, *Aspergillus* and influenza A infection [199-202].

CHEMICAL MUTAGENESIS

The use of X-rays as a mutagen was first reported in 1927 by Hermann Muller when he discovered that X-rays can cause mutations in *Drosophila* that led to phenotypic changes [203]. Before the discovery of *N*-ethyl-*N*-nitrosourea (ENU), procarbazine was the only chemical compound capable of mutagenizing mouse spermatogonia. However, this chemical compound was less potent than X-ray, producing approximately one third as many mutations [204]. As early as 1979, it was noted that a single dose of ENU was a potent mutagen, inducing 12 fold more mutations than the highest effective dose of X-ray, 36 fold more mutations than the most effective dose of procarbazine and over 200 fold more mutations than would arise spontaneously [205].

ENU is an alkylating agent which creates DNA adducts by transferring its ethyl group to nucleophilic nitrogen and oxygen in DNA bases thereby causing mispairing during DNA replication. ENU mainly induces point mutations with the majority resulting in A to T transversions (44%) or A to G transitions (38%) [206]. The resulting effect on amino acids is as follows: missense (64%), splicing (26%), and nonsense mutations (10%) [207]. ENU also has a bias towards genes with a high GC content or sites flanked by G/Cs [208]. It is also well known

that different inbred strains respond differently to ENU doses and there is an increase in the number of mutations generated with a fractionated dose [209].

There are two types of screens that can be used to identify genes that differ in the breeding scheme used: region specific and genome wide.

Region specific ENU screen:

A region specific screen is appropriate when the aim is to identify the functional content of a specific region of the genome or to generate an allelic series of a specific gene. A region specific screen can be generated through non-complementation, deletion or balancer screens [210]. In a non-complementation screen, the mutagenized generation 0 (G0) male is crossed to a female carrying a homozygous mutation in a gene of interest. The resulting G1 offspring would be screened for a phenotype that recapitulates that of the maternal phenotype due to non-complementation.

In a deletion screen, the mutagenized G0 male is crossed to a female carrying a deletion in a known part of the genome. This type of screen allows for identification of loss of function alleles in the G1 offspring, greatly accelerating gene identification. Limitations to the deletion screen include the viability of mutants with haploinsufficiency as well as the availability of mice with deletions in the region of interest.

The final type of region specific screen is the balancer screen. In this screen the mutagenized G0 male is crossed to a female carrying a balancer chromosome achieved by inversion of the chromosome. The aim of the balancer is to suppress recombination between the balancer and its homolog. Balancer screens have two added features: a marker that allows for the visual identification of mice carrying the balancer chromosome and a mutation that either prevents homozygous mice for the balancer to be viable or to differentiate the heterozygous mice [210].

Genome wide screen:

A genome wide screen is appropriate to study diseases in which multiple genetic and biochemical pathways are involved. The genome wide screen can be generated through a dominant screen, a recessive screen or a modifier screen [210].

In a dominant screen, the aim is to identify genes that cause a phenotype that are inherited in a dominant fashion. After the generation of G0 males, they are bred to a wild type female to generate G1 mice that are screened for the desired phenotype of interest. A limitation to this

method of screening is the fact that only about 2% genes cause a phenotype in a dominantly inherited fashion [211]. In a recessive screen, the G1 males would be bred to a wild type female to generate G2 offspring. These G2s can be intercrossed or backcrossed to their G1 father to generate G3s. The resulting G3 offspring is then phenotyped to identify deviant pedigrees. In a modifier screen, the aim is to identify genes that suppress or enhance a phenotype of interest. However, this type of screen requires prior knowledge of at least one gene necessary for the phenotype; nevertheless this type of screen can be useful in mimicking some human diseases.

Global ENU initiatives:

There are a number of ENU initiatives around the world investigating genetic determinants affecting many different phenotypes. These initiatives encompass both region specific and genome wide screens. In addition to the genome wide recessive screen at McGill to identify genetic determinants affecting the outcome to Herpes Simplex Virus, cerebral malaria and acute *Salmonella* infection, there are primary screens with *in vivo* challenge with Murine cytomegalovirus (MCMV) and lymphocytic choriomeningitis (LCMV). In addition, secondary screens looking at hematopoietic cell development, TLR signaling, and *ex vivo* challenges with PAMPs or pathogens such as *Listeria* or influenza have also identified genes and pathways involved in outcome to infection [212-217].

GENE IDENTIFICATION

One bottleneck in the forward genetics approach, either through the use of ENU mutagenesis or the use of congenic mice, is in mapping and gene identification. Conventional strategies require meiotic mapping using SNPs spread across the genome. Further fine mapping requires additional mice and markers within the interval of interest. Finally, identification of causative mutations is done by Sanger sequencing of candidate genes within the mapped region. This approach is time consuming; requiring large sample sizes and extensive genotyping. Next generation sequencing of the whole genome or whole exome is an approach that has the potential to accelerate gene identification. The whole exome sequencing approach still

requires mapping a locus but does not require additional fine mapping. A limitation to whole exome sequencing is that if the causative mutation lies within non-coding regulatory regions or unannotated regions not within the capture library, the causative mutation is difficult to identify. However most causative mutations identified thus far by ENU has been within exonic regions or splice acceptor/donor sites, thus making whole exome sequencing a cheaper alternative to whole genome sequencing [218, 219].

Whole genome sequencing can be used to identify ENU induced mutations without using conventional mapping strategies by looking at SNPs that are identical by descent which could decrease the time from identification of a deviant phenotype to the identification of the causative mutation [220]. As the cost of whole genome sequencing decreases, this approach can be especially useful in identifying variants found within intronic regions or regions that are poorly annotated.

THESIS RATIONALE, HYPOTHESIS & OBJECTIVES:

RATIONALE

Salmonella infection is an important global health problem and the outcome of infection depends on the complex interaction between the host, the pathogen and the environment. We know there are some genetic predispositions to susceptibility to *Salmonella* infection as seen in patients with Sickle cell anemia, β -thalassemia, and MSMD. Inbred strains of mice have also provided information on genes that confer susceptibility to *Salmonella* infection such as *Nramp1*, *Pklr* and *Tlr4*. However, there is a limited amount of natural variation found between inbred strains of mice and a low rate of spontaneous mutations. Chemical mutagenesis is one method that allows for the elucidation of novel variations that affect the outcome to infection. Previously in our laboratory, a pilot ENU mutagenesis screen in 129S1 mice was undertaken in which over 2200 G3 animals were screened [221]. As a result of this pilot project, three deviant pedigrees *Ity9*, *Ity10*, and *Ity11* were identified. The *Salmonella* susceptibility phenotype in *Ity9* and *Ity10* pedigrees were shown to be inheritable in a recessive fashion while the *Ity11*

pedigree presented a dominant mode of inheritance. The gene underlying the *Ity9* locus was identified as *Usp18*. USP18, a deubiquitinating protease, is involved in the negative regulation of type I IFN signaling by interacting with the IFN alpha receptor 2 (IFNAR2) and limiting JAK-STAT1 activation. This discovery emphasizes the importance of type I IFN signaling in the host response to bacterial infection [222]. The pilot project proves the feasibility of using random chemical mutagenesis to identify novel genes involved in *Salmonella* susceptibility.

HYPOTHESIS

We hypothesize that there are an abundance of genes that have not previously been implicated in susceptibility to *Salmonella* disease. We believe the use of genome-wide chemical mutagenesis will help identify novel *Salmonella* susceptibility genes and further our understanding of the complex genetic etiology and the mechanisms of immunity underlying susceptibility to bacterial infection.

OBJECTIVES

Based on the hypothesis outlined above, there were 3 main objectives to my thesis.

My first aim was to initiate a large scale ENU mutagenesis recessive screen to identify deviant pedigrees with increased susceptibility to *Salmonella* infection. Following the identification of deviant pedigrees, the causative mutations are identified using fine mapping and whole exome sequencing.

My second aim was to validate and characterize the function of *Ank1*, underlying the susceptibility of the *Ity16* pedigree. Mice from the *Ity16* pedigree showed increased susceptibility to *Salmonella* infection starting at day 3 post-infection.

My third aim was to validate and characterize the function of *Fam49b*, underlying the susceptibility of the *Ity15* pedigree. Mice from the *Ity15* pedigree exhibited increased susceptibility to *Salmonella* infection starting at day 6 post-infection.

BRIDGING STATEMENT CHAPTER 1 TO CHAPTER 2

Genetic susceptibility to typhoid fever has been studied mostly in mouse models of infection and has provided a deeper understanding of the complex interplay between the host and the pathogen. Several strains of mice show varying degrees of susceptibility to acute and chronic *Salmonella* Typhimurium infection. Classical inbred strains and other reference panels of inbred mice (RIS, RCS, consomic, etc) are powerful tools to dissect the genetic architecture of complex biological traits, such as resistance/susceptibility to infection with *Salmonella* however these panels present limited genetic diversity. To counteract this bottleneck, we have used *N*-ethyl-*N*-nitrosourea (ENU)-induced mutagenesis to identify novel genes involved in host resistance to *Salmonella* infection. A pilot study, where *Usp18*^{ty9} a negative regulator of type 1 interferon was identified, showed the feasibility of such approach. We then embarked on a major initiative to screen 300 G1 pedigrees over a period of 5 years. I am presenting in Chapter 2, the results of the initial years of this large recessive ENU-screen initiative.

CHAPTER 2: MOUSE ENU MUTAGENESIS SCREEN FOR THE DISCOVERY OF NOVEL *SALMONELLA* SUSCEPTIBILITY GENES

Kyoko E. Yuki^{1,2}, Megan M. Eva^{1,2}, Shauna M. Dauphinee², Lou Beaulieu-Laroche², Robert Eveleigh⁵, Guillaume Bourque^{1,5}, Jeremy A. Schwartzentruber⁵, Jacek Majewski^{1,5}, Silvia M. Vidal^{1,2,6}, Danielle Malo^{1,2,6}

¹Department of Human Genetics, McGill University, Montreal, Quebec, Canada; ²Complex Traits Group, McGill University, Montreal, Quebec, Canada; ⁵McGill University and Genome Quebec Innovation Center, Montreal, Quebec, Canada; ⁶Department of Medicine, McGill University, Montreal, Quebec, Canada

ABSTRACT:

Salmonella enterica infection in humans represents a significant economic and public health challenge and is associated with high morbidity and mortality rates in both industrialized and non-industrialized nations. Identification of genes involved in susceptibility to *Salmonella* infection is vital for furthering our understanding of the mechanisms of disease. We report here that the use of a forward genetics approach by *N*-ethyl-*N*-nitrosourea (ENU) can efficiently recover recessive mutations and identify genes involved in susceptibility to infection. We have screened over 1200 G3 progeny and have identified four pedigrees with defects in genes and pathways important in the pathogenesis of *Salmonella* disease.

INTRODUCTION:

Despite advances in prevention, diagnosis and treatment, infectious diseases remain a significant cause of morbidity and mortality worldwide [223]. The global threat from infectious disease increases with the emergence of new pathogens such as those causing SARS (severe acute respiratory syndrome) or MERS (Middle East Respiratory Syndrome) and the increasing incidence of drug resistance.

Salmonella related diseases in humans are significant economic and public health problems. Infection with *Salmonella* can result in four diseases: enteric fever, invasive non-typhoidal *Salmonella*, gastroenteritis and chronic disease. In industrialized nations, *Salmonella* infection is a significant cause of foodborne illness. In non-industrialized nations, particularly in Africa and Southeast Asia, *Salmonella* infection is a substantial source of mortality due to enteric fever and invasive non-typhoidal *Salmonella*. The diverse outcome to *Salmonella* infection is a result of the complex interplay between host genetics, bacterial pathogenicity and the environment (ie: nutrition, hygiene, and/or climate).

Of the approximately 25,000 genes within the mammalian genome about half of the genes have unknown or poorly characterized function. Following the completion of the human genome project, significant progress has been made through projects such as the International HapMap Project, ENCODE, and GENCODE [224-226] to better understand the function of the sequences found within our genome. However the understanding of the function of genes responsible for pathogenesis of infectious diseases in humans has been limited due to confounding factors like the extent of pathogen exposure within the population as well as genetic variation from the pathogen itself [14].

Mouse models have been used extensively to investigate the complex genetics underlying infectious diseases due to the availability of a number of resources for easy genetic manipulation. These include studying the innate natural variation of the host response to infection in inbred laboratory strains, recombinant congenic strains, recombinant inbred strains of the Collaborative Cross [169, 170, 195, 196, 199, 202].

N-ethyl-*N*-nitrosourea (ENU) is a potent chemical mutagen that induces random germline point mutations within spermatogonia. ENU mutations can be used to generate various allelic series

such as gain-of-function, loss-of-function, hypermorph, hypomorph, dominant negative (antimorph) or neomorph mutations which can mimic variants found in human disease [206]. One major advantage of ENU mutagenesis is to provide an invaluable resource of new animal models for the study of host resistance to infection that will result in a deeper understanding of the complex interplay between the host and the pathogen.

An ENU mutagenesis screen was established at McGill University with the aim of identifying genes involved in the host response to malaria, herpes viruses and *Salmonella* [227]. A pilot study using the mouse model of *Salmonella* infection *in vivo* identified the first ENU-induced mutant named *Ity9* (*Immunity to Typhimurium 9*) that carries a mutation in *Usp18* resulting in hyperactivation of type I IFN signalling [221]. Subsequent screens identified additional loci among them *Ity16* that carries a mutation in *Ank1*, a red blood cell structural membrane protein, which demonstrated the importance of iron metabolism in resistance to infection ([228] and Chapter 3 of the current thesis). In these particular screens, highly resistant 129S1 mice were mutagenized and were outcrossed to a wild type female of a different background for mapping purposes (either C57BL/6 or DBA/2). Even though this breeding strategy allowed early mapping of heritable mutations it introduces some modifier gene effects and affects the robustness of the phenotype [229].

We then designed and implemented an ENU mutagenesis screen using highly resistant 129S1 and genetically related 129X1 mice to identify new genes involved in regulating outcome to acute *Salmonella* infection. We report here the results using this new ENU mutagenesis breeding strategy and the identification, mapping and positional cloning of four pedigrees (*Ity14*, *Ity15*, *Ity19* and *Ity21*) that show increased susceptibility to *Salmonella* infection.

MATERIALS & METHODS:

Mice and ENU mutagenesis:

All animal experiments were performed as per the conditions specified by the Canadian Council on Animal Care. Animal use protocols were approved by the McGill University Facility Animal Care Committee. ENU mutations were induced by single intraperitoneal injection of 150 mg/kg ENU (Sigma) into 129S1/SvImJ male G0 mice aged 8-12 weeks. Infertility in G0 mice was confirmed by pairing with a wild type CD1 female 3 weeks after ENU treatment. Fertility was regained by 9 weeks post treatment. At this point, G0 males were crossed to wild type females, either 129X1 or 129S1 (Jackson, Bar Harbor ME). A three-generation breeding scheme was used to study recessive inheritance.

***Salmonella* infection and survival monitoring of G3 animals:**

G3 animals were infected at 7-9 weeks of age with 10,000 CFUs of *Salmonella* Typhimurium strain Keller by intravenous injection. G3 mice were monitored for survival using clinical endpoints defined by a body condition score less than 2, body weight decrease >15%, piloerection, decreased mobility, or hunched posture.

Identification of deviant pedigrees:

A minimum of 5 mice per litter per pedigree was screened for susceptibility to infection. Pedigrees in which one or more mice succumbed to infection between days 3 and 10 post infection were flagged for further investigation. Deviant pedigrees were defined as those in which at least 25% of the mice succumbed to infection in 3 or more litters.

DNA preparation and genetic mapping:

DNA was extracted from a tail biopsy by proteinase K digestion and phenol-chloroform extraction. Loci responsible for susceptibility were mapped using the medium density SNP panel in which 708 SNPs were polymorphic between the parental 129S1 and DBA/2 (Medium Density SNP Panel, Illumina GoldenGate, The Centre for Phenogenomics, U. of Toronto, ON, Canada) for the *Ity14* and *Ity15* pedigrees. To identify a genetic locus, samples from at least six

susceptible and six resistant offspring were used. Mapping was validated by genotyping additional samples by SNP sequencing (McGill University and Genome Quebec).

Exome Sequencing and gene identification:

Identification of ENU induced mutations was done by exome sequencing. High quality DNA was prepared by phenol/chloroform extraction from two or three susceptible animals per pedigree. Exome sequencing was performed using the SureSelect Mouse All Exon kit (Agilent Technologies, USA) at Centre National de Génotypage (Évry, France), Genome Quebec (Montreal, Canada) or Australian Phenomics Facility (Acton, Australia). Analysis was done as previously published [230]. Briefly, raw sequencing data were aligned to the mm9 reference genome with BWA [231]. This was followed by a variant discovery step in which single nucleotide variants and short insertions and deletions were called using tools such as Genome Analysis Toolkit or Samtools [232-234]. Variants were annotated to identify whether they affected the protein coding sequence and excluded if present in the mouse SNP database or in a database of ENU induced mutations to reduce the number of candidate mutations. Unless otherwise stated, variants identified in all samples sequenced for a given pedigree were flagged for further confirmation by Sanger sequencing in all animals in the same pedigree.

RESULTS:

Mutagenesis screen design and identification of deviant pedigrees:

Two breeding schemes were used to identify deviant pedigrees. In the first scheme, G0 mutagenized males were crossed to wild type 129X1 females. The resulting G1 males were then crossed again to 129X1 females to generate G2 females which were subsequently backcrossed to the G1 male. The resulting G3 progeny were screened with 10,000 colony forming units (CFUs) (Fig 1a). This breeding scheme was used to screen 643 G3 animals from 39 G1 males and to identify the *Ity14* and *Ity15* deviant pedigrees. The *Ity14* pedigree displayed early susceptibility with 30% mortality by day 6 post infection (Fig 2a) which is consistent with a recessive mode of inheritance. The *Ity15* pedigree expressed later susceptibility with 40% mortality by day 10 post infection which may suggest a co-dominant mode of inheritance (Fig2b).

In the second breeding scheme, we used a pure 129S1 background such that the G1 male and G2 females were generated by crossing with a 129S1 female (Fig 1b). We screened 580 G3 animals from 41 G1 males and identified the *Ity19* and *Ity21* deviant pedigrees. The *Ity19* pedigree has 25% mortality by day 10 post infection (Fig 2c) consistent with a recessive trait and the *Ity21* pedigree presented 60% mortality by day 12 post infection suggestive of a co-dominant mode of inheritance (Fig 2d).

Overall, we have screened 1223 G3 animals from 80 G1 males and 133 G2 females for susceptibility to *Salmonella* infection. A total of 4 deviant pedigrees were identified: *Ity14*, *Ity15*, *Ity19* and *Ity21* (Table 1).

Mapping and gene identification:

In the first breeding scheme, 129S1 G0 males were initially crossed with the genetically related wild-type 129X1 females for mapping purposes. There were nearly 20,000 polymorphic SNPs identified between 129S1 and 129X1 using the Jackson Diversity Array spread across the genome (Fig 3a). However, some chromosomes were poorly covered and >20 gaps exceeding 25 Mb in length were evident which unfortunately prevented the use of this panel for mapping the *Ity14* and *Ity15* mutations.

In order to map the mutations underlying these two pedigrees, the G1 male and G2 female were outcrossed to DBA/2 mice to generate F1 progeny. F1 progeny were randomly intercrossed to generate F2 mice that were phenotyped for survival. F2 progeny from F1 breeders producing susceptible animals were propagated and used for mapping with a medium density SNP panel comprising 708 polymorphic markers between the parental 129 and DBA/2 strains (Fig 3b). Using this approach *Ity14* was mapped to chromosome 1 between position 47.85 and 54.48 Mb [230] and *Ity15* to chromosome 15 between position 63.7 and 68.1 Mb. In the F2 cross used for mapping, *Ity14* and *Ity15* are both inherited as recessive traits ([230] and Chapter 4 of the current thesis).

Whole-exome sequencing of coding exons and flanking splice junctions in two susceptible *Ity14* mice identified 15 novel ENU-induced mutations. The mutation within *Stat4* (signal transducer and activator of transcription 4) was the only one that was located within the mapped interval and segregated with the survival phenotype. The mutation consisted of a guanosine to adenosine substitution within the splice donor site of exon 15, at position +5 of intron 15 (c.1335+5G to A) [230]. STAT4 is a crucial mediator of inflammation following activation by IL-12 resulting in the transcriptional regulation of the immune response such as the production of IFN γ , Th1 differentiation, and Ig isotype switching [235]. The mutation in *Stat4* results in impaired IFN γ production by NK and NKT cells favoring increased bacterial replication in spleen and liver [230].

For the *Ity15* pedigree, whole exome sequencing identified 4 homozygous mutations with two located within the mapped interval. A c.728+2A to T transversion within the splice donor site of intron 9-10 in the gene *Fam49b* (family with sequence homology 49 member b) was identified and a non-synonymous mutation (p.F56V) within the gene *Gsdmc4* (gasdermin c4). FAM49B and GSDMC4 currently have no known function. Expression of *Fam49b* is ubiquitous and that of *Gsdmc4* is limited to the gastrointestinal tract and kidneys. Gene complementation experiments showed that *Fam49b* is the causative gene. At the protein level, the ENU-induced mutation in *Fam49b* results in the loss of protein expression. Detailed phenotypic characterization of *Ity15* is reported in Chapter 4.

Because of prior success in identifying causative ENU-induced mutations without the need for meiotic mapping [236], we initiated pedigrees using only 129S1 mice. For the *Ity19* pedigree, exome sequencing was done on three affected mice. The coverage across the coding portion of the genome at >5 times depth was 52-59%. We detected between 22 and 25 variants per mouse (1-3 homozygous, 14-21 heterozygous and 1-5 other) (Fig 4a and Table 3). 15 SNPs were present in all samples but none in a homozygous state in all three samples. The best hit was a variant in the gene *Cnp*. The *Cnp* variant was homozygous in two samples and heterozygous in one. CNP is an enzyme that hydrolyzes 2',3'-cAMP to 2'-AMP and has recently been shown to be induced by type I IFNs [237-239].

For the *Ity21* pedigree, exome sequencing was also performed in three susceptible mice. In this batch, the coverage was better with >85% at >5 times depth. We identified between 49 and 54 variants (10-17 homozygous, 21-34 heterozygous and 9-14 other) per mouse (Fig 4b and Table 3). 11 SNPs were present in all samples with 2 in the same gene (*Slc22a16* on chromosome 10) (Fig 4b). We have identified a number of potential candidate genes that need to be validated by Sanger sequencing and correlated with the phenotype in the pedigree. The number of homozygous mutations is small enough to allow validation of each SNP in siblings. Prioritization of candidate mutations will be done using the PolyPhen2 score applied to novel mutations (mutations with a score greater than 0.95 will be tested first).

Further characterization of these mutants will include primary phenotyping to investigate bacterial load, serum cytokines and histopathological analysis. The candidate genes identified for the *Ity19* and *Ity21* deviant pedigrees will need to be further validated by methods such as complementation assay using knockout mice, shRNA knockdown *in vitro*, or CRISPR/Cas9 technology.

DISCUSSION:

The recessive ENU screen for susceptibility to *Salmonella* infection was initiated in 2005 as a pilot study and then pursued between 2008 and 2013. Overall, 8415 G3 progeny issued from 491 G1 pedigrees were screened. My involvement in the project started in 2008 with the screening of 1223 G3 animals from 80 G1 males and 133 G2 females and the identification of 4 deviant pedigrees: *Ity14*, *Ity15*, *Ity19* and *Ity21*. The breeding schemes using the resistant 129S1 or 129X1 as the wild type female proved to be very efficient; producing the equivalent of 3 deviant pedigrees per 800 G3 animals screened (Fig 5a). This is more efficient than the previous ENU screen for *Salmonella* susceptibility that identified approximately one deviant pedigree for every 800 G3 animals screened [221]. The ability to identify more than the expected number of deviant pedigrees using highly resistant wild type females may be attributed to a number of factors: first the susceptibility range was relaxed to include animals that succumbed at any point before day 14 post infection; and second our ability to identify susceptibility resulting from the ENU induced mutation was not confounded by genetic heterogeneity conferred by outcrossing G1 and G2 animals to another mouse strain presenting some degree of susceptibility to infection.

Different breeding schemes were tested to improve the efficacy and the speed at which ENU-induced causal mutations were identified. Identification of mutations was initially based on meiotic mapping and sequencing of all candidate genes within the linked interval [222] which was efficient but time-consuming. It took about 2 years between the first description of the deviant *Ity9* pedigree and the identification and validation of the causative mutation in *Usp18*. The advent of mouse exome sequencing in combination with meiotic mapping information was efficient but did not significantly improve the speed at which the mutations were identified in *Ity14* and *Ity15*, most likely because of the impossibility in mapping the disease phenotype in the 129S1 x 129X1 cross despite the significant sequence divergence between the two strains. Although there are nearly 20,000 SNPs between 129S1 and 129X1, these SNPs tend to be clustered within the genome and were not informative for mapping purposes. This was well illustrated by the fact that *Ity14* and *Ity15* could not be mapped using this panel since both loci are located within regions where there are no informative SNPs. This necessitated outcrossing

the parental G1 male and G2 female to DBA/2 mice for mapping which added two more rounds of breeding.

The sole use of exome capture and sequencing to identify causative mutations has the potential to consistently shorten the time between description of the pedigree and identification of the causative mutation. However we did not definitively identify the causative mutations in *Ity19* and *Ity21*. There are a number of factors that may explain these results. First, the exome only covers approximately 1% of the genome. It is possible that the underlying mutation may be found within non-coding regulatory regions or within regions of the genome that is not targeted by the exome capture technique. It is possible that in the *Ity19* and *Ity21* pedigrees, the mutations may lie outside the chromosomal regions enriched by exome capture. Although the Agilent technology has been proven to be efficient to capture coding sequences, about 15% of exonic regions were reported to be absent [236]. We noticed that the coverage in *Ity21* was as expected at around 85%. For *Ity19*, it was only about 50-60%. In addition, for co-dominant alleles, it seems that in some specific sequence context, the mutant genotype is out-competed by the reference genotype [236]. Second, the exome capture and the reference genome used to identify variants is based on C57BL/6J sequence and it is possible that natural sequence variants present on the 129S1 background interferes with proper capture or that they are called as ENU induced SNPs. Third, variants already present in a large database of ENU induced mutations were removed during filtering which may have resulted in the causative variant to be removed. In the *Ity19* and *Ity21* pedigrees, biological and technical replications of exome analyses may be necessary to detect the causal mutations. One way to get around this would be to use whole genome sequencing to be able to identify regions that are inherited by descent. This method has been successfully used in a homogenous C57BL/6 background to identify genes involved in B cell development [220].

Despite these drawbacks, the genes and mutations we have identified add to a growing compendium of mutations identified using ENU mutagenesis involved in regulating the outcome to infectious diseases. Overall, we have confirmed 9 deviant pedigrees, and the causative genes have been identified for 6 of them (*Usp18*^{*Ity9*}, *Stat4*^{*Ity4*}, *Fam49b*^{*Ity15*}, *Ank1*^{*Ity16*}, *Ncoa7*^{*Ity17*}, *Adam9*^{*Ity18*}) ([222, 228, 230], chapter 3, chapter 4 and unpublished data). The

involvement of three of these genes in different aspects of the pathogenesis of *Salmonella* infection has been elucidated: USP18 is a negative regulator of Type I IFN signaling [181, 222], *Stat4* mutants present an early innate defect in NK cell-derived IFN γ -mediated immunity [230] and ANK1 plays a critical role in iron homeostasis regulated by hepcidin ([228] and chapter 3). The study of these genes has furthered our understanding of host susceptibility to *Salmonella* infection. In addition, the genes identified in the screen for *Salmonella* susceptibility have been shown to be important in other infectious diseases both in animal models and human populations. Lack of USP18 has been shown to be associated with protection against a number of viral infections including hepatitis C, vaccinia virus, influenza, lymphocytic choriomeningitis virus and vesicular stomatitis virus [240-243]. On the other hand, mutations in *Usp18* leading to interferonopathy was shown to cause susceptibility to *Mycobacterium tuberculosis* [240, 244]. ANK1 has been shown to be important in resistance to blood stage malaria [245-247] and variants within *STAT4* were associated with susceptibility to pulmonary tuberculosis as well as invasive non-typhoidal *Salmonella* in humans. [239, 248-250].

Our ENU *Salmonella* susceptibility screen was part of a larger ENU initiative at McGill to identify genes involved in outcome to infection, in particular resistance to malaria and susceptibility to Herpes simplex virus (HSV) and *Salmonella*. Mutations in *Jak3*, *Themis* and *Ccdc88b* were identified in an *in vivo* screen for resistance to cerebral malaria and demonstrated the importance of proper T cell function in the response to this infection model [251-253]. A mutation in *Ptprc* has also shown the importance of T cell function in susceptibility to *in vivo* HSV infection [254]. An *in vivo* screen for genetic determinants of outcome to murine cytomegalovirus (MCMV) infection was initiated by Beutler and colleagues. Mutations in *Stat1*, *Flt3*, *Unc13d* and *Slf2* were identified highlighting the importance of DC production of type I IFN, defects in DCs or natural killer (NK) cells and maintaining quiescence of immune cells (reviewed in [255]).

Secondary screens looking at individual pathways also have the potential to identify genes that are important in regulating the outcome to infection. An *in vitro* screen to identify genes within the TLR signaling pathway has identified *Tlr9*, *Trif*, *Ikbkg*, *Unc93b1*, *Gimap5*, *Eif2ak4*, *Ptpn6*, *Cd36*, and *Map3k8*. These were later shown to be important in susceptibility to influenza,

MCMV, *Staphylococcus aureus* and group B streptococcus [212, 213, 256-260]. A screen to identify genes involved in hematopoietic cell development identified a mutation in *Gfi1*, which was shown to be important for neutrophil development [261]. The mutation in *Gfi1* was then shown to confer resistance to *Brucella abortus* as well as susceptibility to oral infection with *Salmonella* Typhimurium SfiA mutant [217, 262].

Overall, these results demonstrate the usefulness of ENU mutagenesis to identify genes and pathways controlling *Salmonella* susceptibility.

ACKNOWLEDGEMENTS:

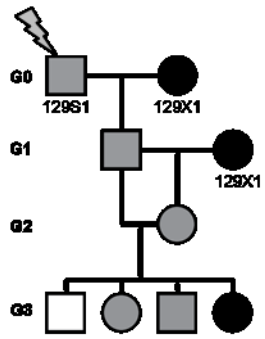
The following work was part of a larger collaborative effort with the CIHR Team in Mutagenesis and Infectious Diseases. We would like to thank Melissa Herman, and Line Larivière, as well as the many animal technicians who helped with infections and maintenance of the animal colony: Nadia Prud'homme, Patricia D'Arcy, Geneviève Perreault, Vanessa Guay, Cynthia Villeda-Herrera and Leigh Piercey-Brunet. This work was funded by the Team Program of the Canadian Institutes of Health Research (CIHR) to SMV and DM (CTP-87520). KEY was funded by an internal studentship from the Faculty of Medicine, McGill University. MME was funded by a studentship from the McGill University Health Centre. SMD was funded by a fellowship from the Fonds de Recherche du Québec-Santé.

FIGURES AND FIGURE LEGENDS:

FIGURE 1: ENU MUTAGENESIS BREEDING SCHEMES.

Generation 0 (G0) males are mutagenized on a 129S1 *Salmonella*-resistant background. G0 males were crossed with a wild-type female 129X1 or 129S1 to generate G1 offspring. G1 males were crossed with a wild-type female 129X1 or 129S1 to generate G2 females. G2 females were backcrossed to their G1 fathers to generate G3 offspring. G3 offspring were challenged with 10,000 CFUs of *Salmonella* Typhimurium. Black denotes wild type alleles; gray denotes heterozygous alleles and White denotes homozygous mutant alleles. **A)** *Ity14* and *Ity15*. **B)** *Ity19* and *Ity21*.

A



B

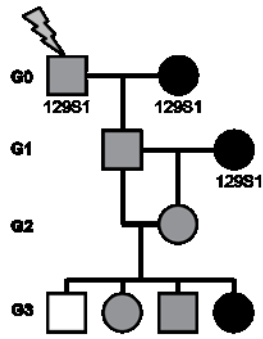


FIGURE 2: SURVIVAL ANALYSIS OF *SALMONELLA*-SUSCEPTIBLE PEDIGREES
IDENTIFIED IN MUTAGENESIS SCREEN

Survival curves of the G3 animals from the *Ity14* (A), *Ity15* (B), *Ity19* (C), and *Ity21* (D) deviant pedigrees (solid line) compared to the parental 129S1 strain (dashed line). Curves represent the cumulative survival of at least 3 litters consisting of 5 or more pups.

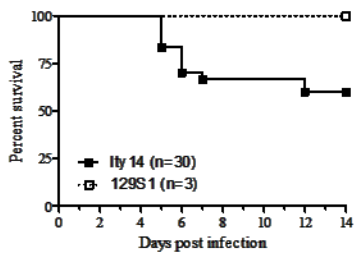
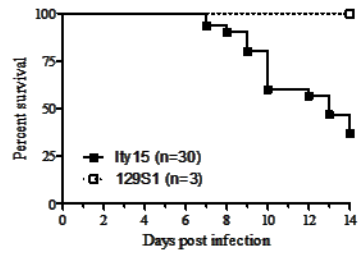
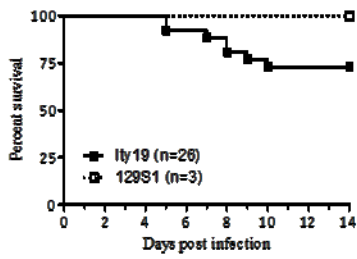
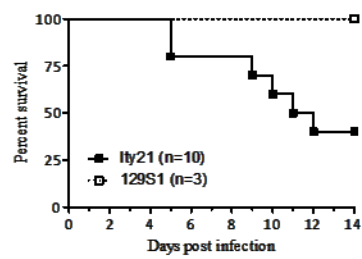
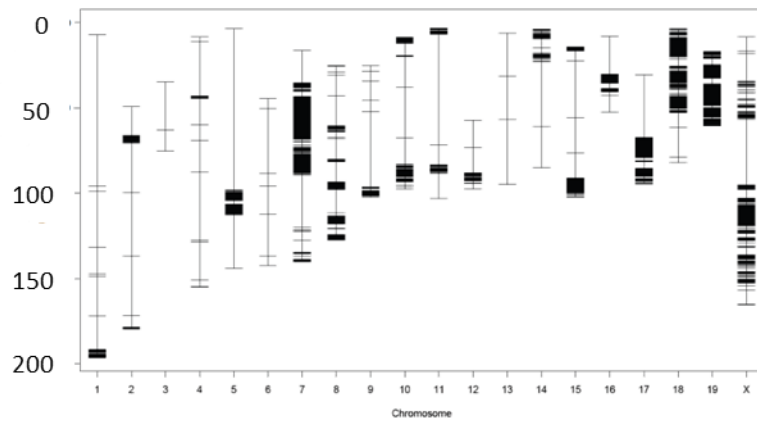
A**B****C****D**

FIGURE 3: MAPPING STRATEGIES USED TO IDENTIFY *ITY14* AND *ITY15*

A) 19,545 SNPs between 129S1 and 129X1 as identified by the Jackson Diversity Array. **B)** 708 SNPs between 129S1 and DBA/2 present in the Illumina Medium Density SNP Panel were used to map *Ity14* and *Ity15*.

A



B

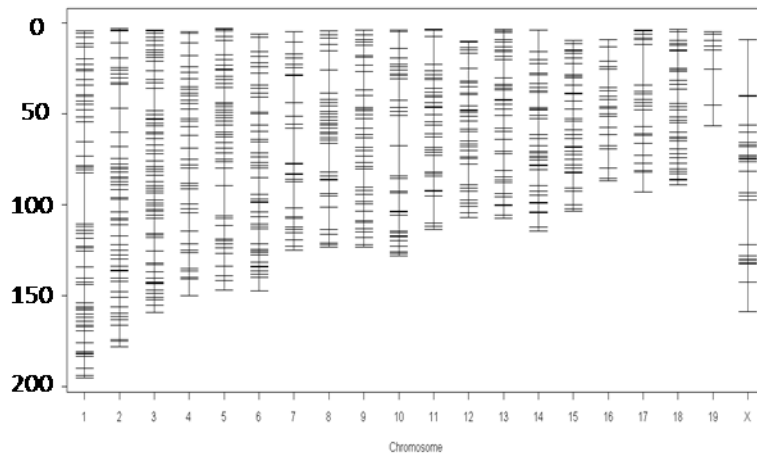
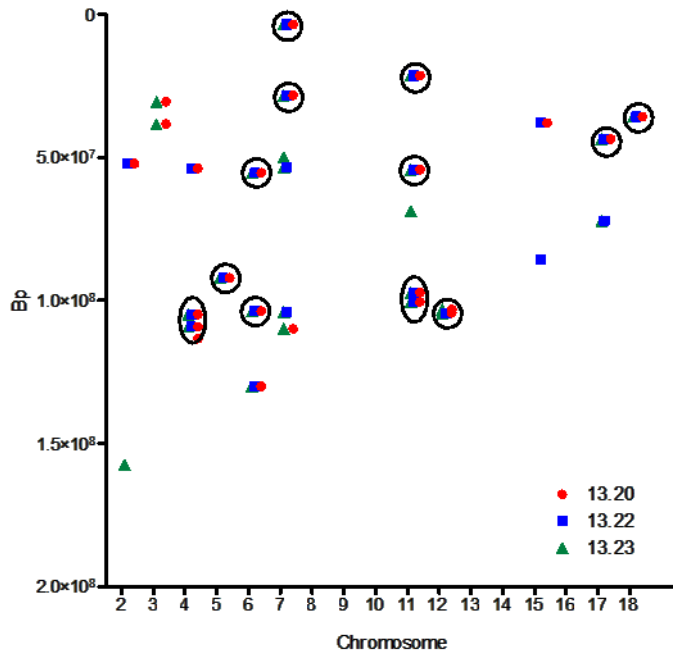


FIGURE 4: MAPPING STRATEGIES USED TO IDENTIFY *ITY19* AND *ITY21*

Exome sequencing was performed in 3 susceptible animals from the *Ity19* and *Ity21* pedigrees. ENU mutations present in each sample after filtering are mapped based on chromosomal position for the *Ity19* pedigree **(A)** and the *Ity21* pedigree **(B)**. Chromosome 1 and 19 were not represented in exome sequencing of *Ity19*. Circles represent mutations present in all 3 samples of each pedigree.

A



B

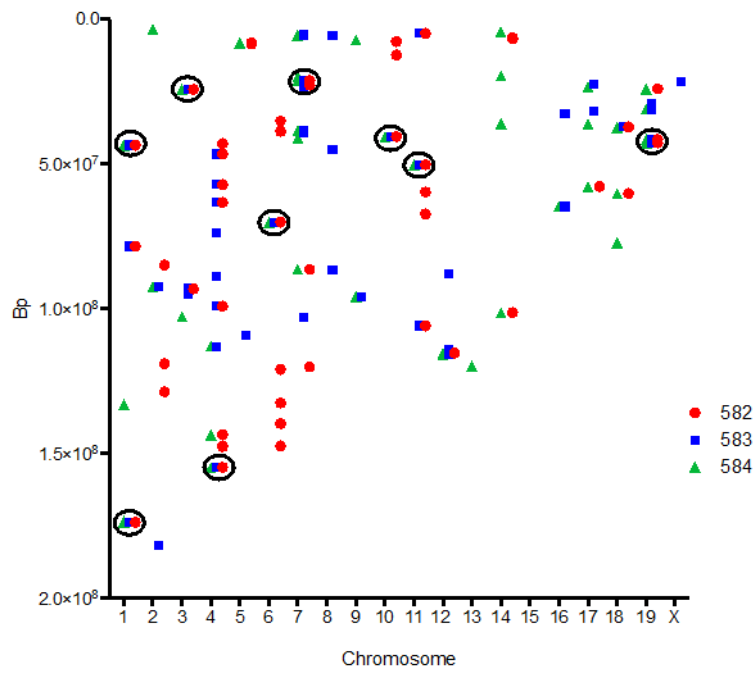


FIGURE 5: EFFICIENCY OF BREEDING SCHEMES TO IDENTIFY DEVIANT PEDIGREES

The number of deviant pedigrees identified per 800 G3 animals screened for the 129X1 and 129S1 breeding schemes **(A)**. The efficiency is shown compared to a previously published Salmonella ENU screen (Richer 2008). The dotted line represents the expected 1 deviant pedigree identified per 800 G3 animals screened.

A

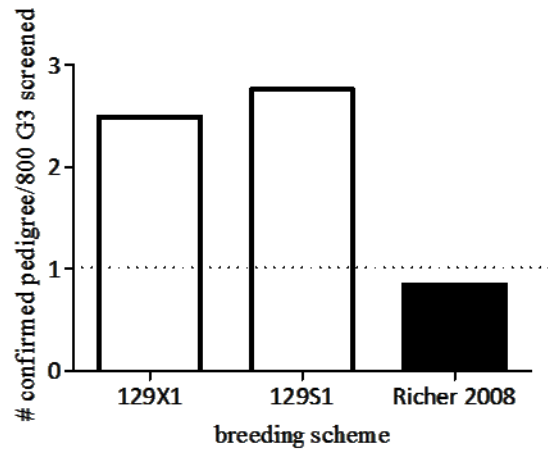


TABLE 1: SUMMARY OF ENU MUTAGENESIS SCREEN FOR SUSCEPTIBILITY TO *SALMONELLA* TYPHIMURIUM INFECTION.

Breeding Scheme	Batch	N3	G2	G1	Deviant	Confirmed	Phenotype	Mapped	Cloned
129X1	1	146	17	10	0	0			
	2	497	45	29	2	<i>lty14</i>	33% mortality by d7	Chr. 1	Stat4
							<i>lty15</i>	40% mortality by d10	Chr. 15
		643	62	39	2	2		2	2
129S1	3	206	33	20	1	Rakeem & Athena (<i>lty19</i>)	25% mortality by d10		Cnp?
	4	374	38	21	1	Lessie & Virgie (<i>lty21</i>)	60% mortality by d12		?
		580	71	41	2	2			1
	TOTAL	1223	133	80	4	4		2	3

TABLE 2: MUTATIONS IDENTIFIED BY EXOME SEQUENCING IN 3 SAMPLES FROM THE *ITY19* PEDIGREE.

Chr	Position	ref_base	var_base	aa_change	polyphen_prediction	snp_exon_type	mgf_name	13.20	13.22	13.23
2	52075749	A	T	D1019E	MODERATE	NON_SYNONYMOUS_CODING	Neb	HET	HET	--
2	157294906	C	T	R387W	MODERATE	NON_SYNONYMOUS_CODING	Src	--	--	HET
3	30554686	A	T	Q404L	MODERATE	NON_SYNONYMOUS_CODING	Lrriq4	HET	--	HET
3	38354137	A	T	V1001E	MODERATE	NON_SYNONYMOUS_CODING	Ankrd50	HET	--	HET
4	53853418	A	G		MODERATE	START_GAINED	Tmem38b	HET	HET	--
4	104748051	A	G	L68	LOW	SYNONYMOUS_CODING	Prkaa2	HET	HET	HET
4	109098963	A	C	T108P	MODERATE	NON_SYNONYMOUS_CODING	Ttc39a	HET	HET	HET
4	113208314	G	C	T1242S	MODERATE	NON_SYNONYMOUS_CODING	Skint5	HET	--	--
5	92051971	T	A	Y273*	HIGH	STOP_GAINED	Parm1	HET	HET	HET
6	55335401	T	C	S330P	MODERATE	NON_SYNONYMOUS_CODING	Ghrhr	OTHER	HOM	HET
6	103661212	T	G	S1004R	MODERATE	NON_SYNONYMOUS_CODING	Chl1	HET	HOM	HOM
6	129942733	C	G		HIGH	SPLICE_SITE_DONOR	Gm15854	HET	HET	HET
7	3562812	A	G	Y160H	MODERATE	NON_SYNONYMOUS_CODING	Oscar	HET	HET	HET
7	28313355	G	A	R169H	MODERATE	NON_SYNONYMOUS_CODING	Hipk4	HET	HET	OTHER
7	49963545	C	A	C301F	MODERATE	NON_SYNONYMOUS_CODING	Gm17067	--	--	HET
7	53484567	A	G		HIGH	SPLICE_SITE_DONOR	Ush1c	--	HET	HET
7	104044094	G	A	R2269H	MODERATE	NON_SYNONYMOUS_CODING	Odz4	--	HET	OTHER
7	109832830	A	T	L53*	HIGH	STOP_GAINED	Trim68	HET	--	OTHER
11	21458542	A	G	S268P	MODERATE	NON_SYNONYMOUS_CODING	Mdh1	HET	HET	HET
11	54150459	G	C	D313H	MODERATE	NON_SYNONYMOUS_CODING	Acsl6	HET	HET	HET
11	68764625	C	T	R492H	MODERATE	NON_SYNONYMOUS_CODING	Arhgef15	--	--	HET
11	97196737	G	A	P1969S	MODERATE	NON_SYNONYMOUS_CODING	Gpr179	HET	OTHER	HET
11	100441997	A	G	T384A	MODERATE	NON_SYNONYMOUS_CODING	Cnp	HOM	HOM	HET
12	103131664	A	C	L388R	MODERATE	NON_SYNONYMOUS_CODING	Trip11	HET	--	HET
12	104321826	G	A	R750H	MODERATE	NON_SYNONYMOUS_CODING	Unc99	HET	HET	HET
15	37938957	T	C	D1040G	MODERATE	NON_SYNONYMOUS_CODING	Ubr5	HET	OTHER	--
15	85648844	T	G	D1107A	MODERATE	NON_SYNONYMOUS_CODING	Pkdrej	--	OTHER	--
17	43567644	A	T	I306L	MODERATE	NON_SYNONYMOUS_CODING	Gpr116	HET	HET	HET
17	72100946	T	C	K359E	MODERATE	NON_SYNONYMOUS_CODING	BC027072	--	OTHER	HET
18	35738952	C	T	H388Y	MODERATE	NON_SYNONYMOUS_CODING	Matr3	HET	OTHER	HET

TABLE 3: MUTATIONS IDENTIFIED BY EXOME SEQUENCING IN 3 SAMPLES FROM THE *ITY21* PEDIGREE.

Chr	Position (bp)	ref_base	var_base	aa_change	polyphen_prediction	snp_exon_type	mgf_name	582	583	584
1	43553956	C	T	R108C	probablydamaging	NON-SYN	Nck2	OTHER	OTHER	OTHER
1	78522757	T	C	V56A	benign	NON-SYN	Mogat1	HET	HOM	--
1	133355548	T	G	S141A	benign	NON-SYN	Ren1	--	--	HET
1	133355549	C	A	S141Y	possiblydamaging	NON-SYN	Ren1	--	--	HET
1	173481380	A	T	F350Y	N/A	NON-SYN	Gm4955	--	--	HET
1	173906193	G	A	A134V	benign	NON-SYN	Mnda	HET	OTHER	HET
2	3453517	A	T	Q609L	probablydamaging	NON-SYN	Dclre1c	--	--	HOM
2	85024990	A	T	W41R	probablydamaging	NON-SYN	P2rx3	HET	--	--
2	92349453	G	A		N/A	SPLICE(5)	Phf21a	--	HET	HET
2	119071939	T	A	C1374S	benign	NON-SYN	Casc5	HET	--	--
2	128831474	T	C	Y228H	probablydamaging	NON-SYN	Tmem87b	HET	--	--
2	181995906	A	C	K258Q	N/A	NON-SYN	Gm14496	--	OTHER	--
3	24333155	G	T	G30C	probablydamaging	NON-SYN	Gm7536	HET	HET	HET
3	93073589	G	T		N/A	SPLICE(1)	Gm4858	--	OTHER	--
3	93219581	A	T	R1933S	probablydamaging	NON-SYN	Flg2	HOM	--	--
3	93219594	G	A	G1939S	probablydamaging	NON-SYN	Flg2	HOM	--	--
3	95240518	C	T	R155Q	possiblydamaging	NON-SYN	Gm128	--	HET	--
3	102820586	A	G	F904L	benign	NON-SYN	Sycp1	--	--	OTHER
4	43034143	T	C	D410G	probablydamaging	NON-SYN	B230312A22Rik	HET	--	--
4	46649805	T	A	Y77F	benign	NON-SYN	Tbc1d2	HET	HET	--
4	57204936	T	A	M742L	probablydamaging	NON-SYN	Ptpn3	HET	HET	--
4	63379280	C	T	V846M	possiblydamaging	NON-SYN	Akna	HET	HET	--
4	73919898	A	G	V17A	N/A	NON-SYN	Gm11756	--	HET	--
4	88835766	G	C	S81T	benign	NON-SYN	lfna5	--	OTHER	--
4	99217977	T	A	M58K	benign	NON-SYN	Atg4c	HET	HET	--
4	112872513	T	C	K847R	benign	NON-SYN	Skint6	--	--	HET
4	113238078	T	C	D128G	benign	NON-SYN	Skint6	--	HET	--
4	143616039	A	T	T239S	benign	NON-SYN	Gm13083	HET	--	HET
4	147541289	A	G	H80R	unknown	NON-SYN	Gm16503	OTHER	--	--
4	147755751	T	A	K214N	possiblydamaging	NON-SYN	Gm13157	OTHER	--	--
4	147755757	A	T	S212R	benign	NON-SYN	Gm13157	OTHER	--	--
4	154892012	T	A	D510E	probablydamaging	NON-SYN	Mmel1	OTHER	HET	HET
5	8181118	G	C	V495L	N/A	NON-SYN	Adam22	HET	--	--
5	8181127	A	G	M498V	N/A	NON-SYN	Adam22	HET	--	HET
5	8603978	C	G	V45L	possiblydamaging	NON-SYN	Rundc3b	HET	--	--
5	109363951	G	C	V675L	benign	NON-SYN	Vmn2r16	--	OTHER	--
6	35241335	T	A	M1761K	possiblydamaging	NON-SYN	Nup205	HET	--	--
6	38737500	T	C	N547S	benign	NON-SYN	Hipk2	HET	--	--
6	70143614	T	A	Q95L	N/A	NON-SYN	AC159715.1	HOM	HOM	HOM
6	121038543	T	C	H178R	probablydamaging	NON-SYN	Mical3	HET	--	--
6	132600439	A	C	T230P	N/A	NON-SYN	Prp2	HOM	--	--
6	139754778	T	C	S147P	N/A	NON-SYN	Pik3c2g	HET	--	--
6	147507788	G	T		N/A	SPLICE(10)	Ccdc91	HET	--	--
7	5488033	A	T	M405K	N/A	NON-SYN	Vmn2r28	--	HET	HET
7	19954311	A	T	M177L	probablydamaging	NON-SYN	Rpl7a-ps8	--	--	OTHER
7	21162676	G	T	Q164H	probablydamaging	NON-SYN	Vmn1r123	HOM	HOM	HOM
7	22843224	G	A	L128F	N/A	NON-SYN	Vmn1r159	HET	--	--
7	23835021	A	C	S236A	N/A	NON-SYN	Vmn1r176	--	OTHER	--
7	38448145	G	T	D342E	N/A	NON-SYN	GM5114	--	OTHER	OTHER
7	39411135	G	A	L97F	N/A	NON-SYN	Gm5114	--	HET	--
7	41157864	T	G	N380K	benign	NON-SYN	Gm2128	--	--	HOM
7	86526750	T	A		N/A	SPLICE(9)	Olfir297	OTHER	--	OTHER

7	103051913	G	A	S205N	benign	NON-SYN	Olf583	--	OTHER	--
7	120195352	A	T	W215R	probablydamaging	NON-SYN	Crym	HET	--	--
8	5639973	G	C	L130F	benign	NON-SYN	Gm1840	--	HET	--
8	45051172	T	A	S4512R	benign	NON-SYN	Fat1	--	HET	--
8	86636594	C	T	S280F	possiblydamaging	NON-SYN	Lonp2	--	HET	--
9	7147741	A	T	V963E	probablydamaging	NON-SYN	Dync2h1	--	--	HET
9	95967703	A	G		N/A	SPLICE(9)	Xrn1	--	HET	HOM
10	7774044	A	G	Y162H	benign	NON-SYN	Ginm1	HET	--	--
10	12406574	A	T	I3227N	probablydamaging	NON-SYN	Utrn	HET	--	--
10	40603920	A	G	K642E	unknown	NON-SYN	Slc22a16	HOM	HOM	HOM
10	40603921	A	G	K642R	unknown	NON-SYN	Slc22a16	HOM	HOM	HOM
11	4939602	T	C	T1006A	unknown	NON-SYN	Nefh	HET	HOM	--
11	50299157	A	T	L458Q	possiblydamaging	NON-SYN	Canx	HOM	HOM	HOM
11	59795757	A	T	V390D	probablydamaging	NON-SYN	Flcn	HET	--	--
11	67364489	A	T	I1562F	benign	NON-SYN	Myh13	HET	--	--
11	105988017	T	C	Y1133H	probablydamaging	NON-SYN	Ace	HOM	HOM	--
12	88176445	T	G		N/A	SPLICE(6)	Gm2042	--	HOM	--
12	114176824	A	G		N/A	SPLICE(5)	Ighv14-4	--	HET	--
12	114788784	G	A	L8F	N/A	NON-SYN	AC073565.5	--	HET	--
12	115359388	A	C	S35A	benign	NON-SYN	Igh-VJ558	HOM	--	--
12	115507729	A	G	V56A	N/A	NON-SYN	AC164609.1	--	--	HET
12	115567220	T	C	N94S	N/A	NON-SYN	AC073939.2	--	HET	--
12	115834374	A	T	L8H	N/A	NON-SYN	AC160473.3	--	OTHER	--
12	115920343	C	T	S96N	N/A	NON-SYN	AC160990.2	--	--	HET
12	116000072	G	T	H103N	N/A	NON-SYN	AC160990.4	--	--	HOM
13	119893692	G	T	L135I	benign	NON-SYN	Tcstv1	--	--	HOM
14	4442708	C	G	P215A	benign	NON-SYN	Gm17143	--	--	HET
14	6443534	C	A	R98M	benign	NON-SYN	Gm3594	OTHER	--	--
14	6767076	T	C	T215A	N/A	NON-SYN	Gm8362	HET	--	--
14	19540914	C	T	E102K	N/A	NON-SYN	Gm2244	--	--	HOM
14	36089365	C	T	S157N	benign	NON-SYN	Gm7853	--	--	HET
14	101444531	T	A		N/A	SPLICE(7)	Tbc1d4	HET	--	HET
16	32755148	C	G	T1674S	benign	NON-SYN	Muc4	--	HET	--
16	64766857	T	G	H168P	probablydamaging	NON-SYN	4930453N24Rik	--	OTHER	OTHER
17	22603447	C	A	P369T	N/A	NON-SYN	Vmn2r112	--	OTHER	--
17	23310978	G	A	L152F	benign	NON-SYN	Vmn2r114	--	--	HET
17	31987432	A	G	Y242H	possiblydamaging	NON-SYN	Hsf2bp	--	HET	--
17	36165863	C	T	V212I	benign	NON-SYN	Gm8909	--	--	HOM
17	57838924	G	C	H104D	benign	NON-SYN	Cntnap5c,Rpl7a-ps5	OTHER	--	HOM
17	57838931	C	A	K101N	benign	NON-SYN	Cntnap5c,Rpl7a-ps5	OTHER	--	HOM
18	37302922	A	T	N647I	probablydamaging	NON-SYN	Pcdhb3	HET	HOM	--
18	37343041	C	G	A410G	benign	NON-SYN	Pcdhb7	--	--	OTHER
18	60270793	G	A	T76I	possiblydamaging	NON-SYN	Gm4841	--	--	OTHER
18	60270794	T	C	T76A	probablydamaging	NON-SYN	Gm4841	OTHER	--	OTHER
18	77295819	A	T	Y138F	unknown	NON-SYN	Loxhd1	--	--	HET
19	24120009	G	A	A516V	probablydamaging	NON-SYN	Tjp2	HET	--	HET
19	29003667	C	A	R59L	N/A	NON-SYN	Gm10136,Cdc37l1		OTHER	--
19	31084439	T	A	D458E	benign	NON-SYN	Cstf2t,Prkg1	--	HET	HET
19	41608377	G	C	N1094K	benign	NON-SYN	Slit1	HET	HOM	HOM
19	41639835	A	T	C445S	probablydamaging	NON-SYN	Slit1	HET	--	HOM
19	42771190	A	T	M61K	possiblydamaging	NON-SYN	Hps1	HET	HOM	HOM
X	21716277	G	A	D31N	probablydamaging	NON-SYN	Slc6a14	--	OTHER	--

BRIDGING STATEMENT FROM CHAPTER 2 TO CHAPTER 3

Our work in the previous chapter and other work from our laboratory using chemical mutagenesis ([221] and Eva et al unpublished) has demonstrated that there are numerous loci controlling different aspects of the host response to *Salmonella* infection. In this chapter we present the phenotypic characterization of the ENU induced mutation in *Ank1* identified in the *lty16* pedigree. This gene is known to play an important role in the formation and stabilization of the red cell cytoskeleton. In humans, mutations within *ANK1* cause hereditary spherocytosis, a disease characterized by hemolytic anemia. This study illustrates that suppression of hepcidin, a key gene involved in iron metabolism, and iron overload contribute to the susceptibility of *Ank1* mutant to *Salmonella* infection.

CHAPTER 3: SUPPRESSION OF HEPCIDIN EXPRESSION AND IRON OVERLOAD MEDIATE *SALMONELLA* SUSCEPTIBILITY IN ANKYRIN1 ENU INDUCED MUTANT

Kyoko E. Yuki^{1,3}, Megan M. Eva^{1,3}, Etienne Richer^{1,3}, Dudley Chung⁵, Marilène Paquet⁴, Mathieu Cellier⁶, François Canonne-Hergaux⁷, Sophie Vaulont⁸, Silvia M. Vidal^{1,3}, Danielle Malo^{1,2,3#}

Departments of ¹Human Genetics, ²Medicine, ³Complex Trait Group of the McGill Life Sciences Complex, ⁴Comparative Medicine & Animal Resources Centre, McGill University, Montréal, QC, Canada, ⁵Department of Biochemistry and Microbiology, University of Victoria, Victoria, BC, Canada, ⁶Centre INRS-Institut Armand Frappier, Laval, QC, Canada, ⁷INSERM U1043-CPTP, Toulouse, F-31300, France; CNRS, U5282, Toulouse, F-31300, France; Université de Toulouse, UPS, Centre de Physiopathologie de Toulouse Purpan (CPTP), Toulouse, F-31300, France, ⁸INSERM, U1016, Institut Cochin, Paris, France

Running title: Ankyrin 1 deficiency causes *Salmonella* susceptibility

#Correspondence should be addressed to D.M. (McGill Life Sciences Complex, Bellini Building, 3649 Promenade Sir William Osler, Room 369, Montreal, QC, Canada H3G 0B1, Tel: 514-398-3907, email: danielle.malo@mcgill.ca)

Published in: PLoS One 8(2): e55331. doi: 10.1371/journal.pone.0055331

ABSTRACT:

Salmonella, a ubiquitous Gram-negative intracellular bacterium, is a food borne pathogen that infects a broad range of hosts. Infection with *Salmonella* Typhimurium in mice is a broadly recognized experimental model resembling typhoid fever in humans. Using a *N*-ethyl-*N*-nitrosurea (ENU) mutagenesis recessive screen, we report the identification of *Ity16* (*Immunity to Typhimurium locus 16*), a locus responsible for increased susceptibility to infection. The position of *Ity16* was refined on chromosome 8 and a nonsense mutation was identified in the ankyrin 1 (*Ank1*) gene. ANK1 plays an important role in the formation and stabilization of the red cell cytoskeleton. The *Ank1*^{Ity16/Ity16} mutation causes severe hemolytic anemia in uninfected mice resulting in splenomegaly, hyperbilirubinemia, jaundice, extramedullary erythropoiesis and iron overload in liver and kidneys. *Ank1*^{Ity16/Ity16} mutant mice demonstrated low levels of hepcidin (*Hamp*) expression and significant increases in the expression of the growth differentiation factor 15 (*Gdf15*), erythropoietin (*Epo*) and heme oxygenase 1 (*Hmox1*) exacerbating extramedullary erythropoiesis, tissue iron deposition and splenomegaly. As the infection progresses in *Ank1*^{Ity16/Ity16}, the anemia worsens and bacterial load were high in liver and kidneys compared to wild type mice. Heterozygous *Ank1*^{+/Ity16} mice were also more susceptible to *Salmonella* infection although to a lesser extent than *Ank1*^{Ity16/Ity16} and they did not inherently present anemia and splenomegaly. During infection, iron accumulated in the kidneys of *Ank1*^{+/Ity16} mice where bacterial loads were high compared to littermate controls. The critical role of HAMP in the host response to *Salmonella* infection was validated by showing increased susceptibility to infection in *Hamp*-deficient mice and significant survival benefits in *Ank1*^{+/Ity16} heterozygous mice treated with HAMP peptide. This study illustrates that the regulation of *Hamp* and iron balance are crucial in the host response to *Salmonella* infection in *Ank1* mutants.

INTRODUCTION:

Salmonella infections in humans are responsible for two major diseases, typhoid fever caused by *Salmonella* Typhi and *Salmonella* Paratyphi and a diarrheal disease known as salmonellosis caused by several non-host specific serotypes including *Salmonella* Typhimurium and *Salmonella* Enteritidis. Typhoid is transmitted by a fecal-oral route through contaminated food and water and is endemic in areas of poor water sanitation. It is estimated by the World Health Organization that there are 21 million new cases of typhoid fever each year resulting in approximately 200,000 deaths. In addition, 1 to 5% of patients become asymptomatic chronic carriers serving as reservoirs from which new *Salmonella* Typhi infections can be transmitted [263]. Early during infection, phagocytes are instrumental in the control of bacterial replication through the production of pro-inflammatory cytokines such as IFN γ , TNF α and IL-12. Immunocompromised patients due to chronic granulomatous disease (deficient in NADPH oxidase activity), defects in the IFN γ or IL-12 signaling pathway or HIV infection are more susceptible to disseminated *Salmonella* infection [264-266]. In addition, patients with hemoglobinopathies resulting in iron overload such as sickle cell anemia and thalassemia present increased susceptibility to *Salmonella* infection [267, 268]. In the mouse, *Salmonella* Typhimurium infection results in a systemic disease with clinical manifestations resembling those found in humans with typhoid fever. The severity of infection depends on a variety of factors including the dose of the inoculum, as well as the interaction of host and bacterial genetic determinants. Several strains of mice show varying degrees of susceptibility to *Salmonella* Typhimurium infection with the mouse strain 129 substrains showing the most resistance. The study of the natural variation of the host response to infection with *Salmonella* Typhimurium in spontaneous mouse mutants have identified important innate immune genes having Mendelian contribution to disease susceptibility and contributing to different mechanisms including pathogen recognition (*Tlr4*^{P712H} in C3H/HeJ), phagosome transport of divalent cations including iron (*Nramp1*^{G169D} in C57BL/6J and BALB/CJ) or erythropoiesis and iron metabolism (*Pklr*^{J90N} in AcB61 mice) [132, 156, 170, 269].

Due to the limited amount of natural variation found in classical inbred mice, we have used *N*-ethyl-*N*-nitrosurea (ENU) mutagenesis to generate novel mutations responsible for increased

susceptibility to *Salmonella* infection. Recessive ENU induced mutations are bred to homozygosity with the use of a three-generation breeding scheme and challenged with *Salmonella* Typhimurium. In the current screen we have evaluated 216 pedigrees for their susceptibility to infection and identified 5 deviant pedigrees. In this paper, we report the identification of one of these ENU mutants named *lty16* that carries a nonsense mutation in the gene *Ank1*. *Ank1* encodes a red blood cell (RBC) adaptor protein consisting of three major functional domains: an N-terminal membrane binding, a spectrin binding and a C-terminal regulatory domain [270]. ANK1 plays an important role in RBC membrane stability by mediating the attachment of band 3 (SLC4A1) and protein 4.2 (EPB4.2) to the spectrin-based membrane cytoskeleton [271]. A number of mutations in murine *Ank1*, both spontaneous and ENU-induced, have been described to cause hemolytic anemia [245, 246, 272-274]. In humans, mutations within *ANK1* cause hereditary spherocytosis, a disease characterized by hemolytic anemia [275-277]. In the current paper, we show that *Ank1*^{*lty16/lty16*} and *Ank1*^{*+/lty16*} mice have increased susceptibility to *Salmonella* Typhimurium infection, although in the latter group the increased susceptibility is delayed and milder. The suppression of hepcidin (*Hamp*) expression and iron overload contribute to their increased susceptibility to *Salmonella* infection.

MATERIALS & METHODS:

Mice and ENU mutagenesis: All animal experiments were performed under conditions specified by the Canadian Council on Animal Care and the animal use protocol was approved by McGill University Facility Animal Care Committee. Generation 0 (G0) 129S1 males were mutagenized with a single injection of 150 mg per kg of body weight of *N*-ethyl-*N*-nitrosurea (ENU) given intraperitoneally. G0 males were outcrossed to 129X1 females to create G1 progeny that were subsequently crossed to DBA/2J. Resulting G2 animals were intercrossed to produce the G3 mice that were phenotyped for their susceptibility to *Salmonella* infection. Hamp^{tm1Svl} knock out mice [278] were transferred onto a 129S6 background, a strain that carries a wild-type allele of *Slc11a1* (129S6.B6*129S2-Hamp^{tm1Svl}).

Genotyping: The genome scan was performed using a 1441 SNP panel (The Centre for Applied Genomics, Toronto, Ontario, Canada) on 22 mice. Additional genotyping was performed by microsatellite analysis or restriction enzyme digests of SNP markers. Sequencing of the *Ank1* gene was performed on cDNA isolated from spleens of *Ank1*^{ty16/ty16} and *Ank1*^{+/+} mice using 3730xl DNA Analyzer (Applied Biosystems) from the McGill University and Genome Quebec Innovation Centre.

In vivo *Salmonella* Infections: Mice were infected with 5000 CFUs of *Salmonella* Typhimurium strain Keller as described by us previously [222]. The infectious inoculum was diluted to 25,000 CFUs per mL and 0.2 mL was injected into the caudal vein of 7 week old mice of both sexes. To determine CFUs in tissues, mice were euthanized with CO₂ at day 2 and day 6 post infection and spleen, liver and kidney were removed aseptically, weighed and homogenized. Homogenates were diluted in saline and plated on trypticase soy agar (TSA) overnight. Other groups of mice were coinfecting with 2500 CFUs of *Salmonella* Typhimurium strain Keller and 2500 CFUs of Δ *tonB* constructed by allelic exchange in serovar Keller [279]. The tissues were collected 2 days after infection and tissue homogenates were plated on TSA containing or not 50 mg/ml of kanamycin.

Western blots: Erythrocyte ghost membranes were prepared by osmotic lysis as previously described ([273]). Primary antibody to detect ANK1 (N13) was purchased from Santa Cruz Biotechnology ([SC-87552](#)) and was used at a 1:200 dilution. This antibody was raised against a peptide sequence spanning exons 8 and 9 of the *Ank1* transcript ([ENSMUST00000121802](#)) and recognized the full length ANK1. The ACTIN antibody and the secondary antibodies for Western detection (anti-rabbit IgG) were purchased from Cell Signaling Technology.

Hepcidin treatment: Mice were treated with 50 µg of HAMP (Peptide International, Louisville KY) resuspended in 100 µl of PBS intraperitoneally. Four hours later, mice were infected with 5000 CFUs of *Salmonella* Typhimurium and monitored for survival over a period of 14 days. Littermate controls were given 100 µl of PBS intraperitoneally.

Histology: Tissues were collected from *Ank1*^{lty16/lty16}, *Ank1*^{+/lty16} and *Ank1*^{+/+} mice and fixed in 10% neutral buffered formalin for 24 hours at 20°C, then placed in 70% ethanol at 4°C before processing and embedding (Goodman Cancer Research Center histology facility, McGill University). Embedded tissues were sectioned and stained with hematoxylin and eosin or prussian blue.

Hematologic and biochemical parameters: Blood samples from *Ank1*^{lty16/lty16}, *Ank1*^{+/lty16} and *Ank1*^{+/+} mice were collected by cardiac puncture and analyzed for CBC & differential and reticulocyte counts (Diagnostic Research Support Service, Comparative Medicine and Animal Resources Centre, McGill University). Serum was isolated with a serum separator tube (Sarstedt) and analyzed for bilirubin, blood urea nitrogen (BUN), alanine transaminase (ALT) and aspartate transaminase (AST) (Diagnostic Research Support Service, Animal Resources Centre, McGill University).

QRT-PCR: Total RNA was extracted from spleen, liver and kidneys with Trizol Reagent (Invitrogen, Burlington ON) according to manufacturer instructions. cDNAs were synthesized using SuperScript®II Reverse Transcriptase (Invitrogen). Quantitative PCR was performed on a

Chromo4 (BioRad, Mississauga ON) or StepOnePlus (Applied Biosystem, Carlsbad CA) using SYBR Green (Applied Biosystems) for hepcidin (*Hamp*), ferroportin (*Slc40a1*), *Il6*, *Il1*, *Ifng*, erythropoietin (*Epo*), heme oxygenase 1 (*Hmox1*) and growth differentiation factor 15 (*Gdf15*) expression. Two housekeeping genes: *Tbp* (TATA box binding protein) and *Hprt* (hypoxanthine guanine phosphoribosyl transferase) were used. The relative expression of the genes was normalized to the amount of *Tbp* and *Hprt* (endogenous reference) and relative to a calibrator (untreated wild type genotype) for each tissue by using the comparative $2^{(-\Delta\Delta Ct)}$ method. The primer sequences are provided in Supplemental Table 1.

Statistical analysis: Data (unless otherwise specified) was analyzed by two-tailed Mann Whitney test and two-way ANOVA using GraphPad Prism 5. Data for qPCR was analyzed in R by ANOVA and Welch two sample t-test [280].

RESULTS:

Identification of a novel *Salmonella* susceptibility locus using ENU chemical mutagenesis

The breeding scheme used to identify the *Ity16* pedigree is shown in Fig. 1A. Mutagenized 129S1 G0 males were crossed to wild-type 129X1 females to produce G1 males. These G1 males were crossed to DBA/2J females to generate G2 offspring that were randomly intercrossed to produce G3 progeny. G3 animals were phenotyped for susceptibility to *Salmonella* infection with 5,000 CFUs and monitored for a period of 14 days. Mortality in the *Ity16* pedigree was observed between day 3 post infection and continued until day 11 with 25% of mice succumbing to infection by day 6 (Fig. 1B). An initial genome scan was performed using twenty-two G3 animals (8 susceptible and 14 resistant mice) and 708 informative DNA markers. Binary analysis of the genome scan revealed a locus on chromosome 8 at position 25.8 Mb with a LOD score of 3.72 (Fig. 1C). DNA samples used in the genome scan were also genotyped with DNA markers discriminating 129S1 and 129X1 genomes to ensure that mice were homozygous for the mutagenized 129 allele (data not shown). Fine mapping of the chromosome 8 region with 27 additional G3 animals and 9 markers reduced the region to a 2.5 Mb region (Fig. 1D) that includes 23 annotated genes, 10 predicted genes and 2 miRNAs (MGI). The survival curves of the *Ity16* G3 mice were plotted according to their genotype at the peak marker (rs32874474) on chromosome 8 (Fig. 1E). All mice homozygous for the 129S1 allele succumbed to infection by day 6. Mice carrying the DBA/2J alleles at this locus were 100% resistant to infection. Interestingly, mice with a heterozygous genotype at the peak marker had an intermediate survival phenotype, with mortality starting at day 7 (Fig. 1E).

***Ity16* mutant mice present severe hemolytic anemia that worsened during infection**

Compared to wild type and heterozygous littermates, mutant mice are characterized clinically by low body weight (Fig. 2A), pallor of mucosal linings and yellow discoloration of subcutaneous tissues, a consequence of increased levels of bile pigment (bilirubin) in the blood (Fig. 2B). In addition, these mutants exhibit impressive enlargement of the spleen, accounting for up to 10% of their body weight (Fig. 2C). This is accompanied by significant increases in kidney and heart weights (Fig. 2C). Hematological analysis of uninfected mutant *Ity16* mice showed they have

severe constitutive anemia as demonstrated by low hematocrit levels (25% in mutants compared to 50% in wildtype and heterozygous mice) which decreased to as low as 15% 2 days after infection (Table 1). This decrease in hematocrit levels is mirrored by similar decreases in hemoglobin and red blood cell levels during infection (Table 1). Additionally, there were a higher percentage of circulating reticulocytes in the blood of mutants compared to both wild type and heterozygous littermates (Table 1). As a consequence of severe anemia, *Ity16* mutant mice present extensive extramedullary erythropoiesis in the spleen and liver as assessed by histopathological examination that is associated in the spleen with severe lymphoid depletion (Fig. S1). Blood smear examination of mutant *Ity16* mice showed abnormally shaped red blood cells, marked anisocytosis, and reticulocytosis and the presence of spherocytes (data not shown). Total number of WBC, neutrophils and lymphocytes were significantly higher in *Ity16* mutant mice compared to littermate controls before and after infection (Table 1) after correcting for the high percentage of nucleated RBC (Table 1). The total number of neutrophils increased significantly during infection in all three groups although it was more pronounced in *Ity16* mutants.

A mutation within *Ank1* is responsible for susceptibility of *Ity16* mice to *Salmonella* infection

Identification of the causative gene for *Ity16* focused on the region between 23.5 Mb and 26 Mb on mouse chromosome 8. Genes involved in hematopoiesis and causing splenomegaly and anemia were of particular interest because of the distinct phenotype exhibited by the mutant mice. Only the gene ankyrin 1 (*Ank1*) met our criteria. ANK1 is primarily known for its structural role in erythrocytes. *Ank1* is part of a small gene family which members are adaptor structural components linking lipid membranes to the cytoskeleton showing an essential role in the stability of plasma membranes of many cell types [281]. The *Ank1* gene comprises a total of 44 exons. Several *Ank1* splice variants are observed and the full-length isoform encodes for a protein of 1907 amino acids (200–210 kDa). Erythroid *Ank1* consists of three major conserved domains including an N-terminal membrane-binding domain, a spectrin-binding domain and a C-terminal regulatory domain containing a death domain motif [282, 283]. *Ity16* mutant showed a C to T transition at cDNA position 4069 (c.4069C>T) resulting in a nonsense mutation

in exon 33 at amino acid position 1357 (p.Gln1357Ter) (Fig. 3A). This pre-mature stop codon results in a predicted truncation of the ANK1 protein by 550 amino acids with the loss of the C-terminal regulatory and the death domains but retaining the membrane-binding and most of the spectrin-binding domains (Fig. 3B). Immunoblotting analysis of fractioned erythrocyte membrane ghosts revealed that the non-sense mutation abrogated ANK1 protein expression in *Ity16* mutant mice (Fig. 3C). A truncated form of the protein (calculated molecular weight of 144 kDa) could not be detected suggesting that the abnormal protein is targeted for degradation. The frequency of adult mice (older than 4 weeks) on a 129S1/DBA2J hybrid background with a c.4069C>T genotype was not in Hardy-Weinberg equilibrium: we obtained a ratio that was significantly different ($p=.04$) from the expected 1-2-1 ratio for a cross between mice heterozygous (+/m) for the mutation. Genotype frequencies in 249 animals were 29% for wild type mice, 52% for heterozygous and 18% for homozygous mutants.

Iron overload in *Ank1*^{*Ity16/Ity16*} mutant mice facilitates proliferation of *Salmonella* in liver and kidneys

Increased amounts of iron pigment deposition were detected in *Ank1*^{*Ity16/Ity16*} mutant livers and kidneys (Prussian blue positive pigment) compared with wild type and heterozygous littermates in non-infected conditions and in mice at 2 days after infection (Fig. S1). Iron accumulates predominantly in the hepatocytes and in the cytoplasm of the epithelium of the renal tubules. The high levels of iron in the liver and kidneys of *Ank1*^{*Ity16/Ity16*} mutant mice suggest that the rapid turnover of RBC in these mice leads to accumulation of iron in the liver and kidneys (secondary hemochromatosis). In contrast, splenic iron content was markedly decreased in *Ank1*^{*Ity16/Ity16*} mutant mice compared to wild type littermates (Fig. S1). In *Ank1*^{*Ity16/Ity16*} mutant mice, iron overload is associated with increased bacterial proliferation in the liver and kidneys. In infected mice, there was a gradation of microabscesses present in the liver that worsened with genotype but was not influenced by the age at the time of infection (Fig. S2). In addition, significant higher bacterial loads were observed in the liver (30-100 times higher) and kidneys (10 times higher) of *Ank1*^{*Ity16/Ity16*} mutant compared to wild type and heterozygous littermates 2 days post infection (Fig. 4B and 4C). Because of the high bacterial burden present in the liver

and kidney, biochemical measures of hepatic (alanine transaminase, ALT and aspartate transaminase, AST) and kidney function (blood urea nitrogen, BUN) were evaluated before and after infection. ALT and AST were elevated after infection only in *Ank1^{lty16/lty16}* mutant mice (Fig. 5A and 5B) whereas BUN levels were significantly higher in uninfected and infected *Ank1^{lty16/lty16}* mice compared to controls (Fig. 5C). These data may indicate the presence of abnormal organ function in naïve *Ank1^{lty16/lty16}* mice (kidney) and during infection (liver and kidney). In fact, we observed glomeruli with enlarged mesangium in *Ank1^{lty16/lty16}* mice, a pathological change that may be compatible with membranoproliferative glomerulonephritis (Fig. S2).

To examine if iron accumulation in tissues has an impact on the bacterial load phenotype in *Ank1^{lty16/lty16}* mutant mice, we infected mice with Δ *tonB* *Salmonella* Typhimurium. The *tonB* mutation is known to inactivate several siderophore-dependent Fe³⁺ uptake systems in *Salmonella* and Δ *tonB* *Salmonella* are as virulent as the wild-type strain in *Slc11a1*-deficient mice [279]. In the spleen where there is no iron accumulation, there was no significant genotype difference for the proliferation of Δ *tonB* and wild-type *Salmonella* (Fig. 4D). In contrast, the levels of both Δ *tonB* and wild-type bacteria were significantly higher (by a factor of ~2 Log) in the liver of mutant mice where there is iron overload (Fig. 4E). At this early time point, there was no iron accumulation in the liver of heterozygous mice (Fig. S1) and the mice were able to control bacterial growth as well as wild-type mice (Fig. 4E). The growth of Δ *tonB* *Salmonella* appears to be affected by the presence of iron in the cellular microenvironment, suggesting that iron uptake via *tonB* is not limiting when iron is abundant in tissue. Overall, these data support the observation that tissue iron overload in *Ank1^{lty16/lty16}* mutant promotes *Salmonella* growth.

Increased expression of *Epo* and *Gdf15* paralleled low levels of *Hamp* expression in *Ank1^{lty16/lty16}* mice

Because of the severe iron overload present in the liver and kidney of *Ank1^{lty16/lty16}* mice, the expression of key genes involved in iron metabolism including hepcidin (*Hamp*), ferroportin (*Slc40a1*) and heme oxygenase 1 (*Hmox1*) and regulators of *Hamp* expression (*Epo*, *Gdf15*, *Il1*

and Il6) were investigated (Fig. 6 and 7). The liver is a major site of iron storage and in clinical conditions of iron overload, the liver become a major site of iron deposition. The kidneys have been shown also to play a role in iron homeostasis and to express both HAMP and SLC40A1 [284-286]. In *Ank1^{lty16/lty16}* mice, the liver and the kidneys are major site for *Salmonella* replication and growth during infection. The expression of *Hamp* in both uninfected and infected *lty16* mutant mice was significantly downregulated in the liver and kidneys compared to wild type littermates (Fig. 6A). On the other hand, the liver and kidney expression of the membrane iron exporter, *Slc40a1* and *Hmox1* was significantly higher in *Ank1^{lty16/lty16}* mice at day 0 and day 2 post infection compared to *Ank1^{+/+}* (Fig. 6C and 7C). In the spleen of *Ank1^{lty16/lty16}* mutant mice, *Slc40a1* and *Hmox1* mRNA levels were significantly lower compared to wild-type littermates (Fig. 6C and 7C). In *Ank1^{lty16/lty16}* mice, low *Hamp* expression had only a modest impact on the expression of liver *Slc40a1* both at the mRNA (Fig. 6C) and protein levels (data not shown). We investigated the expression of two inhibitory erythroid regulators of *Hamp* expression, erythropoietin (*Epo*) (Fig. 6B) and growth differentiation factor 15 (*Gdf15*) (Fig. 6D). These analyses revealed a major significant increase in the expression of both *Epo* and *Gdf15* only in *Ank1^{lty16/lty16}* mutant mice that could explain, at least in part, the low *Hamp* expression levels observed in these mice. During infection, the levels of *Gdf15* were significantly more elevated in *Ank1^{lty16/lty16}* mutant mice compared to wild type littermates (Fig. 6D). In addition, cytokine mRNA levels (*Il1*, and *Il6*) known to be upregulated during *Salmonella* infection and to impact on *Hamp* transcription were measured (Fig. 7A-B). The spleen of *Ank1^{lty16/lty16}* mutant mice appeared to be underresponsive to infection-induced cytokines as measured by very little or no induction of *Il1* and *Il6* (Fig. 7A-B). In the liver and the kidneys, the situation is different and *Ank1^{lty16/lty16}* mice showed marked increases in *Il1* (liver and kidneys) and *Il6* (liver) mRNA expression during infection (Fig. 7A). In these two tissues, high levels of *Il1* and *Il6* cytokines did not promote *Hamp* transcription in *Ank1^{lty16/lty16}* mutant. To further demonstrate the importance of *Hamp* during *Salmonella* infection, we did challenge *Hamp* knockout mice with *Salmonella* Typhimurium (Fig. 6E). We showed that mice deficient for *Hamp* (*Hamp^{-/-}*) were significantly more susceptible to infection than mice carrying one (*Hamp^{+/-}*) or two (*Hamp^{+/+}*) wild type allele at *Hamp*. These results

confirm the importance of *Hamp* during acute systemic model of *Salmonella* Typhimurium infection.

***Salmonella* susceptibility in *Ank1*^{+/*Ity16*} heterozygous mice is associated with low levels of *Hamp* and iron accumulation in tissues**

Ank1^{+/*Ity16*} heterozygous mice present an intermediate phenotype with respect to susceptibility to infection (survival) when compared to *Ank1*^{+/+} and *Ank1*^{*Ity16*/*Ity16*} littermates (Fig. 1E).

Clinically, *Ank1*^{+/*Ity16*} mice did not present any sign of anemia (Table 1) or splenomegaly (Fig. 2C). However, we did observe a small but significant increase in the number of RBCs (Fig. 8A). In addition, the *Ank1*^{+/*Ity16*} mice presented moderate extramedullary hematopoiesis in the spleen (Fig. S1) and lower levels of *Hamp* expression in the liver (Fig. 8B) and kidneys (Fig. 8C) that was paralleled by increased expression of *Gdf15* (data not shown).

Early during infection (day 2), *Ank1*^{+/*Ity16*} mice behaved as wild type littermates for most subphenotypes we have measured including different blood parameters (Table 1) and organ CFUs (Fig. 4). To understand the pathophysiology of the underlying susceptibility of *Ank1*^{+/*Ity16*} mice, we followed the animals for a longer period of time during infection. At day 6 post infection when the animals become clinically diseased, *Ank1*^{+/*Ity16*} mice presented consistent increase in bacterial load in the spleen, liver and kidney with a significant difference detected in the kidney (Fig. 8D). At day 6 post infection, iron pigment deposition was detected in the liver and kidneys of *Ank1*^{+/*Ity16*} mice and not in wild type littermates (Fig. S3). The increase in kidney bacterial load together with iron deposition following infection clearly induced a local inflammatory response that is reflected by higher expression of renal *Il1* (Fig. 8E) and *Il6* (Fig. 8F) mRNA levels by a factor of 2.5 fold compared to wild-type controls. During infection, both wild-type and *Ank1*^{+/*Ity16*} heterozygous mice developed a mild anemia although the *Ank1*^{+/*Ity16*} heterozygous mice still presented higher RBC counts compared to control mice (Fig. 8A). The higher red cell mass present in *Ank1*^{+/*Ity16*} heterozygous mice during infection could be explained by increased *Epo* expression by the kidneys (Fig. 8G). During infection, liver *Hamp* expression levels were not significantly modulated in both wild-type mice and *Ank1*^{+/*Ity16*} heterozygous mice (Fig. 8B) although we did observe a modest but significant increase in kidney

Hamp expression in *Ank1*^{+/*Ity16*} mice later during infection (Fig. 8C). To test the involvement of Hamp in the susceptibility phenotype of *Ank1*^{+/*Ity16*} heterozygous mice, we treated the mice with HAMP peptide. *Ank1*^{+/*Ity16*} heterozygous mice treated with HAMP peptide showed significant survival benefits (Log Rank (Mantel-Cox) test p=0.008) compared to heterozygous mice treated with PBS confirming the importance of HAMP in the host response to *Salmonella* infection (Fig. 8H).

DISCUSSION:

We report here the identification of a novel mutation (*Ity16*) in the gene *Ank1* identified in an ENU recessive screen for susceptibility to typhoid-like disease in mice. The mutation consists in a nonsense mutation (p.Gln1357Ter) located in the spectrin binding domain of *Ank1*. ANK1 protein was not detected in RBC ghosts suggesting that *Ank1*^{*Ity16*} is a null allele although we could not exclude the possibility that low levels of other ANK1 isoforms lacking the N-terminal region may remain undetected. Mice carrying the homozygous allele for *Ank1*^{*Ity16*} present clinicopathological features of human hereditary spherocytosis (HS) which is the most common cause of inherited chronic hemolysis in Europe and North America with a prevalence in population of 1 in 2000 [287, 288]. Clinical manifestations of the human disease range from mild subclinical to severe life-threatening [271]. HS is characterized by spherocytic erythrocytes, splenomegaly, hyperbilirubinemia, thrombosis, leukocytosis and cardiac hypertrophy [276] and is predominantly caused by mutations in one of the erythroid membrane cytoskeleton components including ANK1, Band 3 (SLC4A1), α -spectrin (SPNA), β -spectrin (SPNB), and protein 4.2 (EBP4.2) [271]. Mutations in the *ANK1* gene accounts for about 50% of genetically defined cases of HS and most cases of HS associated with *ANK1* mutations [276](>80%) show a dominant mode of inheritance [271]. In HS and in mice lacking ANK1, the consequence of the ineffective erythropoiesis, extramedullary hematopoiesis and retention of abnormal RBC is splenomegaly and tissue iron overload leading to oxidative damage and cardiac failure (reviewed in [289]).

In addition to the mutation described in the current paper, five mutations within the *Ank1* locus have been reported (Fig. 3B). Two of them were spontaneous recessive mutations (*Ank1*^{*nb*} and *Ank1*^{*pale*}), two additional one were identified in dominant ENU screens for blood cell phenotypes (*Ank1*^{*RBC2*} and *Ank1*^{*E924X*}) and the last one, in a dominant screen for resistance to malaria in SJL/J mice (*Ank1*^{*MRI23420*}) [245, 246, 272-274]. Mice carrying the *Ity16*, *nb*, *RBC2*, *E924X* or *MRI23420* allele at *Ank1* present characteristic clinicopathological features of HS including severe anemia, reticulocytosis, splenomegaly with complete effacement of the normal splenic architecture, multiorgan iron overload and low body weight. Embryonic and neonatal lethality is observed and may vary according to the genetic background and the

position of the mutation ([245, 273] and current paper). *Ank1*^{lty16/lty16} mutants are on a mixed DBA/2J X 129/S1 background and most homozygous are viable (18%; the expected ratio is 25%) and survive to at least 6 months of age. In mutant *Ank1* mice where there is 100% neonatal mortality, the death was associated with severe clinical signs of jaundice due to massive hemolysis [246].

The severity of anemia in *Ank1*^{lty16/lty16} mutant mice and other ENU-induced *Ank1* mutants (*Ank1*^{RBC2} and *Ank1*^{E924X}) was similar with hematocrit levels varying between 22-27%.

Reticulocytosis was present in all mutants and significantly different from control mice.

Ank1^{lty16/lty16} mutant mice exhibit extensive iron accumulation in several organs including the kidneys, a pathological observation that was not reported in other *Ank1* mutants [245, 272-274].

A normal iron balance in the host is required for adequate innate and adaptive immune responses. This is well illustrated by the observation that both iron overload and iron depletion impaired the host immune response in humans and in animal models of infections [156, 267, 268, 290]. Iron overload is known to influence the course of infection by favoring microbial replication and also by affecting antimicrobial immune effector mechanisms. Iron overload has several consequences on the immune system including decreased capacity of macrophage to phagocytose, reduced neutrophil migration, modifications of T-cell subsets, suppression of the complement system, and increased oxidative stress leading to tissue damage [291]. Additionally, acute iron depletion in mice increased their susceptibility to *Salmonella* infection because of impaired NADPH-dependent respiratory burst activity [292]. In the current study, we present several evidences showing that iron overload is an important mechanism in influencing bacterial load including the concomitant presence of iron overload and high bacterial burden in liver and kidneys and the observation that *Salmonella* strain deficient in iron uptake grows better in the iron rich environment of *Ank1*^{lty16/lty16} liver. We do also show that in heterozygous *Ank1*^{+/lty16} mice, higher bacterial load is detected only in tissues where iron accumulation is detected. These results clearly show the importance of iron overload in susceptibility to *Salmonella* infection in *Ank1*^{lty16/lty16} and *Ank1*^{+/lty16} mice.

In *Ank1* mutant mice and HS patients, the normal life span of erythrocytes in the peripheral blood is substantially shortened and retention of abnormal erythrocytes by the spleen was

shown to be the dominant mechanism for their reduced life-span [245, 271]. Hemolysis of erythrocytes results in the liberation of heme which induces the expression of *Hmox1*. HMOX1 catalyzes the degradation of heme to carbon monoxide, biliverdin that is converted to bilirubin and ferrous iron [293]. In *Ank1^{lty16/lty16}* mutant mice, we observed high serum bilirubin levels and iron overload in the liver and the kidneys but not in the spleen. High *Hmox1* mRNA levels was observed in the liver and the kidneys but not in the spleen of mutant mice suggesting that the iron overload present in the liver and kidneys resulted from degradation of heme by *Hmox1*. Low levels of *Hmox1* in the spleen of mutant mice are most likely a consequence of splenic macrophage depletion (data not shown) and could explain the observation that there is no iron deposition in the spleen of mutant mice and less bacterial growth considering that hemophagocytic macrophages may provide a survival niche for *Salmonella* [294]. Of particular interest, increased levels of *Hmox1* has been recently shown to impair resistance to *Salmonella* infection in a context of hemolysis through the suppression of the oxidative burst capacity of neutrophils [295], suggesting that high *Hmox1* levels in *Ank1^{lty16/lty16}* mutant mice may contribute to their susceptibility.

It has been shown that the kidney plays an important role in iron metabolism. It has also been reported that a significant amount of serum iron is filtered by the glomeruli and is reabsorbed [296]. In *Ank1^{lty16/lty16}* mutant mice, the excessive iron load in the kidneys most likely results from the high rate of hemoglobin filtration and reabsorption by renal tubular cells. Iron deposition in glomeruli, and proximal and distal tubules of the kidney has been observed in chronic experimental hemosiderosis [297]. With aging, *Ank1^{lty16/lty16}* mutants develop a more severe nephropathy compared to heterozygous and wild type animals and are more susceptible to infection as measured by increased in bacterial proliferation upon infection. The higher degree of iron accumulation in liver and kidneys in older animals is most likely responsible for these observations.

Another hallmark of ineffective erythropoiesis in *Ank1^{lty16/lty16}* mutant mice is an increase in *Epo* and *Gdf15* levels associated with suppression of *Hamp* expression. *Hamp* expression is known to be regulated by intestinal iron absorption, iron recycling by macrophages and iron mobilization from hepatic stores by inhibiting iron export through its binding to *Slc40a1* causing

its internalization [146]. In *Ank1^{lty16/lty16}* mice, low *Hamp* expression had a modest impact on the expression of *Slc40a1* in the liver. The synthesis of *Hamp* is also upregulated in hepatocytes by inflammatory cytokines and inhibited by anemia, hypoxia and erythropoietic activity [298, 299]. As a consequence of anemia and in response to tissue hypoxia, increased expression of *Epo* is detected in the kidneys. Despite these changes to compensate for erythrocyte demand, erythropoiesis is not efficient and led to massive expansion of the erythroid compartment. GDF15 is a member of the TGF β superfamily that was shown to negatively regulate the expression of *Hamp* *in vitro* [300, 301]. In fact, upregulation of GDF15 and suppression of *HAMP* have been observed in β -Thalassemia and it is thought that erythroid expansion influences the regulation of *HAMP* expression through systemic release of GDF15 from erythroblasts [286, 302]. Low levels of *Hamp* in response to ineffective erythropoiesis, as observed in *Ank1^{lty16/lty16}* mutant mice, clearly exacerbate extramedullary erythropoiesis, tissue iron deposition and splenomegaly. During infection, liver *Hamp* expression levels remain suppressed and *Gdf15*, *Il1* and *Il6* expression increased significantly in *Ank1^{lty16/lty16}* mutant mice compared to wild type littermates. *Gdf15* has been shown to be highly expressed in macrophages stimulated with LPS and to be modulated by several cytokines including IL-1 [303] and by intracellular iron depletion *in vitro* [304]. The high *Gdf15* expression observed during infection in *Ank1^{lty16/lty16}* mutant mice could be explained by the progression of anemia and expansion of the erythroid compartment, by the high expression of cytokines induced by infection with *Salmonella* or as a consequence of intracellular iron deprivation due to low levels of *Hamp* expression.

Salmonella susceptibility in *Ank1^{lty16/lty16}* differs from that observed in the iron overload disorder, hereditary hemochromatosis (HFE). *Hfe*-deficient mice do not lack *Hamp*, present excessive accumulation of iron in the liver and improve resistance to *Salmonella* infection [305]. In *Hfe*-deficient mice, high lipocalin-2 (*Lcn2*) levels were observed in the liver and the spleen prior infection and increased resistance to infection in these mice was associated with higher induction of *Lcn2* expression that was shown to reduce the availability of iron for *Salmonella* within macrophages [305]. In *Ank1^{lty16/lty16}* mutant mice, the spleen and liver expression of *Lcn2* did not differ from that observed in littermate controls prior infection however we did observe a significant increase in the spleen and liver expression of *Lcn2* during infection (data not

shown). There were no significant differences between genotypes in the spleen in contrast levels of *Lcn2* were significantly higher (by a factor of 1.5 LOG) in the liver of *Ank1^{lty16/lty16}* mutant mice compared to littermate controls and parallel the high bacterial loads detected in this organ. Altogether, these data suggest that high levels of *Lcn2* expression in a context of low *Hamp* expression do not protect *Ank1^{lty16/lty16}* mutant mice from systemic *Salmonella* infection.

Of particular interest was the intermediate susceptibility of *Ank1^{+/lty16}* mice to infection with *Salmonella* Typhimurium. In heterozygous mice, there is only one functional copy of *Ank1* which may be limiting to confer a normal structure to the RBC membrane and cause a partial loss of membrane surface. Although the half-life of RBC appears not to be affected in *Ank1^{+/lty16}* mice, small increase in osmotic fragility has been reported which may lead to more RBC destruction by the spleen [245]. In fact, we did observe an increase in extramedullary erythropoiesis in the spleen of *Ank1^{+/lty16}* mice although the mice were not anemic. The phenotype observed in *Ank1^{+/lty16}* mice may correspond to the human mild form of HS where patients have compensated hemolysis without anemia. As observed in uninfected *Ank1^{lty16/lty16}* homozygous mice, liver and kidneys *Hamp* levels were low compared to controls and levels of *Gdf15* were increased. *Hamp* is mainly produced by the liver but it has been found also to be highly expressed in the apical pole of epithelial cells of distal tubules and collecting ducts of the kidney [285, 306]. In humans, diminished serum hepcidin concentration has been observed in human erythroid pathologies where there is no anemia but an increased in red cell mass as seen in primary polycythemia [307]. In *Ank1^{+/lty16}* mice, the *Salmonella* susceptible phenotype appears to be expressed predominantly in the kidney where we found significant accumulation of iron and bacteria. Low levels of *Hamp* expression in *Ank1^{+/lty16}* heterozygous mice at the time of infection appears to contribute to iron accumulation in the kidney and liver and consequently favor bacterial growth. The central role of *Hamp* in the host response to *Salmonella* infection was validated using mice deficient for *Hamp*. These mice are not anemic and present an important iron overload secondary to low level of *Hamp* a phenotype similar to the one observed in heterozygous mice [278] and are highly susceptible to *Salmonella* infection (current paper). Finally, direct evidence of the role of *Hamp* in the host response to *Salmonella*

infection was obtained by treating $Ank1^{+/Ity16}$ mice with hepcidin. Hepcidin treatment did not improve resistance of $Ank1^{Ity6/Ity16}$ mutant mice where iron accumulation in tissues is massive however it was clearly beneficial in $Ank1^{+/Ity16}$ heterozygous mice. We do not know at the moment the exact mechanism of how hepcidin is improving resistance to infection in $Ank1^{+/Ity16}$ heterozygous mice. Induction of hepcidin through transgenesis in mouse models of hemochromatosis and β -Thalassemia was shown to alter the pattern of cellular iron accumulation and limit iron overload [308, 309]. In addition, administration of an hepcidin agonist in $Hamp^{-/-}$ mice caused a partial redistribution of iron from the liver to the spleen [310]. An antimicrobial effect of hepcidin could be also considered although the impact of hepcidin on bacterial growth has been shown only *in vitro* [311]. Overall, the current study shows that the suppression of *Hamp* expression and iron overload contributes to the susceptibility of $Ank1^{Ity16/Ity16}$ mutant and $Ank1^{+/Ity16}$ heterozygous mice to *Salmonella* infection. This emphasizes the importance of iron metabolism and a role for HAMP in susceptibility to systemic *Salmonella* infection.

ACKNOWLEDGEMENTS:

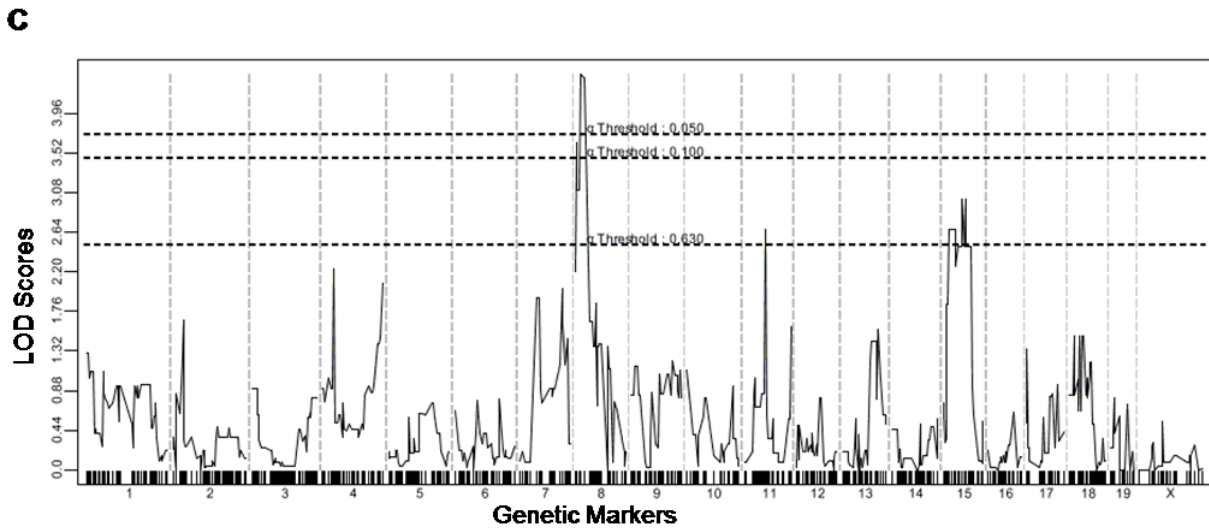
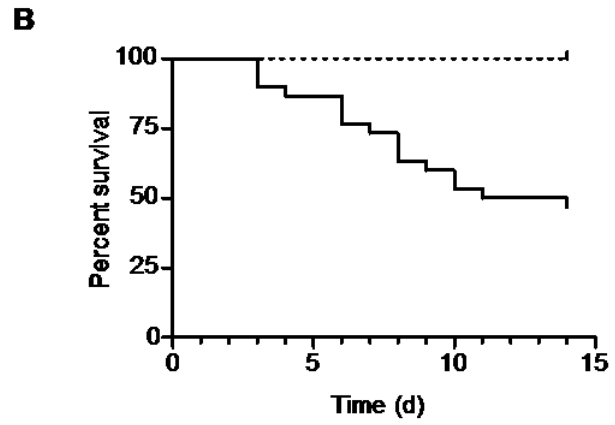
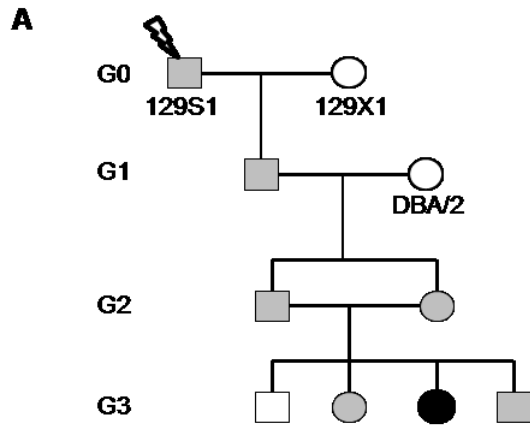
We are grateful for the excellent technical assistance of Nadia Prud'homme and Line Larivière.

We wish to thank Sean Beatty for his help with the analysis of the data, and Pratixa Gandhi from CMARC for the hematology analyses and Jo-Ann Bader and Caroline Therien from the GCRC histology facility for their excellent work.

FIGURES AND FIGURE LEGENDS

FIGURE 1: IDENTIFICATION AND MAPPING OF THE *ITY16* PEDIGREE

A) Breeding scheme used to identify and map the mutant family. Females and males are represented by circles and squares respectively with black representing the homozygous mutant alleles, gray representing the heterozygous alleles, and white representing the wild type alleles. **B)** Survival curve of the G3 mice from the *Ity16* pedigree is represented by the solid line (n=30) while wild type 129S1 (n=5) mice are represented by dotted lines. Log-Rank (Mantel-Cox) $p=0.01$. **C)** Linkage analysis in 8 *Salmonella*-susceptible and 14 *Salmonella*-resistant mice identifies a significant peak on chromosome 8. **D)** Fine mapping of the *Ity16* locus to a 2.5 Mb region on chromosome 8. Black fill represents homozygous 129S1 allele. White fill represents heterozygous or homozygous DBA/2 genotypes. **E)** Survival curves of *Ity16* mice according to their genotypes at peak marker on chromosome 8. Solid line represents homozygous 129S1 alleles (n=6), dashed line represents heterozygous (n=12), and dotted line represents homozygous DBA/2 alleles (n=12). Log-Rank (Mantel-Cox) for $Ank1^{+/+}$ and $Ank1^{Ity16/Ity16}$ $p<0.0001$, $Ank1^{+/+}$ and $Ank1^{+/Ity16}$ $p=0.001$.



D

markers	Mb
Rs13479608	11.7
Rs32549327	12.3
Rs13479619	15.3
D8Mit61	15.6
Rs32892593	16.9
Rs33527586	23.5
Rs32874474	24.2
Rs33420248	24.3
CEL-	
8_25963079	26.0
Rs32926278	28.0
D8Mit94	32.8
D8Mit4	33.5
Rs13479716	38.8

Affected	0	0	1	1	1	2	0	0	0	0
Unaffected	1	1	0	0	0	0	6	6	7	1

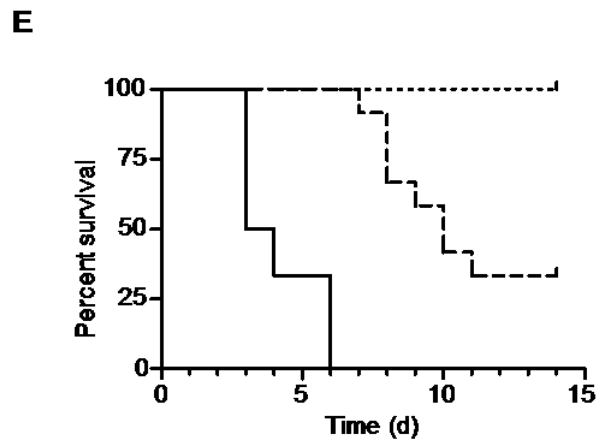


FIGURE 2: *ITY16* MUTANT MICE PRESENT MASSIVE SPLENOMEGALY, MODERATE INCREASE IN KIDNEYS AND HEART WEIGHTS AND BILIRUBINEMIA

A) Body weight of wild type littermates and *Ity16* mice by sex (males are represented by squares, females by circles) at 7 weeks (open and black fill) and 24 weeks (open and black fill) n=3 per sex and genotype. **B)** Serum bilirubin levels were measured at day 0 and day 2 post infection in wild type (open circle), heterozygous (gray circle) and *Ity16* mutant (black circle) mice. **C)** Increased spleen, kidney and heart weights in *Ity16* mutant (black fill) mice compared to wild type littermates (open fill). The data are presented by sex (males are squares, females are circles). Results are representative of at least two experiments. An * represents a P-value of less than 0.05; ** represents a P-value of less than 0.001; *** represents a P-value of less than 0.0001.

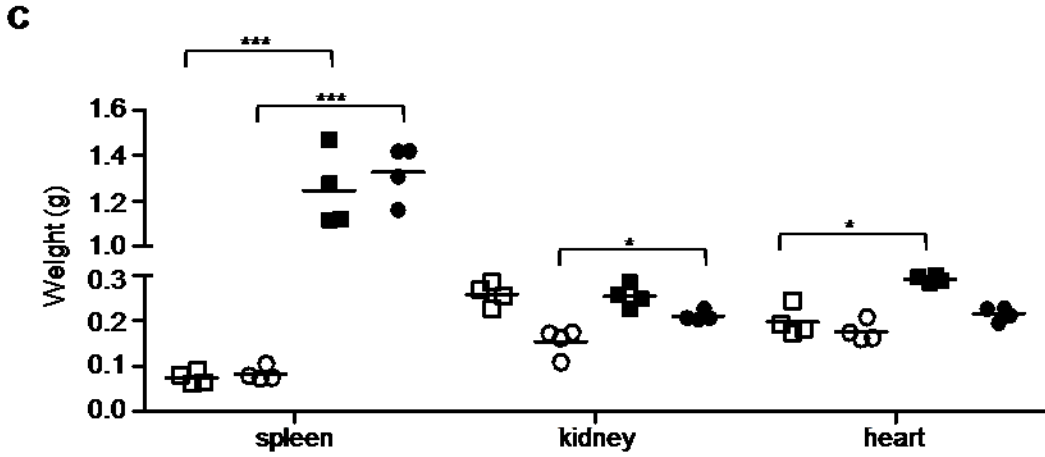
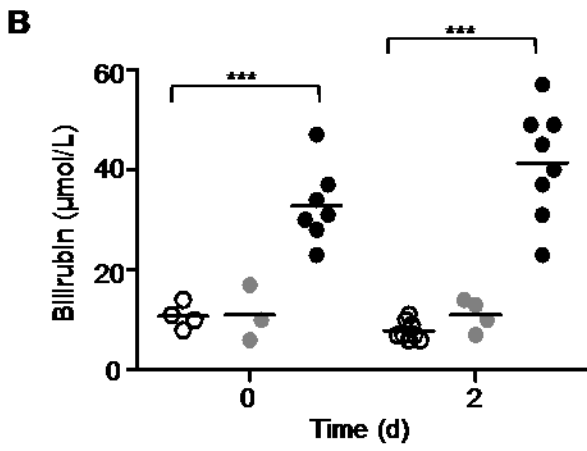
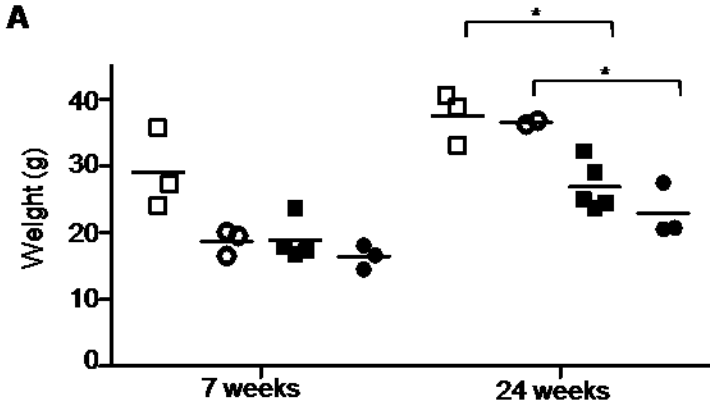


FIGURE 3: *ITY16* MUTANT MICE CARRY MUTATION WITHIN THE *ANK1* GENE

A) A C to T transition (arrow) at cDNA position 4069 (c.4069C>T) resulting in a stop codon at amino acid position 1357 (p.Gln1357Ter) was detected in *Ank1*^{*ity16/ity16*} mutant. The *Ity16* mutation is located in exon 33 using the exon numbering of the *Ank1* transcript ID ENSMUST00000121802 (Ensembl build 37). **B)** Schematic representation of the different domains of ANK1 (adapted from [312]) and location of mutations previously identified in human (small ticks) [275] and mouse ANK1 [245, 246, 272-274]. The *Ity16* allele is shown together with two spontaneous ANK1 recessive mutations (*nb* and *pale*) and three dominant mutants (*RBC2*, *M1W1st* and *MRI23420*). **C)** Immunoblot of RBC ghosts prepared from wild-type (+/+), heterozygous (+/m) and mutant *Ank1* (m/m) littermates probes with ANK1 antibody. The size of the molecular markers in kDa are shown on the left. An expected band of about 210 kDa was observed in samples from the wild-type and heterozygous mice while this band or any smaller bands corresponding to a truncated version of the protein could not be detected in mutant mice.

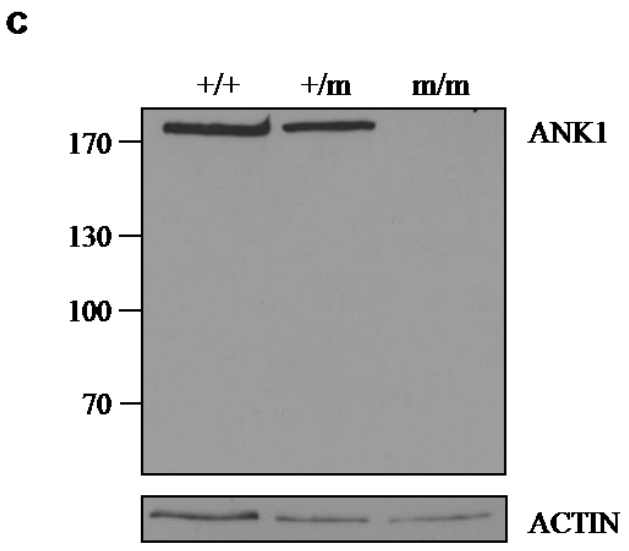
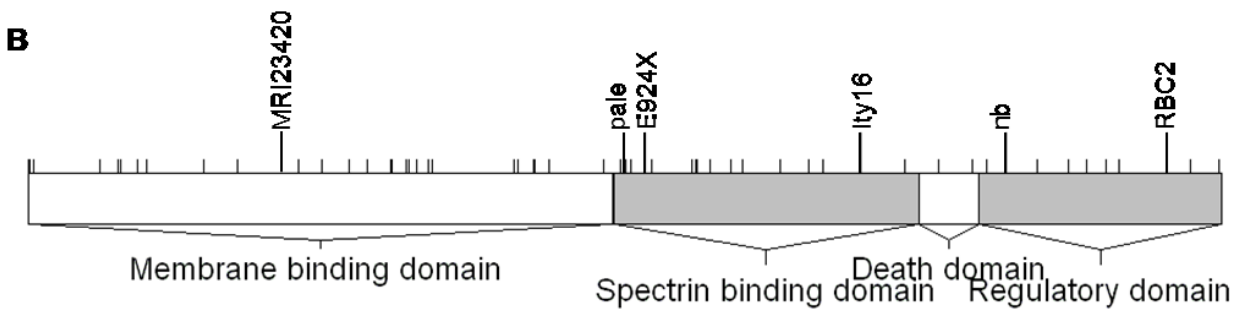
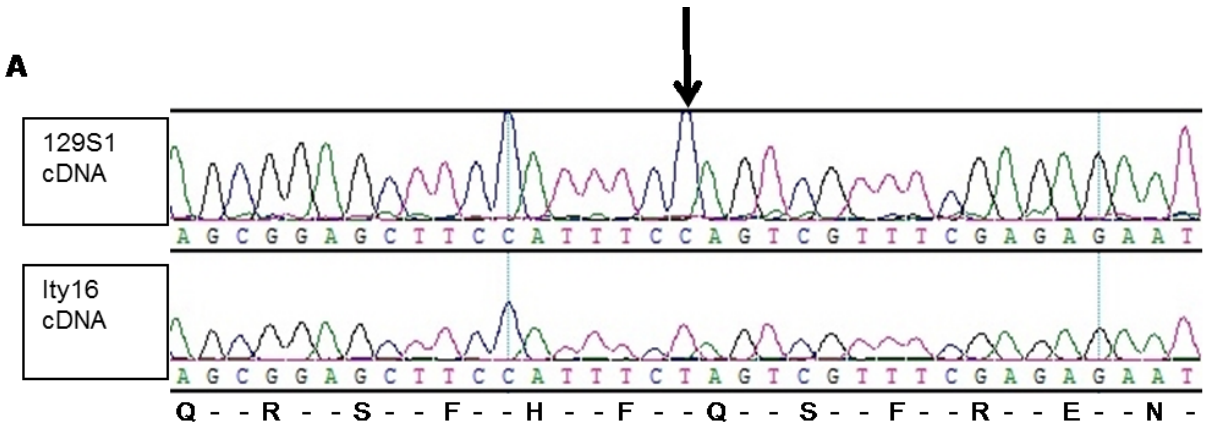


FIGURE 4: BACTERIAL LOAD IN SPLEEN, LIVER AND KIDNEY AFTER INFECTION WITH *SALMONELLA* TYPHIMURIUM IN *ITY16* MUTANT, HETEROZYGOUS AND WILD TYPE MICE

The bacterial load was measured 2 days after infection in the spleen (**A**), liver (**B**), and kidney (**C**) of wild type aged 7 weeks (open circle), and 24 weeks (open circle), heterozygous mice at 7 weeks (gray circle) and 24 weeks (gray circle) and *Ity16* mutant mice at 7 weeks (filled circle) and 24 weeks (filled circle) (n=3-5 per genotype and age). *Ity16* mutant mice present higher bacterial load in the liver and kidneys compared to heterozygous and wild type littermates. Bacterial load of *Salmonella* Typhimurium and $\Delta tonB$ *Salmonella* Typhimurium was measured 2 days after infection in spleen (**D**) and liver (**E**) of wild type (open circle), heterozygous (gray circle) and *Ity16* (black circle) mice aged 7-12 weeks (n=3-8 per genotype). Results are representative of at least two experiments. An * represents a P-value of less 0.05; **represents a P-value of less than 0.001; ***represents a P-value of less than 0.0001.

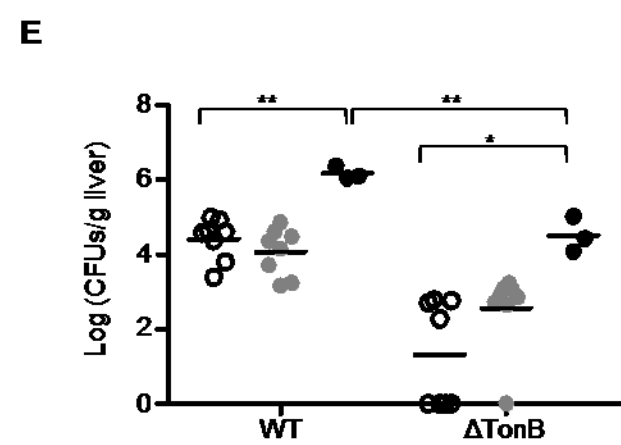
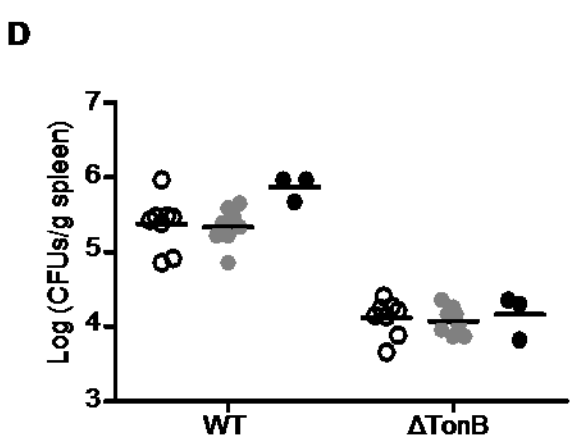
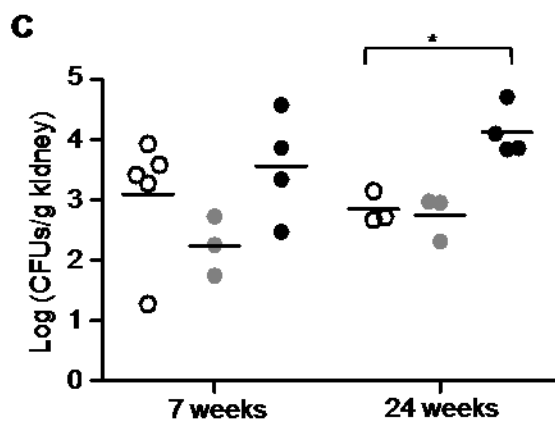
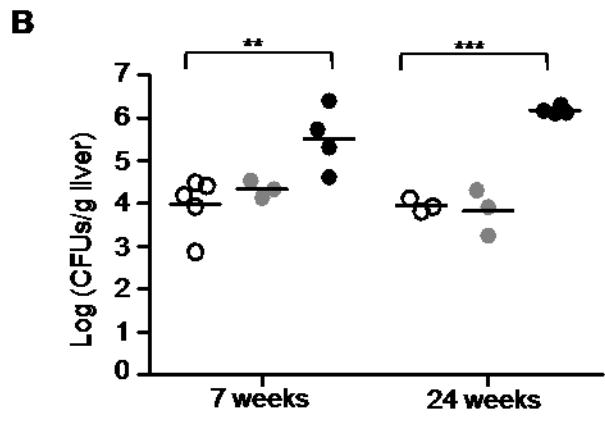
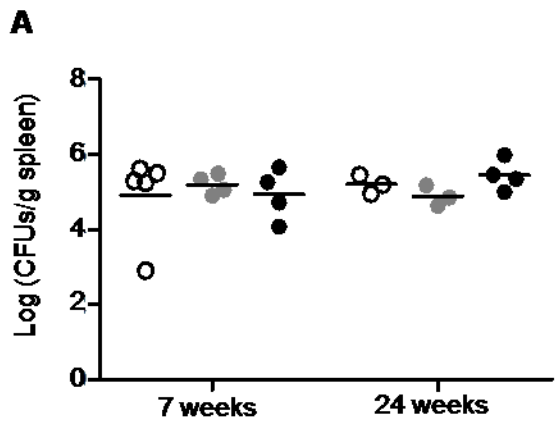


FIGURE 5: *ITY16* MUTANT MICE PRESENT ELEVATED BLOOD UREA NITROGEN (BUN), ALANINE TRANSAMINASE (ALT) AND ASPARATATE TRANSAMINASE (AST) DURING *SALMONELLA* INFECTION

BUN (A), ALT (B) and AST (C) levels were measured at day 0 (prior to infection) and day 2 post infection in 7 week old *Ank1*^{+/+} wild type, *Ank1*^{+/Ity16} heterozygous and *Ank1*^{Ity16/Ity16} mutant mice. The values for each individual mouse are shown (n=3-8 per genotype). Wild type mice are represented by open circles, heterozygous by gray circles and *Ity16* mutant by black circles. The high levels of BUN levels detected in mutant mice at day 0 most probably reflect the nephrotoxicity of iron accumulation in the kidney. During infection BUN, ALT and AST levels increased in mutant mice denoting kidney and liver damage. An *represents a P-value of less than 0.05; *** represents a P-value of less than 0.0001.

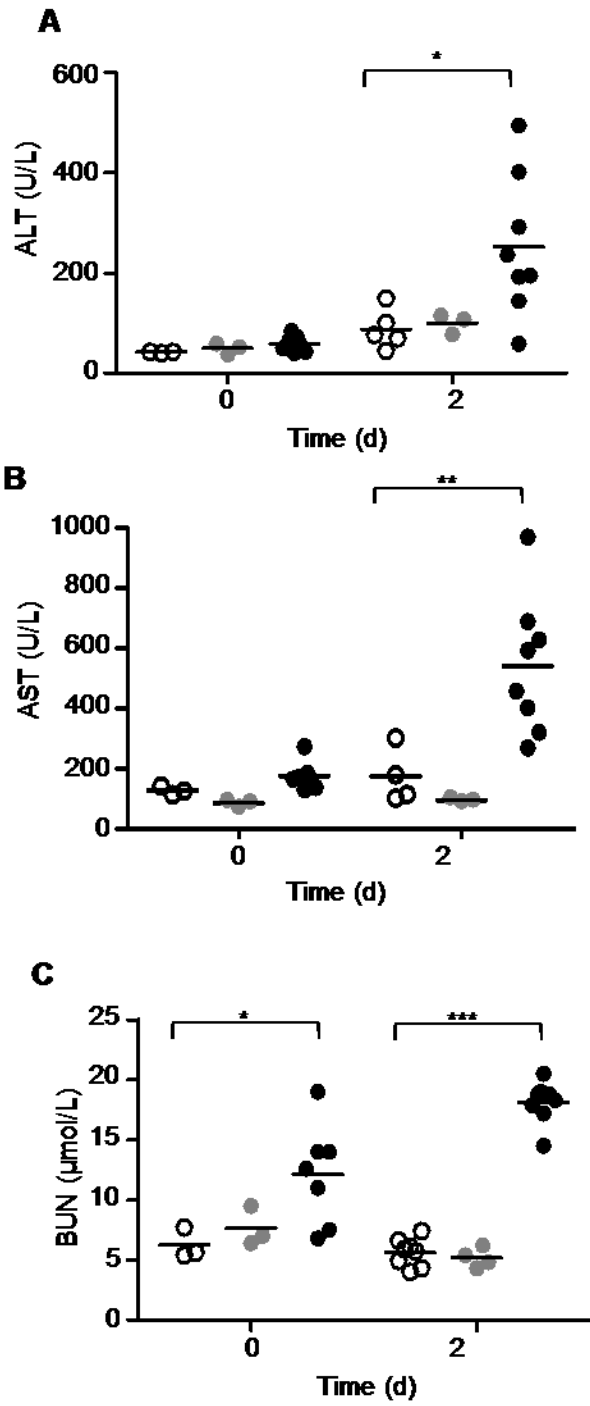


FIGURE 6: TISSUE EXPRESSION OF GENES INVOLVED IN IRON METABOLISM IN 7 WEEK OLD $ANK1^{+/+}$ WILD TYPE AND $ANK1^{ITY16/ITY16}$ MUTANT MICE

Real-time PCR expression of liver *Hamp* (A), kidney *Epo* (B), spleen, liver and kidney *Slc40a1* (C), and spleen and liver *Gdf15* (D). The relative mRNA levels at day 0 and day 2 post infection are shown in $ANK1^{+/+}$ wild type (clear bar, n= 3) and $ANK1^{ITY16/ITY16}$ mutant (black bar, n=3) mice. *Epo* mRNA levels are represented on a LOG_{10} scale. (E) Survival curves of *Hamp* knock out mice (129S6.B6*129S2- $Hamp^{tm1Svl}$) infected with 8000 CFUs of *Salmonella* Typhimurium. Solid line represents homozygous $Hamp^{-/-}$ knock out (n=8), dashed line represents heterozygous $Hamp^{+/-}$ (n=12), and dotted line represents homozygous wildtype $Hamp^{+/+}$ alleles (n=10). Log-Rank (Mantel-Cox) for $Hamp^{+/+}$ and $Hamp^{-/-}$ p=0.0071. An *represents a P-value of less than 0.05; ** represents a P-value of less than 0.001; *** represents a P-value of less than 0.0001.

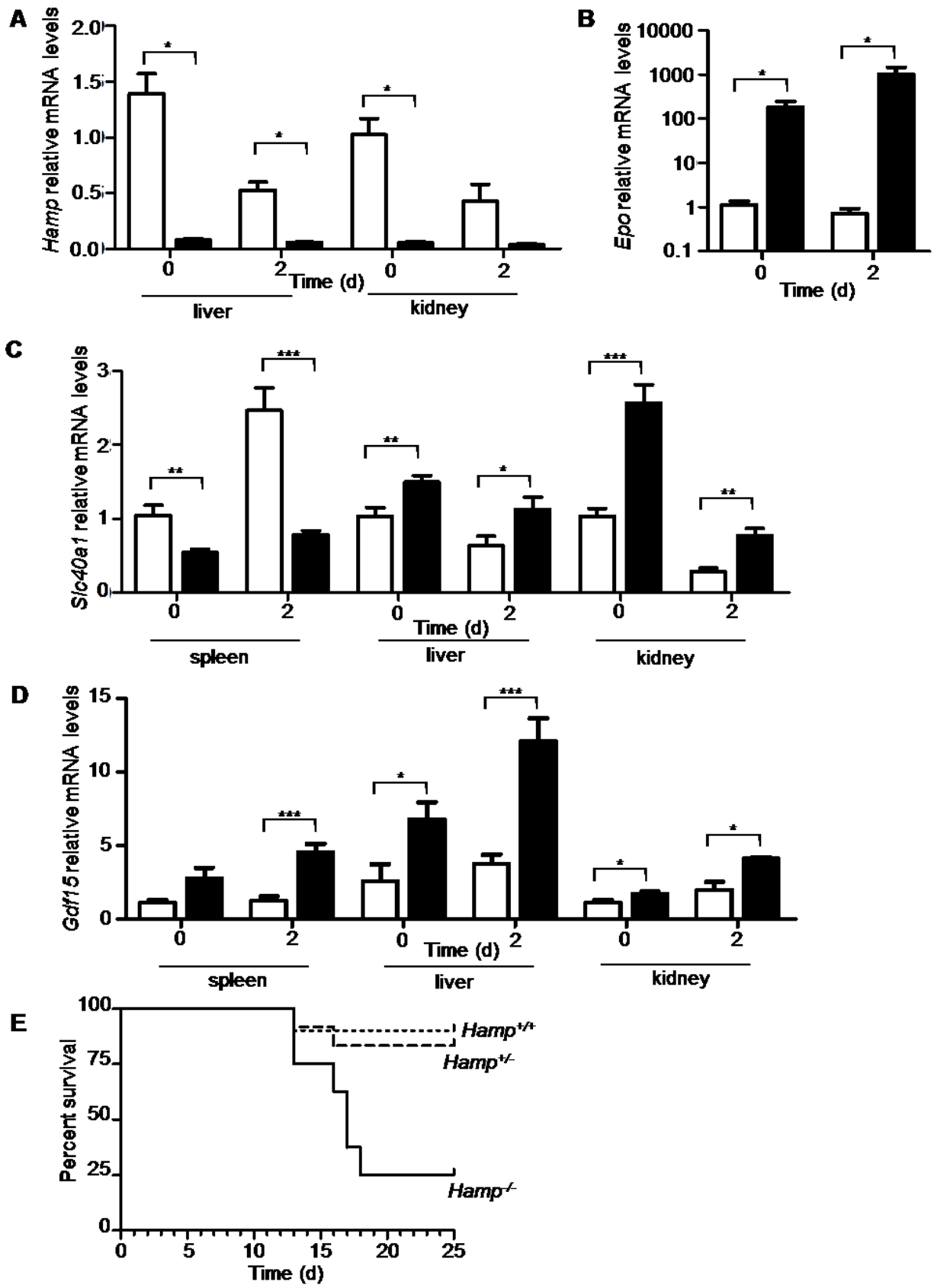


FIGURE 7: CYTOKINE PROFILES IN 7 WEEK-OLD $ANK1^{+/+}$ WILD TYPE AND $ANK1^{lTY16/lTY16}$ MUTANT MICE DURING INFECTION WITH *SALMONELLA* TYPHIMURIUM

Relative spleen, liver and kidney mRNA levels are shown for *Il1* (A), *Il6* (B), and *Hmox1* (C) at day 0 and day 2 post infection. $Ank1^{+/+}$ wild type mice (n=3) are represented by clear bar and $Ank1^{lty16/lty16}$ mutant mice (n=3) by a black bar. All values are compared to wild type mRNA levels at day 0 and presented on a LOG_{10} scale. An * represents a P-value of less than 0.05; ** represents a P-value of less than 0.001; *** represents a P-value of less than 0.0001.

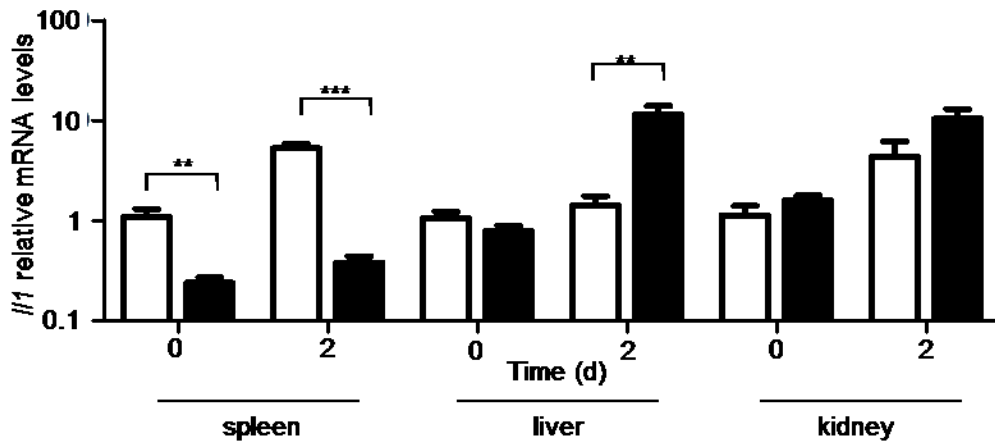
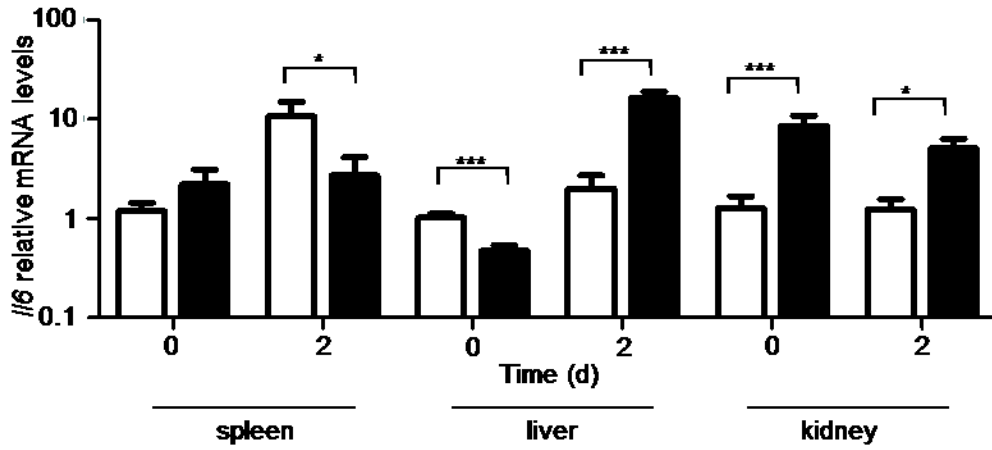
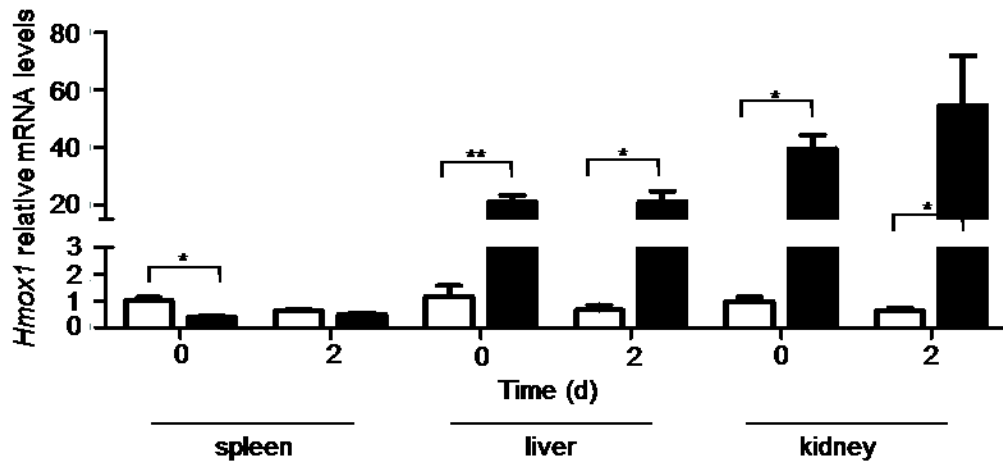
A**B****C**

FIGURE 8: CHARACTERIZATION OF $ANK1^{+/ITy16}$ HETEROZYGOUS MICE

RBC counts **(A)** and bacterial burden in spleen, liver and kidney **(D)** were measured in 7 week old $Ank1^{+/+}$ wild type and $Ank1^{+/Ity16}$ heterozygous mice at day 0 (prior infection), day 2 and day 6 post infection. Wild type $Ank1^{+/+}$ mice are represented by clear circles and $Ank1^{+/Ity16}$ heterozygous mice by gray circles. Relative kidney mRNA levels are shown for *Hamp* **(C)**, *Il1* **(E)**, *IL6* **(F)** and *Epo* **(G)** at day 0, day 2 and day 6 post infection. **(B)** Relative liver *Hamp* levels at day 0, day 2 and day 6 post infection. Wild type $Ank1^{+/+}$ mice are represented by clear bars (n=3 for day 0 and day 2; n=4 for day 6) and $Ank1^{+/Ity16}$ heterozygous mice by gray bars (n=3 for day 0 and day 2; n=4 for day 6). **(H)** Survival curves of $Ank1^{+/+}$ wild type (n=5; open circle) and $Ank1^{+/Ity16}$ heterozygous (n=5; gray circle) mice with (n=5; dashed or dotted line) or without (n=5; solid line) HAMP treatment infected with 5000 CFUs of *Salmonella* Typhimurium. Log-Rank (Mantel-Cox) for $Ank1^{+/Ity16}$ heterozygous with and without HAMP treatment p=0.008. The experiment was repeated twice. An * represents a P-value of less than 0.05; ** represents a P-value of less than 0.001; *** represents a P-value of less than 0.0001.

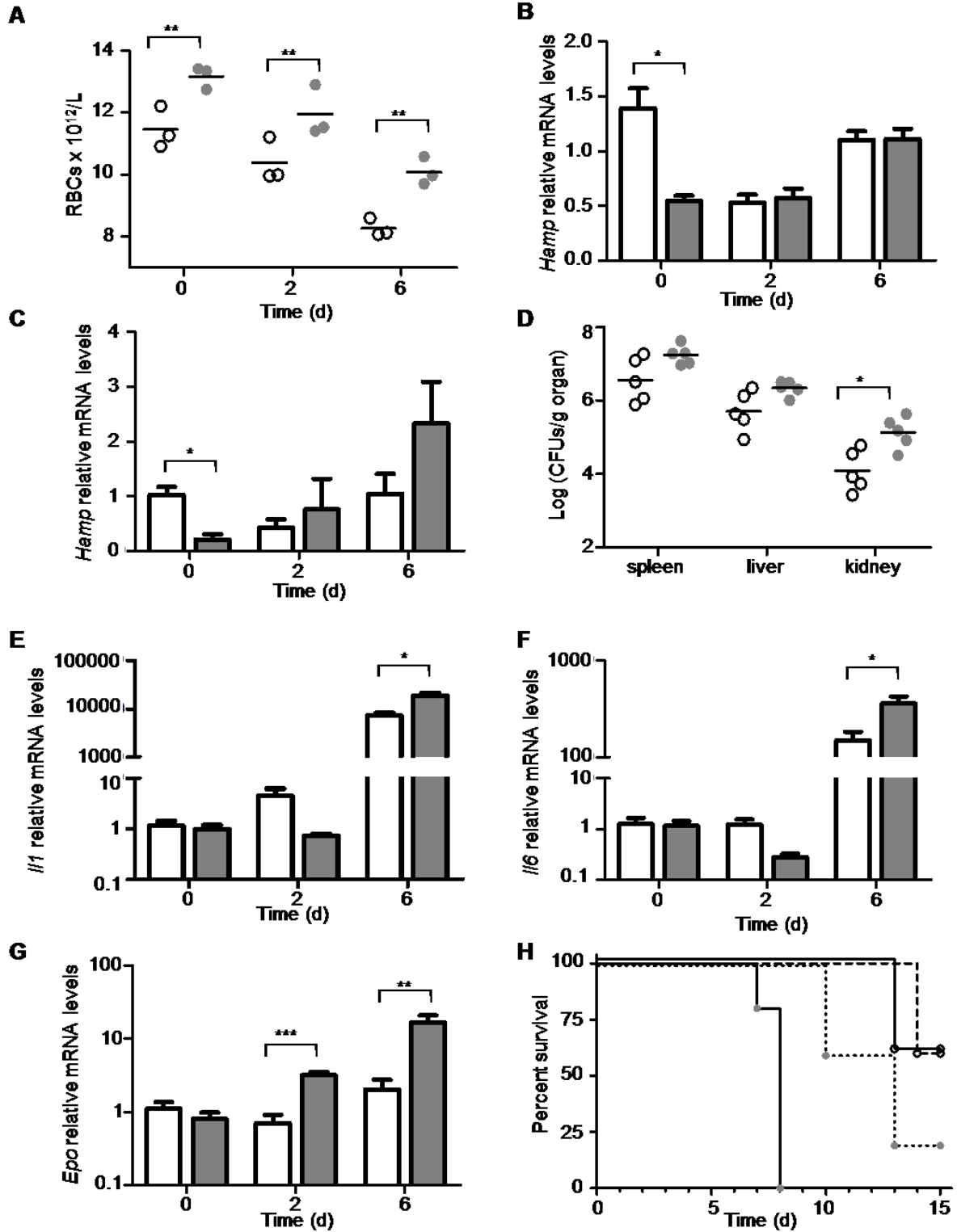


TABLE 1: RBC HEMATOLOGICAL PARAMETERS

Genotype	Day 0			Day 2		
	<u>Wt</u>	<u>Heterozygous</u>	<u>lty16</u>	<u>Wt</u>	<u>Heterozygous</u>	<u>lty16</u>
Hematocrit L/L	0.523 ± 0.007	0.549 ± 0.017	0.252 ± 0.013*	0.519 ± 0.011	0.526 ± 0.023	0.190 ± 0.020*
Hemoglobin g/L	167 ± 0.88	169 ± 5.57	76.9 ± 4.02*	164 ± 3.26	165 ± 7.22	57.5 ± 6.17*
RBCs x 10 ¹² /L	11.5 ± 0.39	13.2 ± 0.21	5.47 ± 0.25*	10.7 ± 0.23	11.9 ± 0.48	3.98 ± 0.39*#
WBCs x 10 ⁹ /L	10.76 ± 2.92	9.73 ± 1.64	35 ± 5.07	9.85 ± 0.65	11.13 ± 1.73	22.92 ± 3.01*
% reticulocytes	5.1 ± 0.17	5.03 ± 0.64	44.9 ± 7.68*	4.7 ± 0.42	5.1 ± 1.36	33.1 ± 5.60*
neutrophils x 10 ⁹ /L	1.17 ± 0.38	0.86 ± 0.12	2.36 ± 0.99	2.08 ± 0.25	2.55 ± 0.38	7.54 ± 0.98*
lymphocytes x 10 ⁹ /L	9.54 ± 2.6	8.82 ± 1.57	32.24 ± 4.59*	7.54 ± 0.52	8.54 ± 1.50	14.88 ± 2.71*
Nucleated RBCs/100 WBCs	0	2.33 ± 1.20	66.86 ± 11.15*	3.38 ± 1.74	3 ± 3	77 ± 5.58*

* p values <0.05 compared to wild type values of the same infection status

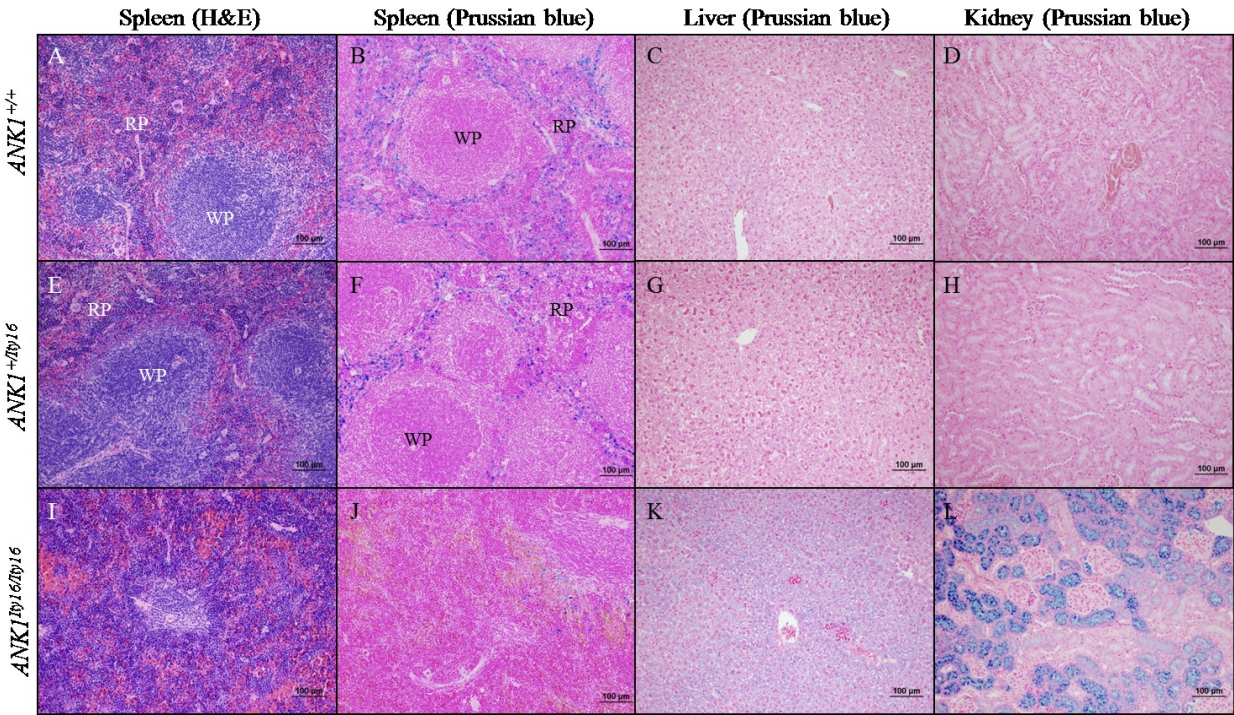
p values <0.05 compared to day 0 of the same genotype

SUPPLEMENTAL FIGURE 1: HISTOPATHOLOGIC EXAMINATION OF THE SPLEEN,
LIVER AND KIDNEY OF 7 WEEK OLD $ANK1^{+/+}$ WILD TYPE, $ANK1^{+/ITy16}$
HETEROZYGOUS, AND $ANK1^{ITy16/ITy16}$ MUTANT MICE BEFORE INFECTION (DAY 0)

H&E stain of uninfected spleen of wild type **(A)**, heterozygous **(E)**, and *Ity16* mutants **(I)**.

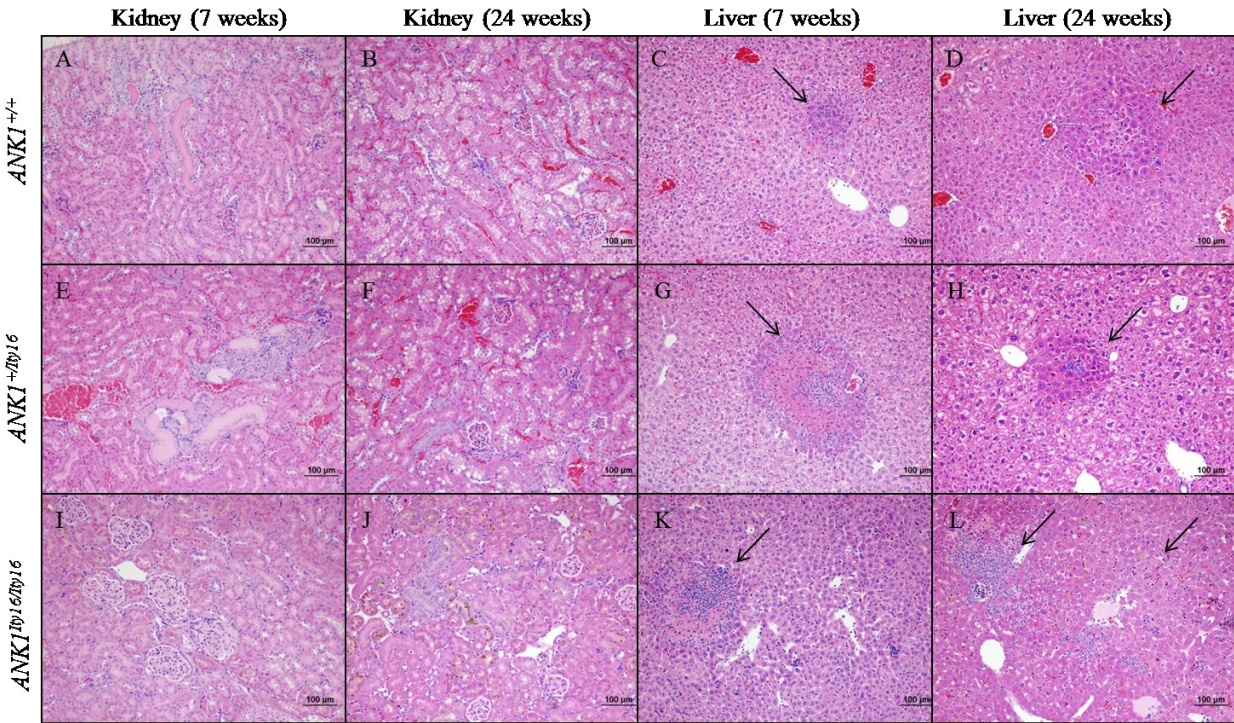
Prussian blue stain of uninfected spleen, liver and kidney, respectively, of wild type **(B,C,D)**, heterozygous **(F,G,H)**, and *Ity16* mutants **(J,K,L)**. All pictures are taken at 200x magnification.

RP = red pulp, WP = white pulp.



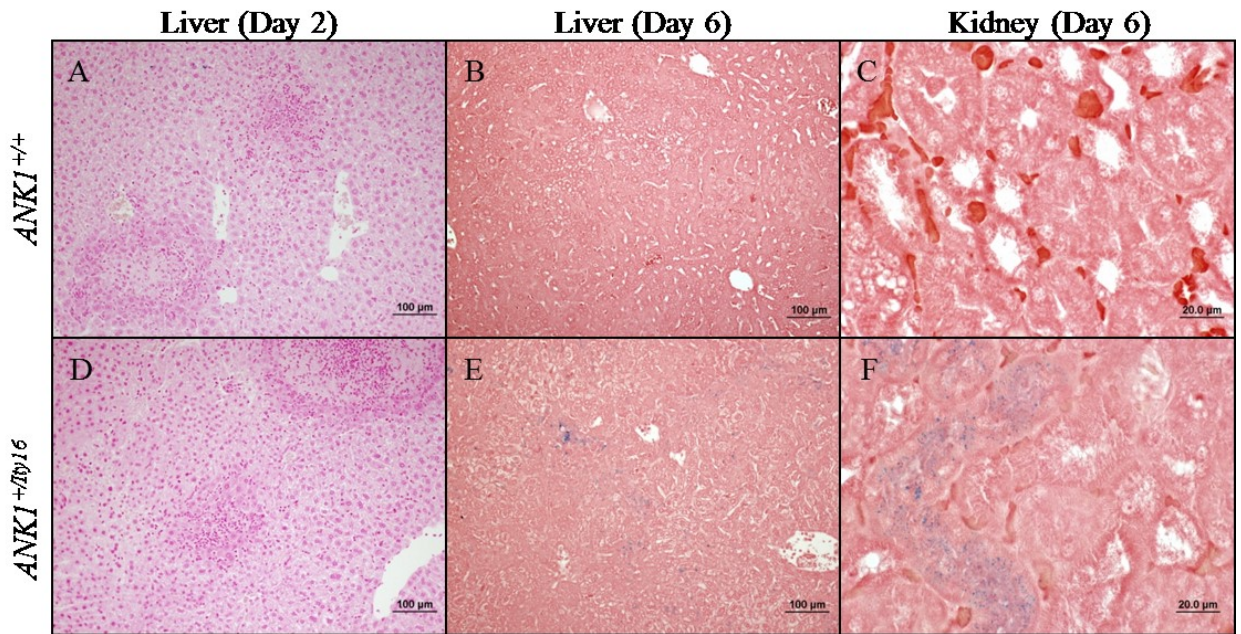
SUPPLEMENTAL FIGURE 2: PROGRESSION OF LESIONS IN KIDNEY AND LIVER 2
DAYS AFTER *SALMONELLA* INFECTION OF *ANK1*^{+/+} WILD TYPE, *ANK1*^{+/*ITY16*}
HETEROZYGOUS, AND *ANK1*^{*ITY16/ITY16*} MUTANT MICE AGED 7 AND 24 WEEKS
USING HEMATOXYLIN & EOSIN STAINING

H&E stain of uninfected kidney of wild type **(A,B)**, heterozygous **(E,F)**, and *Ity16* mutants **(I,J)** at 7 and 24 weeks of age respectively. H&E stain of day 2 post infection liver of wild type **(C,D)**, heterozygous **(G,H)**, and *Ity16* mutants **(K,L)** at 7 and 24 weeks of age respectively. All pictures taken at 200x magnification.



SUPPLEMENTAL FIGURE 3: PRUSSIAN BLUE STAINING OF LIVER AND KIDNEY OF 7 WEEK OLD $ANK1^{+/+}$ WILD TYPE AND $ANK1^{+/TY16}$ HETEROZYGOUS MICE AT DAY 2 AND DAY 6 POST INFECTION WITH *SALMONELLA* TYPHIMURIUM

Prussian blue stain of day 2 post infection liver in wild type **(A)** and heterozygous **(D)** mice at 200x magnification. Prussian blue stain of day 6 post infection liver of wild type **(B)** and heterozygous **(E)** mice at 200x magnification. Prussian blue stain of day 6 post infection kidney of wild type **(C)** and heterozygous **(F)** mice at 1000x magnification.



BRIDGING STATEMENT FROM CHAPTER 3 AND CHAPTER 4

In the previous chapter, we presented the importance of iron metabolism in regulating the outcome to *Salmonella* infection. In chapter 4, we present the phenotypic characterization of another ENU pedigree (*Ity15*) showing increased susceptibility to infection. We showed that a mutation in the gene *Fam49b* (family with sequence similarity 49, member B) underlies the susceptibility we observed in the *Ity15* pedigree. *Fam49b* is a poorly characterized transcript that is ubiquitously expressed and whose expression is regulated by LPS and type I IFN. *Fam49b* expression is modulated during infection in the spleen and liver of wild-type mice and the mutant allele is associated with low mRNA expression and no detectable protein. Although the literature on FAM49B is limited, recent papers highlighted a putative role for FAM49B in the anti-inflammatory response. Upregulation of FAM49B was shown to be associated with multiple sclerosis (MS). In Chapter 4 we showed that absence of FAM49B is accompanied by immunopathology that is detrimental to the host. We also showed that FAM49B localizes with proteins of the host cytoskeleton and may have a role in the intersection of *Salmonella* with the host cell cytoskeleton to regulate inflammation.

MUTATION IN FAM49B CAUSES SUSCEPTIBILITY TO *SALMONELLA* INFECTION

Kyoko E. Yuki^{1,2}, Megan M. Eva^{1,2}, Jessica Tjong², Jarred Chicoine^{1,3}, Gregory Caignard, Jeremy Schwartzenruber^{1,3}, Jacek Majewski^{1,3}, Mathieu Cellier⁵, Pierre-Olivier Vidalain, Rob Sladek^{1,3}, Silvia M. Vidal^{1,2}, Danielle Malo^{1,2,4}

¹Department of Human Genetics, McGill University, Montreal Canada; ²Complex Traits Group, McGill University, Montreal, Canada; ³McGill University and Genome Quebec Innovation Center,

⁴Department of Medicine, McGill University, Montreal Canada

ABSTRACT

We used a genome wide recessive screen in mutagenized mice to identify genes involved in regulating susceptibility to *Salmonella* infection. We report the identification of a novel gene *Fam49b* regulating the outcome to *Salmonella* infection. *Fam49b* is a poorly annotated gene expressed in several tissues and within immune cells. Abrogation of FAM49B resulted in uncontrolled *Salmonella* replication and septic shock. In this study, we have used proximity-dependent biotin identification (BioID) to identify a group of proteins that are found in proximity to FAM49B. The candidate interactors included AHNAK, a large scaffold protein, annexin 2 (ANXA2), a calcium and phospholipid-binding protein and several proteins (actin, vimentin, tubulin, etc) composing the cytoskeleton. Our findings suggest that FAM49B plays a role in the intersection of *Salmonella* with the host cell cytoskeleton to regulate inflammation.

INTRODUCTION:

Globally, *Salmonella* is a significant cause of mortality and disease with an estimated 150 million new cases and 1 million deaths annually resulting from three main diseases: enteric fever, invasive non-typhoidal *Salmonella* and gastroenteritis. In particular, enteric fever (consisting of typhoid and paratyphoid fever) is responsible for nearly 20 million new cases and 200,000 deaths annually [8, 9]. Typhoid, which is transmitted through the fecal-oral route through ingestion of contaminated food or water, causes a systemic disease found mainly in populations within Southeast Asia, Africa and South America with poor access to clean water and proper sanitation.

Once ingested, *Salmonella* preferentially traverses the intestinal epithelial layer through M cells overlying the Peyer's patches. Following invasion of the gut barrier, *Salmonella* is engulfed by professional phagocytes such as macrophages, dendritic cells (DCs) and neutrophils resulting in the dissemination of bacteria through the blood to secondary lymphoid organs like spleen and liver where the bacteria replicates. Final resolution and clearance of bacteria from the host is dependent on the adaptive immune response where T cells and B cells play a vital role. The final outcome to disease is a result of a complex interplay between host genetics, bacterial pathogenicity and the environment.

The host is able to detect pathogens by recognition of their numerous pathogen associated molecular patterns (PAMPs). These PAMPs are detected by Toll-like receptors (TLR) and NOD-like receptors (NLR). In particular, TLR4 and TLR5 recognize lipopolysaccharide (LPS) and flagellin expressed by *Salmonella*, respectively. The binding of ligand to its respective TLRs starts a signaling cascade that results in the production of pro-inflammatory mediators such as TNF α , IL-6, IFN γ and IFN β which orchestrates the early host response to infection. Type I IFNs have been shown to be an important player in the development of LPS-induced shock. Mice that is deficient in type I IFN production are resistant to the toxic effects of LPS [313]. In addition, hyper type I IFN production as seen in mice with a mutation in *Usp18* is susceptible to *Salmonella* infection [222]. The production of type I IFNs results in the production of a number of IFN stimulated genes which have a wide range of functions including inhibition of cell growth and the control of apoptosis [314].

In mice, infection with *Salmonella* Typhimurium manifests in a systemic disease that mimics the clinical symptoms of typhoid fever. Studies in mice have identified several immune genes important for survival to *Salmonella* including phagosome activity (*Slc11a1*^{G169D} in C57BL/6 mice), pathogen recognition (*Tlr4*^{P712H} in C3H/HeJ mice), iron metabolism and erythropoiesis (*Pknox1*^{J90N} in AcB60 mice, *Ank1*^{Gln1357Ter} in *Ity16* mice) as well as IFN signaling (*Usp18*^{L361P} in *Ity9* mice, *Stat4*^{G418_E445} in *Ity14* mice) [156, 169, 170, 222, 228, 230].

Using *N*-ethyl-*N*-nitrosourea (ENU) chemical mutagenesis recessive screen, we have identified a pedigree, *Ity15*, showing increased susceptibility to *Salmonella* Typhimurium infection. The gene underlying this pedigree was mapped and identified using exome sequencing of two affected mice. In this paper, we report the identification and characterization of a novel poorly annotated gene, *Fam49b* that influences the outcome of infection with *Salmonella*.

MATERIALS & METHODS:

Mice and ENU mutagenesis: All animal experiments were performed under conditions specified by the Canadian Council on Animal Care and the animal use protocol was approved by McGill University Facility Animal Care Committee. Generation 0 (G0) 129S1 males were mutagenized with a single injection of 150 mg per kg of body weight of *N*-ethyl-*N*-nitrosourea (ENU) given intraperitoneally. G0 males were outcrossed to 129X1 females to create G1 progeny that were subsequently outcrossed to 129X1 females. Resulting G2 females were backcrossed to parental G1 males to produce the G3 mice that were phenotyped for their susceptibility to *Salmonella* infection. The G1 male was outcrossed to a DBA/2J female to generate F1 offspring. F1s were intercrossed to generate F2s which were then used for mapping. *Fam49b* KO mice were obtained from the Canadian Mutant Mouse Repository NorCOMM.

Genotyping and exome sequencing: DNA was extracted from a tail biopsy by proteinase K digestion and phenol-chloroform extraction. The genome scan was performed using the Medium Density SNP Panel from Illumina (708 SNPs were informative between 129 and DBA/2 strains) (The Centre for Applied Genomics, Toronto, Canada). The mapping was done using 24 mice (9 susceptible and 15 resistant). Exome sequencing was performed in two susceptible animals. Exon capture was done with the SureSelect Mouse All Exon Kit (Agilent Technologies, Santa Clara, USA) and sequencing of 100-bp paired end reads on Illumina HiSeq2000 which generated over 8 Gb of sequence for each of the two susceptible samples at Centre National de Génotypage (Évry, France). Reads were aligned to mm9 with BWA and coverage assessed with BEDTools. Single nucleotide variants and short insertions and deletions were called using samtools pileup and varFilter with the base alignment quality adjustment disabled and quality filtered to require $\geq 20\%$ of reads supporting the variant call. Variants were annotated using both Annovar and custom scripts to identify whether they affected the protein coding sequence and whether they had previously been seen in mouse dbSNP131 or in any of the 21 other mouse exomes in a database of ENU exomes generated at McGill. ENU induced mutations identified by exome sequencing were further validated by Sanger sequencing in

additional progenies of the pedigree. Subsequent genotyping of the mice was done by TaqMan SNP Genotyping Assay (Thermo Fisher).

In vivo *Salmonella* infection: Mice were infected with 5000 CFUs of *Salmonella* Typhimurium as previously described [228] unless otherwise stated. Briefly, the infectious inoculum was diluted to 25,000 CFUs per mL and 200 μ L was injected into the caudal vein of 7-10 week old mice of both sexes. To determine bacterial burden in tissues, mice were humanely euthanized at day 4 or 5 post infection. Spleen and liver were removed aseptically, weighed and homogenized. Homogenates were diluted in saline and plated on trypticase soy agar (TSA) overnight.

Generation of plasmids and induction of transient and stable plasmid expression: Fam49b was amplified by PCR from a murine fetal brain cDNA library. To generate a 3x-FLAG fusion protein for transient expression, Fam49b was amplified with the following Fam49b specific primers (in caps) flanked with Gateway cloning sites:

5'- *ggggacaactttgtacaaaaaagttggcatgGGAATCTTCTTAAAGTTTTGA-3'* and

5'- *ggggacaactttgtacaagaaagttggtaCTGCAGCATGGACCTAATTTG-3'*. PCR products were cloned *in vitro* recombination into pDONR207 (BP cloning kit, Gateway system, Invitrogen) according to manufacturer's instructions. 3x-FLAG fusion protein was achieved by LR cloning (Invitrogen) into pCI-neo-3xFLAG [315] according to manufacturer's instructions. HeLa or Raw264.7 cells were transfected with X-tremeGENE HP DNA transfection reagent (Roche) according to manufacturer's instructions.

To generate a FLAG- BirA^{R118G} fusion protein, *Fam49b* was amplified using the following *Fam49b* specific primers (in caps) flanked with BirA-infusion-adapter sequences:

5'- *cagatatctgcggccATGGGGAATCTTCTTAAAGTTTTG-3'* and

5'- *tcgagtttagcggccgcTTACTGCAGCATGGACCTAATTTG – 3'*. The N-term pcDNA5 FRT/TO FLAG- BirA^{R118G} vector was linearized by NotI digestion. The Fam49b PCR product was cloned into the linearized N-term pcDNA5 FRT/TO FLAG-BirA^{R118G} vector by In-Fusion HD EcoDry cloning (Clontech) according to manufacturer's instructions. The construct was transformed and amplified in Stellar™ competent cells (Clontech) and sequence verified.

Stable expression cell lines were generated in Flp-In T-Rex HeLa cells (Stephen Taylor, University of Manchester). HeLa cells were transfected with 9 µg of pOG44 vector (Invitrogen) and 1 µg N-term FLAG-BirA^{R118G}-FAM49B using X-tremeGENE HP DNA transfection reagent (Roche). Stably transfected cells were maintained in 4 µg/mL of Blasticidin (InvivoGen) and 200 µg/mL of Hygromycin (InvivoGen).

Proximity biotinylation coupled to mass spectrometry: 5 x 10⁶ HeLa cells per stable cell line were plated in three 15 cm tissue culture dishes (Sarstedt). Cells were either left unstimulated, stimulated with 1 µg/mL LPS (Sigma) or infected with *Salmonella* Typhimurium at MOI 30. 24 hours before cell collection, 10 ng/mL of tetracycline and 50 mM of biotin (Sigma) were added to the culture medium to induce transgene expression and biotin labelling respectively. Affinity capture was done in three biological replicates using streptavidin-sepharose beads (GE) as previously described [316]. Mass spectrometry for the identification of interacting partners was performed by the Proteomics Platform of the McGill University Health Center. Briefly, proteins associated with FAM49B were analyzed by nano-electrospray LC/MS. The proteins were digested with trypsin. After lyophilization and re-solubilization in 1% aqueous formic acid, the peptides were loaded onto a Thermo Acclaim Pepmap (75µM ID X 2cm C18 3µM beads) precolumn and then onto an Acclaim Pepmap Easyspray (75µM X 15cm with 3µM C18 beads) analytical column separation using a Dionex NLC 3000 LC at 200 nl/min with a gradient of 2-30% organic (0.1% formic acid in acetonitrile) over 2 hours. Peptides were analyzed using a Thermo Orbitrap Fusion mass spectrometer operating at 120,000 resolution (FWHM in MS1, 60,000 for MS/MS) with HCD sequencing all peptides with a charge of 2+ or greater. The raw data were converted into *.mgf format (Mascot generic format) for searching using the (X!Tandem search engine) against human sequences (Uniprot). The database search results were loaded onto Scaffold Q+ for statistical treatment and data visualization.

Western blot analysis: The following antibodies were used for western blot analysis: FAM49B antibody (1:1000 5% BSA Proteintech), M2 FLAG antibody (1:10,000 5% BSA Sigma), STAT3

(1:500 5% BSA Santa Cruz), Phospho-STAT3 (Tyr705) antibody (1:500 5% BSA Cell signaling), and β -ACTIN (1:10,000 5% BSA Cell Signaling).

Bone marrow chimeras: 5-7 week old mice of both sexes were irradiated with two consecutive doses of 450 rads using the RS2000 X-ray machine. After irradiation, mice were reconstituted by i.v. injection of 1.5×10^6 bone marrow cells in sterile PBS. Mice were kept on sterile tap water containing 2 g/L neomycin sulfate (Bioshop) for 3 weeks. Six weeks following irradiation, mice were tested for chimerism by collecting blood from the saphenous vein and looking at the expression of *Fam49b* wild type or mutant allele by isolating DNA and genotyping with TaqMan.

Immunofluorescence: Following treatment, cells were fixed with 4% PFA for 10-15 mins at 37°C and permeabilized with 0.5% TritonX-100 for 5 mins at 40°C. Following blocking with 10% FBS for 30 minutes at room temperature, cells were incubated with anti-*Salmonella* (1:500 5% FBS) and/or anti-FLAG (1:500 Sigma) for 1 hour at room temperature, followed by secondary antibody (Alexa Fluor 488 goat anti-rabbit, AlexaFluor 568 goat anti-mouse), and Alexa Fluor 647 Phalloidin (1:100) for 45 minutes at room temperature. Finally cells were incubated with DAPI (1:100) for 5 minutes at room temperature and mounted onto slides with ProLong Gold and imaged by confocal microscopy.

RNA extraction and real time quantitative PCR: Total RNA was extracted from snap frozen organs using Trizol Reagent. cDNA was synthesized using M-MLV Reverse Transcriptase (Invitrogen). qPCR was done using SyberGreen reagent and calculated by the $2^{-\Delta\Delta Ct}$ method using HPRT as the housekeeping gene. The primers used are as follows: *Fam49b* 5'-CACGAAATACGAGAGGCAATC-3' and 5'-AAGGCCTCTTAGTGCTGCTTC-3'.

Genome wide expression analysis: Spleens were collected from three uninfected and three day 4 *Salmonella* Typhimurium infected from age-matched *Ity15* wildtype or mutant mice and snap frozen with liquid nitrogen. Total RNA was extracted using Trizol Reagent. RNA yield was determined using a NanoDrop spectrophotometer and quality assessed by denaturing agarose

gel. Genome wide expression profiling was done using Illumina Mouse WG-6 v2.0 Expression BeadChip. Quality control, hybridization and array analysis was performed at the McGill University and Genome Quebec Innovation Center. Raw data was normalized in FlexArray 1.6 software (Genome Quebec, Montreal Canada) using the lumi algorithm with Robust Spline Normalization. Gene lists for each sample group were generated in FlexArray by selecting for genes with a false discovery rate $p < 0.1$ by CyberT test. Pathway analysis for the gene lists was generated using DAVID bioinformatics resource [317, 318].

FACS and cell sorting: Spleens were aseptically from naïve and infected mice. Single cell suspensions were isolated by collagenase digestion followed by passage through a 70 μm strainer. Following RBC lysis, the cells were irreversibly stained for dead cells using Zombie Aqua viability dye (BioLegend). The following antibodies were purchased from eBioscience: CD3 ϵ (145-2C11), CD19 (eBio1D3), CD4 (GK1.5), CD8 α (53-6.7), and Gr-1 (RB6-8C5). CD11b (M1/70) was purchased from BioLegend. Cell sorting was performed by the Cell Vision Single Cell Analysis facility (Life Sciences Complex, McGill University).

Statistics: Statistical analysis was done, unless otherwise stated, with GraphPad Prism (Graphpad, La Jolla CA).

RESULTS:

A mutation in *Fam49b* confers susceptibility to *Salmonella* infection in the *Ity15* pedigree

Using a three-generation recessive breeding screen following chemical mutagenesis of 129S1 male mice, we have identified a pedigree with increased susceptibility to *Salmonella* infection that we named *Immunity to Typhimurium locus 15 (Ity15)*. This pedigree shows 40% mortality by day 10 post infection (Fig 1a). *Ity15^{m/m}* mice do not present any overt phenotypes prior to infection. Examination of naïve *Ity15^{m/m}* mice indicates normal hematological parameters (Table 1) and serum biochemistry including markers of tissue damage and electrolytes (data not shown) compared to wild type littermates. In addition, *Ity15^{m/m}* mice are born at the expected Mendelian ratio of 25% when crossing two heterozygous (*Ity15^{+/m}*) parents. However, we did observe perinatal mortality in litters from *Ity15^{m/m}* mothers but not *Ity15^{m/m}* fathers. To facilitate mapping of the causative mutation, the G1 male and G2 female were outcrossed to wild type DBA/2J mice. F2 mice were then phenotyped using a lower dose of *Salmonella* since the DBA/2J background presented intermediate susceptibility to infection (Fig 1b). In the F2 progeny, we observed 30% mortality by day 8 consistent with previous survival data with the 129S1 background. These F2 mice were genotyped using 708 informative SNPs between the parental DBA/2J and 129S1 strains. Genome wide linkage analysis detected a single linkage peak on chromosome 15 with a LOD score of 4.54 (Fig 1c) between markers rs3677062 and rs13482628 delineating an interval of 4.4 Mb (Fig 1d). Homozygous 129S1 alleles were associated with susceptibility to *Salmonella* infection and were inherited as a recessive trait (Fig 1e). Exome sequencing was performed in two susceptible F2 animals. We identified four ENU specific homozygous SNPs shared by the two animals, two of which were located under the mapped linkage peak (Table 2). Sanger sequencing in all F2 progeny validated two genes – gasdermin c4 (*Gsdmc4*) and family with sequence homology 49 member b (*Fam49b*). The mutation in *Gsdmc4* is an A to C transversion resulting in a phenylalanine to valine change at amino acid position 56. The mutation in *Fam49b* is an A to T transversion at position +2 of the splice donor site of intron 9-10. This is predicted to result in exon 10 skipping thereby introducing a frameshift and a premature stop codon within exon 11. These two genes are found within 40 kb of each other on chromosome 15.

To identify which one of these two genes is the one underlying *Ity15*, we first studied mRNA expression in target tissues during infection (Fig 2a). *Gsdmc4* was expressed at low levels in spleen, liver and kidneys and its expression was not different between wild type (*Ity15^{+/+}*) and mutant (*Ity15^{m/m}*) littermates before and during infection (Supp Fig 1). In contrast, the expression of *Fam49b* showed lower levels in heterozygous mice (*Ity15^{m/+}*) and *Ity15^{m/m}* before (spleen) and during infection (spleen, liver and kidney) compared to *Ity15^{+/+}* littermates (Fig 2a). In addition, the expression of wild type *Fam49b* mRNA increased significantly ($p < 0.0001$) during infection in all tissues (Fig 2a). Immunoblotting analysis of spleen and liver tissues revealed that the splicing mutation abrogated FAM49B protein expression in *Ity15^{m/m}* mice (Fig 2b). Owing to the close proximity of *Fam49b* and *Gsdmc4*, we validated *Fam49b* as the causal gene in the *Ity15* pedigree by allelic complementation. *Ity15^{m/m}* mice were crossed to mice heterozygous for a knock out allele at *Fam49b* (*Fam49b^{+/-}*) and susceptibility to infection was determined by survival in F1 animals. We observed lack of complementation with *Fam49b^{Ity15^{-/-}}* mice as susceptible as *Ity15^{m/m}* mice (Log Rank Mantel-Cox, $p < 0.0001$) (Fig 2c) confirming that the mutation in *Fam49b* is responsible for *Salmonella* susceptibility in the *Ity15* pedigree.

Loss of FAM49B results in early *Salmonella* dissemination and septic shock

Ity15^{m/m} mice showed significantly higher bacterial load in spleen and liver compared to littermate controls both after systemic (Fig 3a) and *per os* infection (Supp Fig 2). *In vivo* imaging with bioluminescent *Salmonella* showed a progressive increase in bacterial load in *Ity15^{m/m}* mice over the course of infection starting as early as four days post infection (Fig 3b). *Ity15^{m/m}* presented multiples abscesses in spleen and liver distributed randomly. These lesions were more diffuse and the inflammatory infiltration was similar to control mice. The white pulp showed marked lymphocytolysis in mutant mice and the liver presented more parenchymal necrosis with the presence of frequent fibrin thrombi in the microvasculature (Supp Fig 3). Overall, these pathological changes indicate that the *Ity15^{m/m}* mice have an overwhelming septicemia with induction of disseminated intravascular coagulation as shown by the numerous microthrombi and foci of fibrin.

Proinflammatory (TNF α and IL-6) and anti-inflammatory (IL-10) cytokines were also significantly higher in mutant mice (Fig 3c). Circulating levels of IFN γ and IL-12 were not affected by the mutation (data not shown). Consistent with high IL-6 and IL-10 levels, we observed that infected *Ity15^{m/m}* mice had elevated levels of phosphorylated STAT3 in the spleen and liver (Fig 3d). In *Ity15^{m/m}* we observed decreased IL-1 β secretion in the serum during infection (Fig 3e) which could be a consequence of increased IL-10 activation of STAT3 signalling. On the other hand, the mRNA expression of the negative regulator of IL-6 response, *Socs3* (suppressor of cytokine signaling 3) was not affected by the mutation (Fig 3f). Altogether these results suggest that both systemic bacterial dissemination in target organs and cytokine-induced septic shock are responsible for susceptibility of *Ity15* mutants to infection.

To further investigate the role of FAM49B during other types of infections, we tested whether the *Ity15* mutation would impact the susceptibility to Gram-positive bacteria (*Listeria monocytogenes*), Coxsackievirus B3 (CVB3) virus or cerebral malaria. *Ity15* mice were not susceptible to *Listeria monocytogenes* as measured by survival analysis and bacterial counts (Supp Fig 4) and the mice were able to clear the infection from liver and spleen by day 15 post infection. *Ity15* mutant mice were also resistant to CVB3 infection and susceptible to cerebral malaria as measured by survival analysis (data not shown).

FAM49B is expressed within the cytoplasm of immune cells and is regulated by LPS and type I IFN

We detected *Fam49b* mRNA by qPCR analysis in all tissues tested with the highest expression found in the spleen (Fig. 2a and Supp Fig 5). In most tissues *Fam49b* expression was upregulated during infection. In order to determine the cellular compartment that expresses FAM49B and which is important for conferring susceptibility to infection, we generated bone marrow chimeras. After 6 weeks of bone marrow reconstitution, the mice were infected with *Salmonella* Typhimurium. *Salmonella* susceptibility could be conferred to wild type mice by transferring mutant bone marrow cells into wild type mice (the mean survival time (MST) of these mice was not significantly different from the MST of mutant mice receiving mutant bone marrow) (Fig 4a and 4b). Conversely, resistance could be conferred to mutant mice by transferring wild type bone marrow cells into mutant mice, which implicates the hematopoietic

compartment in the susceptibility of the *Ity15* mutant mice (Fig 4a and 4b). To further determine which immune cells of the hematopoietic compartment were important for conferring susceptibility, we examined the expression of FAM49B in immune cells by Western blotting of uninfected and infected splenocytes isolated by cell sorting. FAM49B is expressed in all 4 major cell types we examined including T cells, B cells, granulocytes and monocytes (Fig 4c). We also determined cellular localization of FAM49B by transiently transfecting a 3x-Flag-Fam49b fusion plasmid into RAW264.7 cells, a macrophage like cell line. By confocal microscopy FAM49B was primarily located along the cell membrane and with diffuse expression within the cytoplasm (Fig 4d).

Because of the importance of LPS and type I IFN in the development of septic shock during *Salmonella* infection, we studied the response of *Fam49b* to these two stimuli in BMDMs. *Fam49b* mRNA transcript in wild type mice increased more than 2 fold following 24 hours of stimulation with either LPS or type I IFN (Fig 4e). Moreover, the expression of *Fam49b* is significantly lower in IFNAR knock out mice during infection (Fig 4f). Increase *Fam49b* mRNA was paralleled by increased expression of the FAM49B protein after stimulation with both LPS (Fig 4g) and type I IFN (data not shown). Altogether these results showed that FAM49B is expressed ubiquitously in immune cells of the hematopoietic compartment and its expression is regulated by both LPS and type I IFN.

Global transcriptional profile is altered in naïve *Ity15^{m/m}* mice and during infection

Genome-wide expression analysis was performed in spleen tissues from wild type and *Ity15^{m/m}* mice at day 0 and day 4 post infection in order to get a better understanding of the mechanism by which abrogation of FAM49B is causing susceptibility to infection. Cyber T tests were performed to compare wild type and *Ity15^{m/m}* genome-wide expression. The transcriptional profile of *Ity15^{m/m}* mice exhibited 311 differentially regulated genes compared to the 188 differentially regulated genes in wild type littermates upon infection, of which 155 were shared between the two genotypes (Fig 5a). The transcriptional profiles of naïve *Ity15^{m/m}* and control mice were compared and identified 39 genes that were differentially regulated (Fig 5b). Several of these genes encode secreted proteins expressed in granulocytes (*Ltf*, *Ngp*, *Camp*, *Lcn2*,

Pglyrp1) or in platelets (*Cxcl4* also known as *Pf4* and *Ppbp*) and involved in neutrophil recruitment (*Pf4* and *Ppbp*) or in the regulation of inflammatory processes and immune response (*S100a8* and *S100a9*). During infection, there were 192 genes differentially regulated between *Ity15^{m/m}* and wildtype littermates (Fig 5c). We could still observe increased expression of neutrophil associated genes in *Ity15^{m/m}* after infection. The gene *Slpi* (secretory leukocyte peptidase inhibitor) was the most upregulated gene in *Ity15^{m/m}* compared to wild type control during infection. This gene encodes a secreted inhibitor which protects tissues from serine proteases [319] and has been involved in the protection to LPS-induced shock and inflammation. We performed Gene Ontology (GO) enrichment analysis for all three categories (biological process, molecular function and cellular component). It is interesting to note that processes associated with host response to bacteria were overrepresented in naïve *Ity15* mutant mice suggesting that these mice present a subclinical inflammatory state. GO analysis after infection identified additional processes that are also related to the host response to infection including “defense response”, “extracellular region” and “carbohydrate binding” as the most significant terms (Table 3 and Fig 5c). Overall, global expression profiling in *Ity15* mice evokes a perturbation of the inflammatory response prior and during infection.

FAM49B is found in proximity to AHNAK and other proteins of the cytoskeleton

Due to the limited knowledge regarding FAM49B function, we performed a BioID proximity assay to identify potential FAM49B interactors. The BioID assay identifies proteins within a 20 to 30 nm proximity to the bait protein. In this way, we can identify direct interactors as well as proteins found in a complex with FAM49B. *Fam49b* cDNA was cloned into a pcDNA5 FRT/TO FLAG-BirA^{R118G} vector and the FLAG-BirA^{R118G} alone was used as control. FLAG-BirA^{R118G}-FAM49B interactors were identified *in vitro* using HeLa cells that were either unstimulated or exposed to *Salmonella* or LPS. Proteins were identified by mass spectrometry and those that were enriched in FAM49B-BirA samples were scored. Using this method, we identified a total of 27 proteins with an average of >10 peptide counts over 3 biological replicates in at least one of the conditions tested (unstimulated, LPS stimulation and *Salmonella* infection) (Table 4). The FAM49B bait was among the highest-scoring proteins. Most of the potential interactors

included proteins (AHNAK, ANXA2, tubulin, actin etc) known to be associated with the cytoskeleton (23/27) (Table 4). One protein in particular caught our interest: AHNAK (AHNAK nucleoprotein, known as desmoyokin). This protein had the highest score in all three conditions we investigated and was the one that presented the greatest increase in counts after stimulation (either LPS or *Salmonella*). AHNAK is a large protein acting as a scaffold for multi-protein complexes with a diverse range of functions from regulation of calcium influx channels, membrane repair to cell-cell contact (reviewed in [320]). These data suggest that FAM49B may play a role in cytoskeleton and/or membrane biology to regulate inflammation.

DISCUSSION:

We report the identification of a novel *Salmonella* susceptibility gene. The mutation consists of a splice donor site mutation affecting exon 10 of *Fam49b* resulting in the loss of FAM49B protein expression. We show that FAM49B is expressed ubiquitously in tissues and immune cells. Mice carrying the homozygous allele for *Fam49b*^{Ity15} are viable and develop normally presenting no obvious anatomical or cellular anomalies. However, we demonstrate that the loss of FAM49B within the cells of the hematopoietic compartment is sufficient to induce susceptibility to *Salmonella* infection. The defect in *Ity15* mice does not seem to affect a general immune mechanism since mutant *Ity15* mice did not present altered survival to other infectious challenges including *Listeria monocytogenes*, cerebral malaria and coxsackie virus B3. Very little is known about the structure and biochemical function of FAM49B. *Fam49b* is evolutionarily conserved across species from humans to drosophila. It is a member of a protein family that includes *Fam49a*, another poorly annotated gene. This family is defined by sharing a single domain of unknown function (DUF1394). This domain is also found within *Cyfp1* (cytoplasmic FMR (Fragile X Mental Retardation) interacting protein 1), also known as *Sra1* (specifically rac1 associated protein). CYFIP1 has dual roles in mediating inhibition of translation as a part of the FMRP-eIF4E complex and as a part of the WRC (Wave Regulatory Complex) in regulating actin dynamics [321, 322]. Mutagenesis of amino acids within the DUF1394 domain in CYFIP1 results in reduced RAC1 interactions [322]. This suggests that FAM49B may have a role in actin dynamics during infection. The genome-wide transcriptional profile of *Fam49b*^{Ity15} mice during infection add further evidence that *Fam49b* is involved within the cytoskeleton. The viability of mice lacking *Fam49b* suggests that FAM49A may play a redundant role or that FAM49B is necessary only under certain conditions such as inflammation or infection.

We have shown that *Fam49b*/FAM49B expression is regulated by both LPS and IFN β . Studies in multiple sclerosis patients have shown that FAM49B is upregulated in patients compared to controls and that expression of FAM49B is regulated by IFN β treatment [323]. Further evidence for a role for FAM49B in inflammation comes from a study which investigated genes downstream of IL-10 stimulation and STAT3 activation [324].

Our findings using a BioID assay has implicated AHNAK, ANXA2 and cytoskeletal proteins as FAM49B interactors. We propose a mechanism by which FAM49B interacts with the giant scaffold protein AHNAK in the regulation of the cytoskeleton during *Salmonella* infection. AHNAK is a protein with many diverse functions dependent on the cell in which it is expressed (reviewed in [320]). With regards to immune function, AHNAK has been shown to be important in regulating calcium channels affecting T cell activation and proliferation. Mice deficient for *Ahnak* develop normally but when infected with *Leishmania major*, show defects in IFN γ production by CD4⁺ T cells [325]. Production of IFN γ by CD4⁺ cells during infection and serum IFN γ levels were similar between control and mutants after infection. In addition, immunity to *Listeria monocytogenes* relies on T cell activation by macrophages and was not affected in the *Ity15* mutants.

AHNAK has also been shown to interact with ANXA2 and S100A10 (also known as p11) to mediate cytoskeletal and membrane rearrangements during *Salmonella* infection in a SPI1 dependent manner and is essential for *Salmonella* invasion of epithelial cells [56]. ANXA2 is important in the coordination of actin polymerization at the membrane levels and has been shown to be a component of F-actin rich comet tails that propel newly formed endocytic vesicles from the plasma membrane to the cell interior and a component of F-actin pedestals that form at membrane attachment sites of enteropathogenic *E. coli* [326-328]. In *Fam49b* mutants, bacterial invasion in HeLa cells and replication in bone marrow derived macrophages appeared similar to what is observed in littermate controls (data not shown) suggesting that bacterial entry into the cells is not affected by the mutation. Interestingly, more than half of the proteins identified using BioID were listed in the human thymic exosomes database [329] suggesting that FAM49B may play a role in cytoskeleton or membrane biology affecting secretion of inflammatory mediators.

In addition to invasion and phagocytosis, cytoskeleton dynamics are important component of immune function with roles in cell polarization, migration, antigen presentation, and signaling. Mutations resulting in the loss of major actin regulators such as ARP2/3 or WAVE2 or WASH are embryonic lethal. However a small number of actin regulatory proteins function primarily in immune cells and are permissive to mutations. Defects in these proteins such as WAS, WIP,

DOCK8, RAC2, RHOH, Coronin 1A, β -actin, or LSP1 (Leukocyte specific protein 1) result in primary immunodeficiencies (reviewed in [330]).

Although the exact mechanism by which the loss of *Fam49b* interaction with the cytoskeleton, controls the host response to *Salmonella* infection and modulates the inflammatory response remain to be elucidated, we have not only identified a novel gene responsible for regulating the outcome to *Salmonella* infection but we have also identified a potential function for a gene with no previously known function.

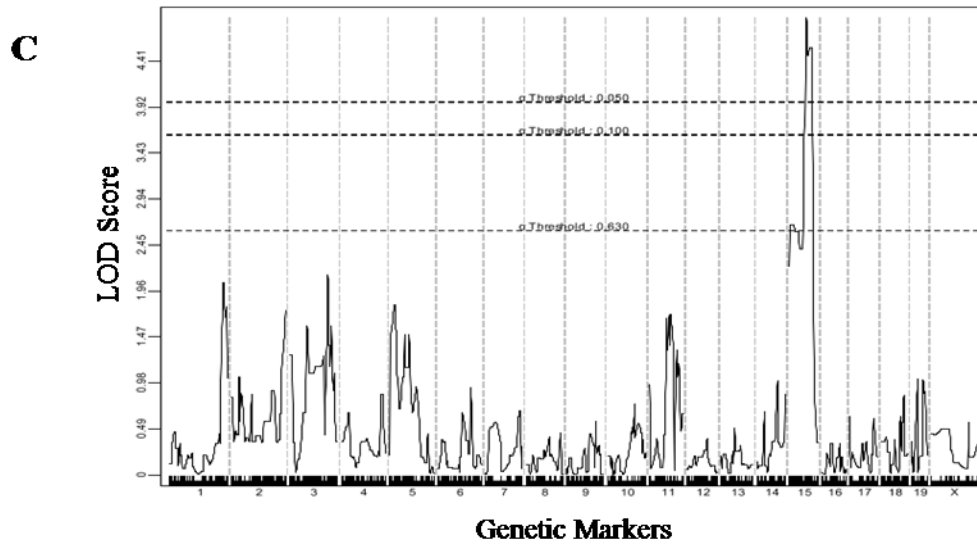
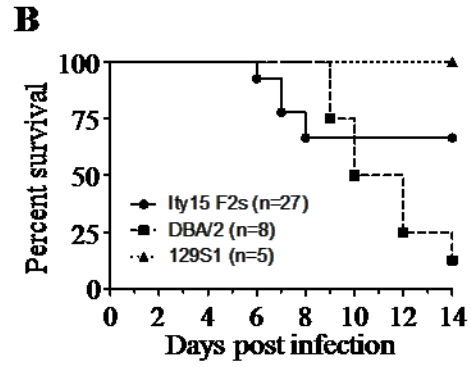
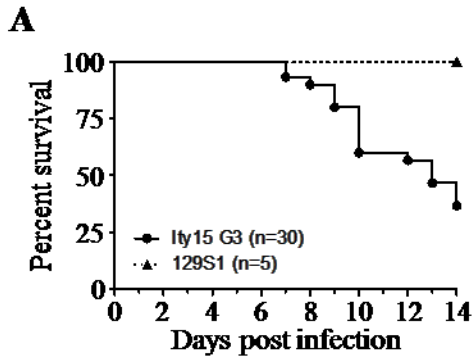
ACKNOWLEDGEMENTS:

We are grateful for the technical assistance of Patricia D'Arcy, Mimi Chen, Nadia Prud'homme, Geneviève Perrault, and Line Larivière. Flp-In T-Rex HeLa cells were obtained from Stephen Taylor (U. Manchester). KEY was a recipient of an Internal Studentship from the Faculty of Medicine. MME is a recipient of a studentship from the Fonds de Recherche du Québec-Santé (FRQS). This work was supported by funds from the Team Program of the Canadian Institutes of Health Research (CIHR) to SMV and DM (CTP-87520) and by CIHR grant to DM (MOP-133700).

FIGURES AND FIGURE LEGENDS:

FIGURE 1: VALIDATION AND MAPPING OF THE *ITY15* PEDIGREE

A) Survival curve of the G3 animals from the *Ity15* pedigree is represented by the solid line (n=30) while wild type 129S1 is represented by the dotted line (n=5) Log-rank (Mantel-Cox) $p=0.02$. **B)** Survival curve of the F2 animals from the *Ity15* pedigree outcrossed to DBA/2 is represented by the solid line (n=27) while the wild type DBA/2 is represented by the dashed line (n=8) and 129S1 by a dotted line (n=5). Log-rank (Mantel-Cox) $p=0.05$. **C)** Linkage analysis in 9 *Salmonella*-susceptible and 15 *Salmonella*-resistant mice identifies a significant peak on chromosome 15. **D)** Fine mapping of the *Ity15* locus to a 4.3 Mb interval. **E)** Survival curves of *Ity15* mice according to their genotypes at the peak marker on chromosome 15. The solid line represents homozygous 129S1 alleles (n=7), dashed line represents heterozygous (n=12) and dotted line represents homozygous DBA/2 alleles (n=4) Log-rank (Mantel-Cox) $p=0.0001$.



D

markers	Mb								
rs13482585	54,1								
rs13482602	61,6								
rs3677062	63,7								
rs13482628	68,1								
rs13482704	90,8								
Affected		0	1	1	1	2	1	0	0
Unaffected		2	0	0	0	0	0	0	12

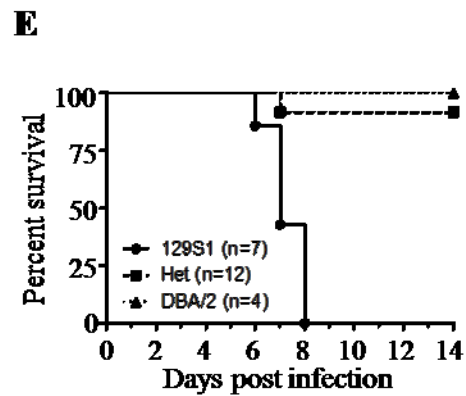


FIGURE 2: A MUTATION IN *FAM49B* CONFERS SUSCEPTIBILITY TO *SALMONELLA*
INFECTION IN THE *ITY15* PEDIGREE

A) Absolute quantities in ng of *Fam49b* mRNA transcript in uninfected or infected spleen, liver and kidney. White fill represents wild type, gray fill represents heterozygous and black fill represents mutant alleles (n=3 for all groups). **B)** FAM49B protein expression in uninfected or infected spleen and liver. + denotes wild type and – denotes mutant alleles. The *ity15* allele results in a loss of function mutation. **C)** Survival curves of F1 mice issued from a cross between *Ity15^{m/+}* and *Fam49b^{+/-}*. *Ity15^m/Fam49b⁻* (n=21), *Ity15^m/Fam49b⁺* (n=15), *Ity15⁺/Fam49b⁻* (n=22) and *Ity15⁺/Fam49b⁺* (n=21). There is no complementation between the *ity15* and KO allele at *Fam49b* confirming that *Fam49b* is the gene underlying *ity15*. ** p<0.01 **** p<0.0001

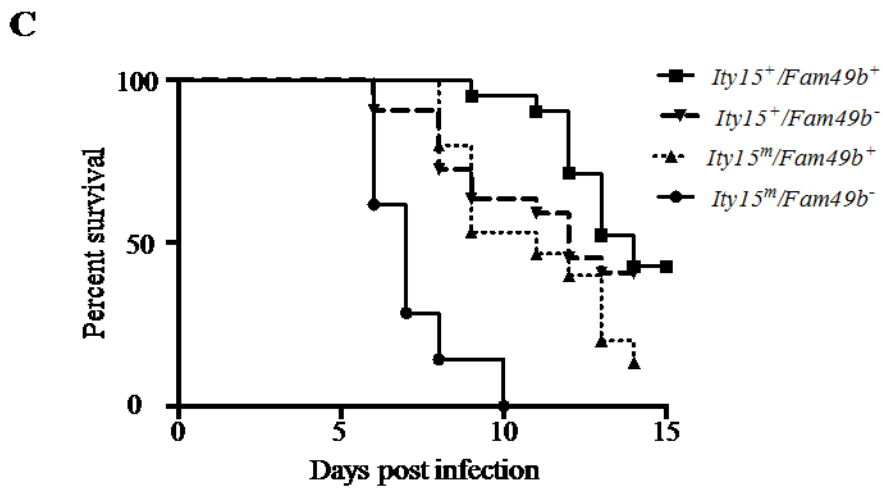
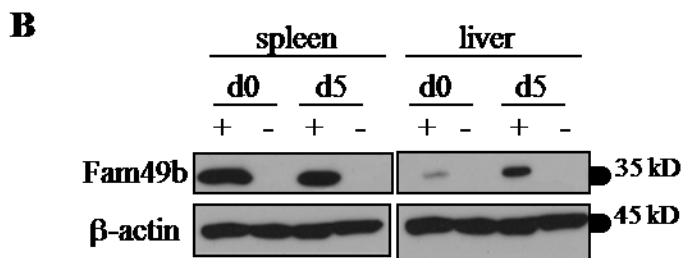
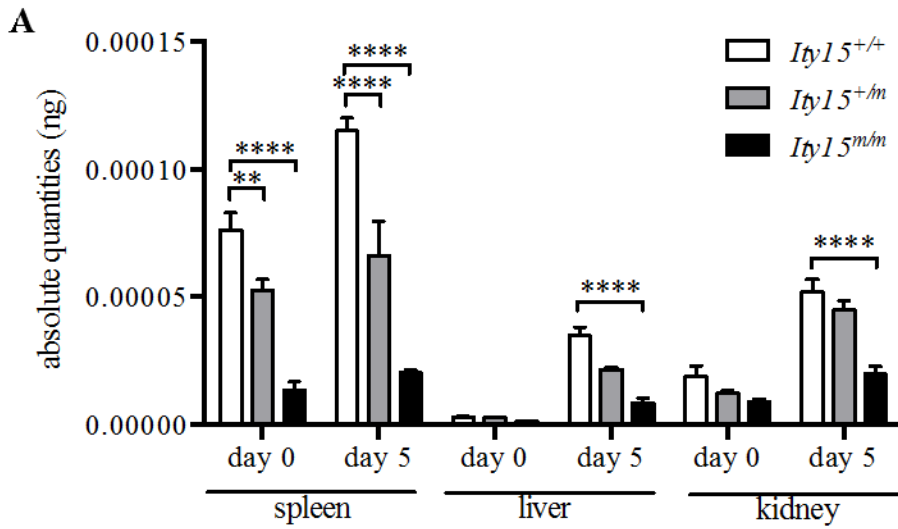


FIGURE 3: LOSS OF FAM49B RESULTS IN EARLY *SALMONELLA* DISSEMINATION
AND SEPTIC SHOCK

A) Bacterial load in spleen and liver at day 5 post infection in *Ity15^{+/+}* (open circle) and *Ity15^{m/m}* (closed circle) mice. **B)** Kinetics of Xen26 luminescent *Salmonella* replication in *Ity15^{+/+}* (open circle) and *Ity15^{m/m}* (closed circle) mice over 7 days. Luminescence of Xen26 *Salmonella* is shown in a representative *Ity15^{+/+}* and *Ity15^{m/m}* mouse at day 6 post infection. **C)** Serum production of TNF α , IL-10, and IL-6 at day 0 and day 5 post infection (n=3 per genotype in 2 independent experiments). **D)** Western blots of protein extracts from spleen and liver at day 0 and day 5 post infection probed with phospho-STAT3, STAT3 and β -ACTIN; **E)** Serum IL-1 β in *Ity15^{+/+}* (white fill) and *Ity15^{m/m}* (black fill) mice during infection; **f)** mRNA expression of *Socs3* in spleen and liver during infection (n=3 per genotype). * p<0.05

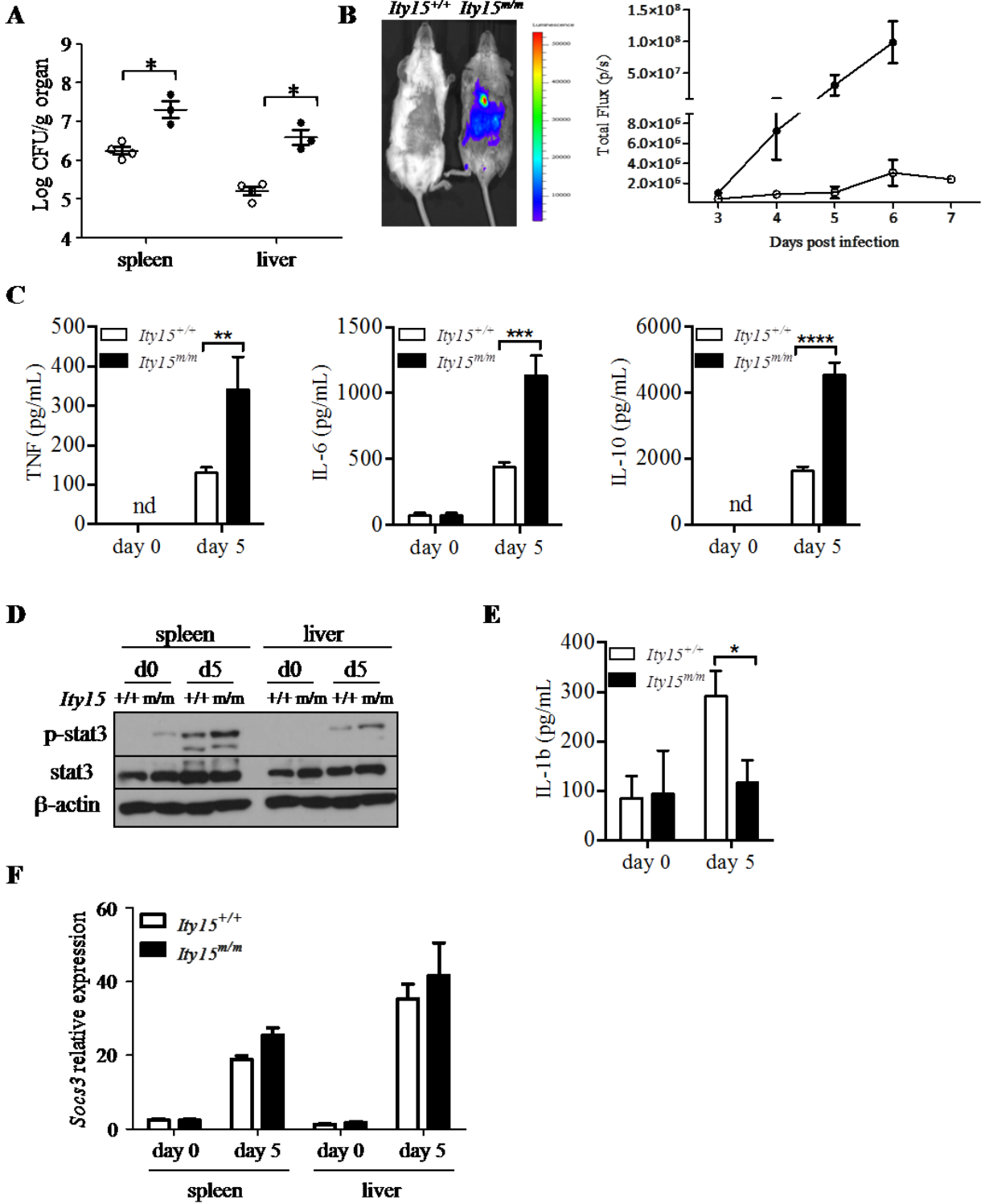


FIGURE 4: FAM49B IS EXPRESSED WITHIN THE CYTOPLASM OF IMMUNE CELLS
AND IS REGULATED BY LPS AND TYPE I IFN

A) Survival curves and **B)** mean survival time of bone marrow chimeras in which bone marrow cells from *Ity15^{m/m}* mice were transferred into *Ity15^{+/+}* (n=4) or vice versa (*Ity15^{+/+}* bone marrow into *Ity15^{m/m}* (n=5)). The hematopoietic compartment confers *Salmonella* resistance or susceptibility. Results for bone marrow chimeras are representative of 2 independent experiments. **C)** Expression of FAM49B was determined in CD4+ and CD8+ T cells (CD3+), B cells (CD19+), granulocytes (CD3-CD19-Gr1+) and monocytes (CD3-CD19-Cd11b+Gr1-) following cell sorting from spleens of uninfected and infected *Ity15^{+/+}* mice. **D)** Intracellular localization of FAM49B is determined by transient transfection of a 3x-FLAG-FAM49B fusion protein into RAW264.7 cells. Red denotes FAM49B, blue denotes nucleus. **E)** *Fam49b* mRNA levels in *Ity15^{+/+}* and *Ity15^{m/m}* BMDM stimulated with either IFN β or LPS/IFN γ over 24 hours. **F)** *Fam49b* mRNA expression in *Ifnar* knock out mice during infection. **G)** FAM49B protein expression in *Ity15^{+/+}* BMDMs stimulated with LPS/IFN γ over 24 hours. ** p<0.01 **** p<0.0001

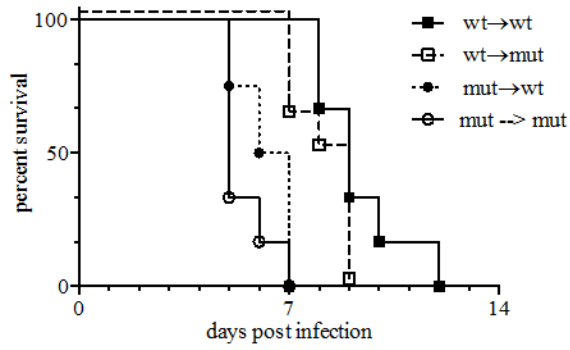
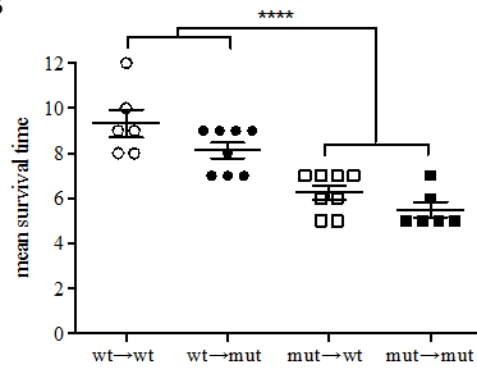
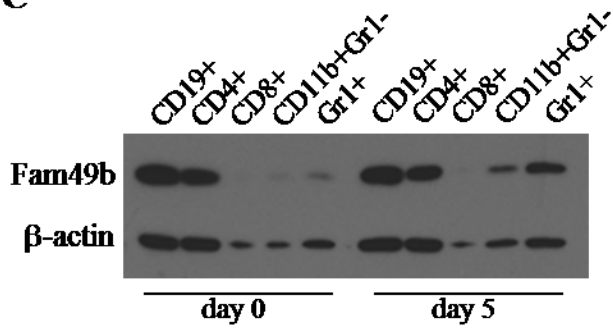
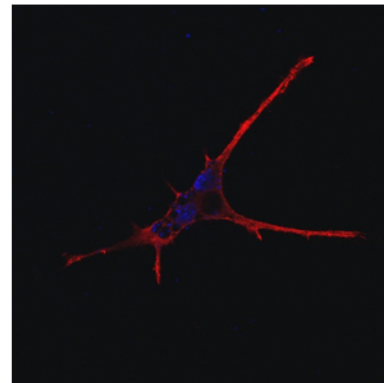
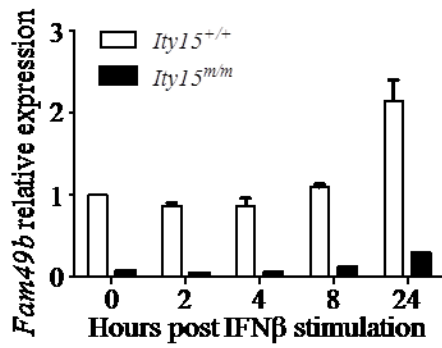
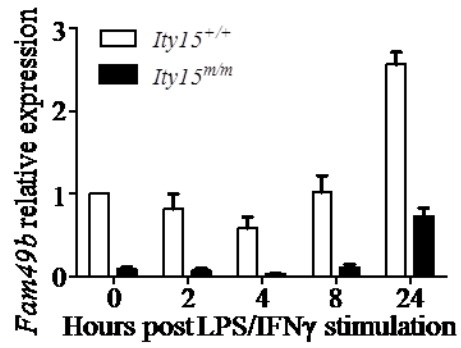
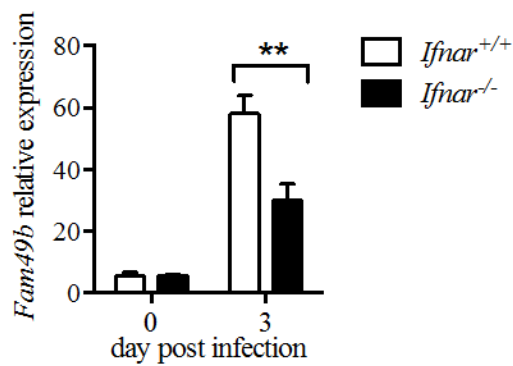
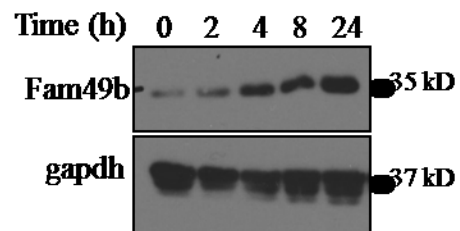
A**B****C****D****E****E****F****G**

FIGURE 5: GLOBAL TRANSCRIPTIONAL PROFILE OF *ITY15^{M/M}* MICE

A) Venn diagram identifies the number of genes that are significantly different with an expression fold change ≥ 2 or ≤ 0.5 in *Ity15^{+/+}* or *Ity15^{m/m}* spleens during infection. **B)** Heat map depicting genes significantly different at day 0 post infection between *Ity15^{+/+}* and *Ity15^{m/m}* mice. **C)** Heat map depicting genes significantly different at day 4 post infection between *Ity15^{+/+}* and *Ity15^{m/m}* mice with the GO terms “extracellular region”, “defense response” and “carbohydrate binding”.

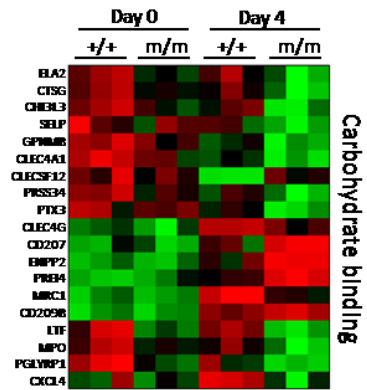
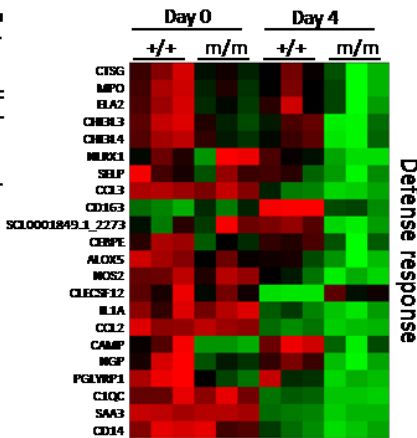
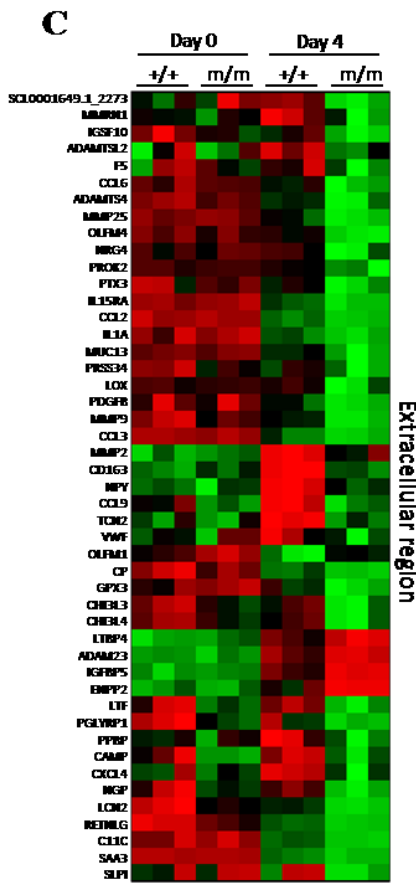
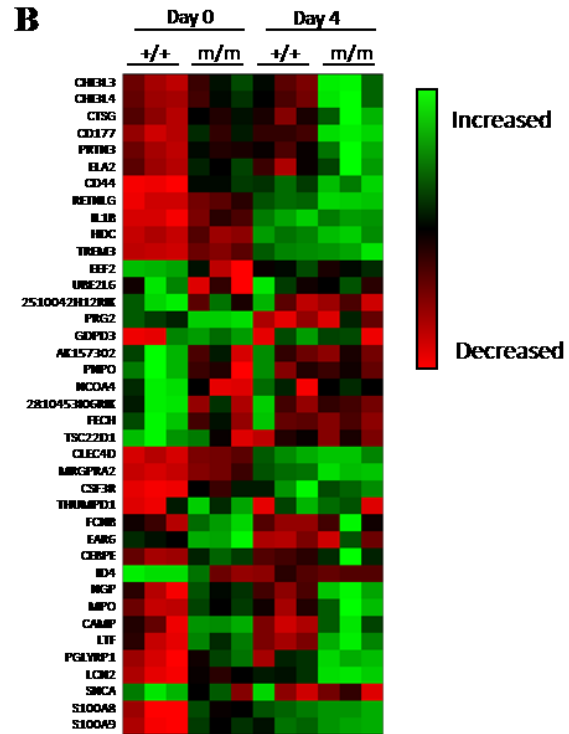
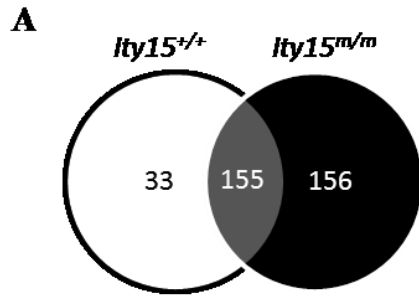


TABLE 1: HEMATOLOGICAL PARAMETERS OF *ITY15^{+/+}*, *ITY15^{+/M}* AND *ITY15^{M/M}* BEFORE AND DURING INFECTION

Genotype	Day 0			Day 5		
	<u>Wt</u>	<u>Heterozygous</u>	<u>Ity15</u>	<u>Wt</u>	<u>Heterozygous</u>	<u>Ity15</u>
Hematocrit L/L	0.554±0.004	0.534±0.037	0.539±0.040	0.468±0.085	0.485±0.03	0.484±0.043
Hemoglobin g/L	168 ± 1.53	162 ± 10.02	166 ± 10.44	145 ± 22.51	150 ± 7.79	149 ± 11.75
RBCs x 10 ¹² /L	12.2±0.68	11.72±0.66	11.62±0.42	9.9±1.77	10.3±0.67	10.6±1.11
WBCs x 10⁹/L	8.53 ± 2.61	7.1 ± 1.57	5.23 ± 1.15	10.2 ± 2.79	11.02 ± 1.8	10.73 ± 1.6
% reticulocytes	5.13±0.25	4.43±0.81	3.43±1.14	3.88±1.44	3.98±1.15	1.92 ± 1.13
neutrophils x 10⁹/L	0.79 ± 0.54	1.38 ± 0.22	0.79 ± 0.27	2.69 ± 1.02	2.73 ± 0.22	2.66 ± 1.3
lymphocytes x 10 ⁹ /L	7.71±2.6	5.66±1.43	4.42±0.93	6.44±1.72	7.07±1.34	6.58±0.53
monocytes x 10⁹/L	0	0.04 ± 0.036	0.02 ± 0.034	1 ± 0.48	1.21 ± 0.59	1.41 ± 0.41
platelets x 10 ⁹ /L	828 ± 64	900 ± 66	541 ± 434	568 ± 87	515 ± 51	328 ± 54

TABLE 2: ENU INDUCED MUTATIONS IDENTIFIED BY EXOME SEQUENCING IN THE
ITY15 PEDIGREE

Position (Mbp)	Variation	ref	alt	19.05	20.10	# alt	# read	# alt	# read	Gene	Phast	Protein change
chr15:63,770,217	splicing	A	T	hom	hom	59	59	71	71	<i>Fam49b</i>	541	NA
chr15:63,734,320	nonsynonymous SNV	A	C	hom	hom	80	80	51	51	<i>Gsdmc4</i>		p.F56V
chr18:38,460,155	nonsynonymous SNV	C	T	hom	hom	42	42	44	44	<i>Rnf14</i>	581	p.A22V
chr15:57,653,375	nonsynonymous SNV	A	T	hom	hom	30	30	15	15	<i>Zhx2</i>	381	p.D195V

TABLE 3: GO TERMS ASSOCIATED WITH GENES DIFFERENTIALLY REGULATED AT DAY 0 AND DAY 4 POST INFECTION

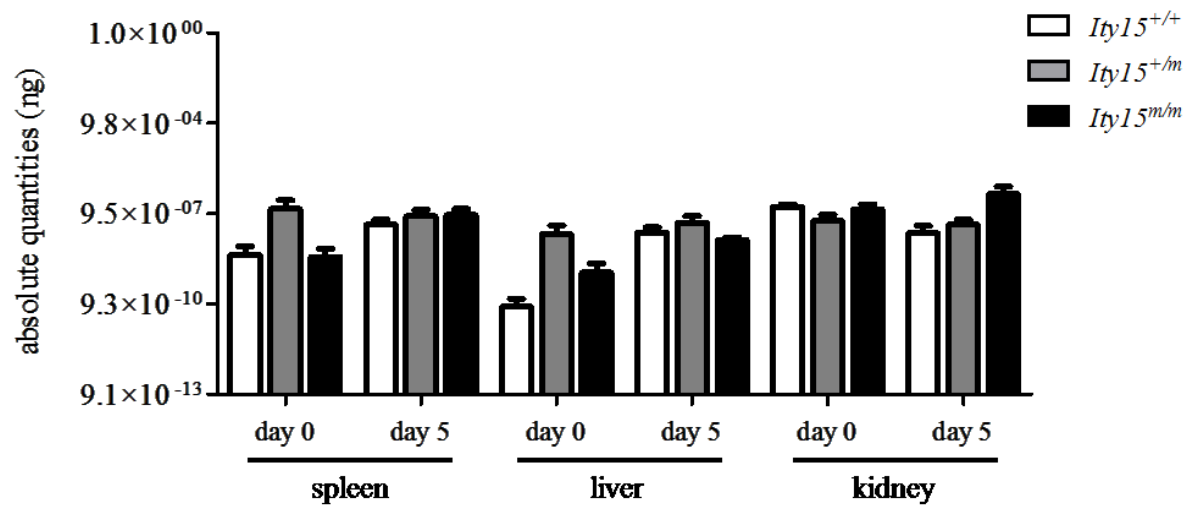
Day 0						
Category	Term		%	PValue	Fold Enrichment	FDR
GOTERM_BP_FAT	GO:0006952	defense response	33,3	7,19E-11	12,72	1,02E-07
GOTERM_BP_FAT	GO:0009617	response to bacterium	17,9	1,02E-06	19,54	1,45E-03
GOTERM_BP_FAT	GO:0042742	defense response to bacterium	15,4	3,52E-06	24,35	4,98E-03
GOTERM_CC_FAT	GO:0030141	secretory granule	17,9	9,04E-08	28,77	8,32E-05
GOTERM_CC_FAT	GO:0031410	cytoplasmic vesicle	23,1	4,12E-06	8,52	3,79E-03
GOTERM_CC_FAT	GO:0031982	vesicle	23,1	4,83E-06	8,34	4,45E-03
GOTERM_CC_FAT	GO:0016023	cytoplasmic membrane-bounded vesicle	20,5	1,19E-05	9,29	1,09E-02
GOTERM_CC_FAT	GO:0031988	membrane-bounded vesicle	20,5	1,31E-05	9,16	1,20E-02
GOTERM_MF_FAT	GO:0030246	carbohydrate binding	25,6	1,47E-08	13,97	1,65E-05
GOTERM_MF_FAT	GO:0030247	polysaccharide binding	17,9	2,81E-07	24,22	3,15E-04
GOTERM_MF_FAT	GO:0001871	pattern binding	17,9	2,81E-07	24,22	3,15E-04
GOTERM_MF_FAT	GO:0005539	glycosaminoglycan binding	15,4	4,29E-06	23,31	4,80E-03
Day 4						
GOTERM_BP_FAT	GO:0009611	response to wounding	11,7	1,21E-10	6,23	1,88E-07
GOTERM_BP_FAT	GO:0006952	defense response	12,2	1,75E-09	5,06	2,72E-06
GOTERM_BP_FAT	GO:0001878	response to yeast	2,8	1,22E-07	85,78	1,90E-04
GOTERM_BP_FAT	GO:0006955	immune response	11,1	1,23E-07	4,37	1,91E-04
GOTERM_BP_FAT	GO:0006954	inflammatory response	7,8	2,58E-07	6,41	4,01E-04
GOTERM_BP_FAT	GO:0006935	chemotaxis	5,6	1,03E-06	9,44	1,61E-03
GOTERM_BP_FAT	GO:0042330	taxis	5,6	1,03E-06	9,44	1,61E-03
GOTERM_BP_FAT	GO:0006909	phagocytosis	3,9	7,13E-06	14,71	1,11E-02
GOTERM_BP_FAT	GO:0009620	response to fungus	2,8	1,78E-05	30,28	2,77E-02
GOTERM_BP_FAT	GO:0009617	response to bacterium	5,6	2,08E-05	6,56	3,23E-02
GOTERM_CC_FAT	GO:0005576	extracellular region	26,1	5,52E-09	2,43	6,77E-06
GOTERM_CC_FAT	GO:0005615	extracellular space	11,7	1,41E-06	3,57	1,73E-03
GOTERM_CC_FAT	GO:0044421	extracellular region part	14,4	2,07E-06	2,92	2,54E-03
GOTERM_MF_FAT	GO:0030246	carbohydrate binding	10,6	4,17E-09	5,77	5,59E-06
GOTERM_MF_FAT	GO:0030247	polysaccharide binding	7,2	7,60E-09	9,78	1,02E-05
GOTERM_MF_FAT	GO:0001871	pattern binding	7,2	7,60E-09	9,78	1,02E-05

TABLE 4: FAM49B PROXIMITY INTERACTORS IDENTIFIED BY BIOID

Gene name	Gene description	MW	Unstimulated	Salmonella	LPS
AHNAK	AHNAK nucleoprotein (desmoyokin)	629 kDa	24,5	114	136,5
FAM49B	Family With Sequence Similarity 49, Member B	37 kDa	18,5	44	54
VIM	vimentin	54 kDa	32,5	45	43
TUBB	Tubulin, Beta Class I	48 kDa	29	43	44
TUBB4B	Tubulin, Beta 4B Class IVb	50 kDa	27,5	37,5	36,5
KRT2	Keratin 2, Type II	65 kDa	19,5	22	47,5
PLEC	plectin	532 kDa	17,5	32	35
CPS1	Carbamoyl-Phosphate Synthase 1, Mitochondrial	165 kDa	21,5	19	41
TUBA4A	Tubulin, Beta 4B Class Iva	50 kDa	22	27,5	31
TUBA1A	Tubulin, Alpha 1a	50 kDa	22,5	27,5	31
TUBB3	Tubulin, Beta 3 Class III	50 kDa	22,5	28	26
ACTB	Actin, Beta	39 kDa	16,5	23,5	25,5
DBT	Dihydrolipoamide Branched Chain Transacylase E2	53 kDa	11,5	21,5	15,5
ANXA2	Annexin A2	39 kDa	14	18,5	18
PKM	Pyruvate Kinase, Muscle	58 kDa	12,5	19	16
HSP90AA1	Heat Shock Protein 90kDa Alpha (Cytosolic), Class A Member 1	85 kDa	15,5	16,5	18
EEF1A2	Eukaryotic Translation Elongation Factor 1 Alpha 2	50 kDa	13	17	15,5
ACTC1	Actin, Alpha, Cardiac Muscle 1	42 kDa	14,5	15,5	17
HSPB1	Heat Shock 27kDa Protein 1	23 kDa	8,5	15,5	14,5
KRT7	Keratin 7, Type II	51 kDa	13,5	16,5	13
TUBB6	Tubulin, Beta 6 Class V	50 kDa	9	14	14,5
KRT6A	Keratin 6A, Type II	60 kDa	6	10,5	14
KRT6B	Keratin 6B, Type II	60 kDa	7	10	14,5
HNRNPM	Heterogeneous Nuclear Ribonucleoprotein M	78 kDa	5	11,5	11
ATP5B	ATP Synthase, H+ Transporting, Mitochondrial F1 Complex, Beta Polypeptide	57 kDa	6	10	12,5
KRT18	Keratin 18, Type I	48 kDa	6	10,5	9,5
KRT5	Keratin 5, Type II	62 kDa	4	9,5	10,5

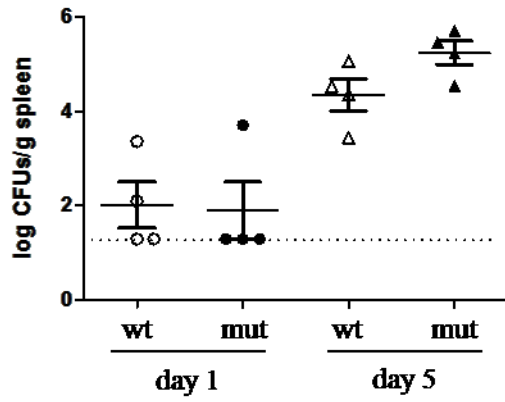
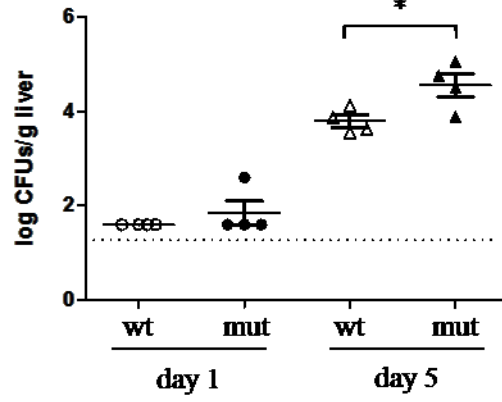
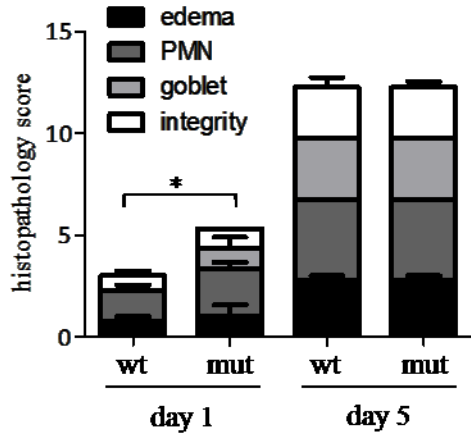
SUPPLEMENTAL FIGURE 1: EXPRESSION OF *GSDMC4* IN THE *ITY15* PEDIGREE

Absolute quantities (in ng) of *Gsdmc4* mRNA are shown for uninfected and infected spleen, liver and kidney. White fill represents wild type, gray fill represents heterozygous and black fill represents homozygous mutant alleles (n=3 for all groups).



SUPPLEMENTAL FIGURE 2: LOSS OF FAM49B RESULTS IN *SALMONELLA*
DISSEMINATION AND EARLY INTESTINAL PATHOLOGY

A) Bacterial load at day 1 and day 5 post infection in spleens of wild type (open circle) and mutant (black circle) mice. **B)** Bacterial load at day 1 and day 5 post infection in livers of wild type (open circle) and mutant (black circle) mice. **C)** Histopathological scores of ceca from infected mice at day 1 and day 5 post infection. Black fill represents edema, dark gray fill represents polymorphonuclear cell infiltration to the submucosa, light gray represents goblet cell numbers, white represents epithelial integrity. * $p < 0.05$

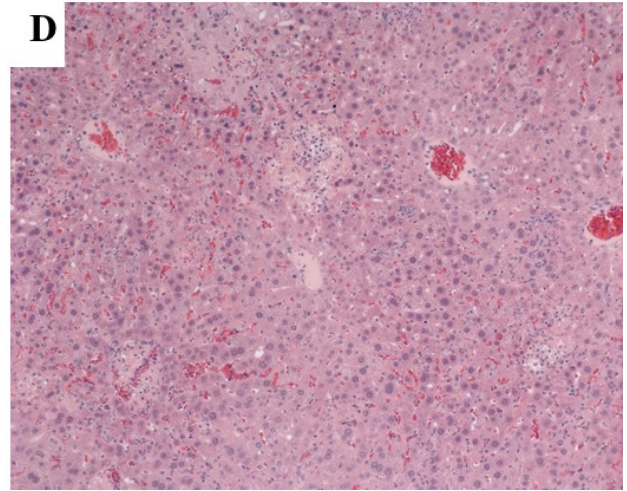
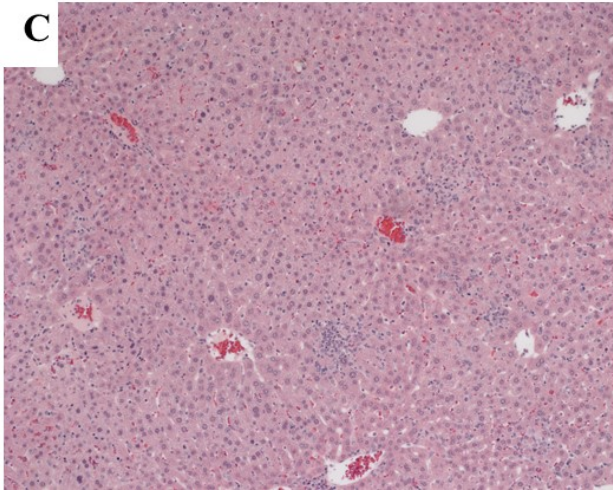
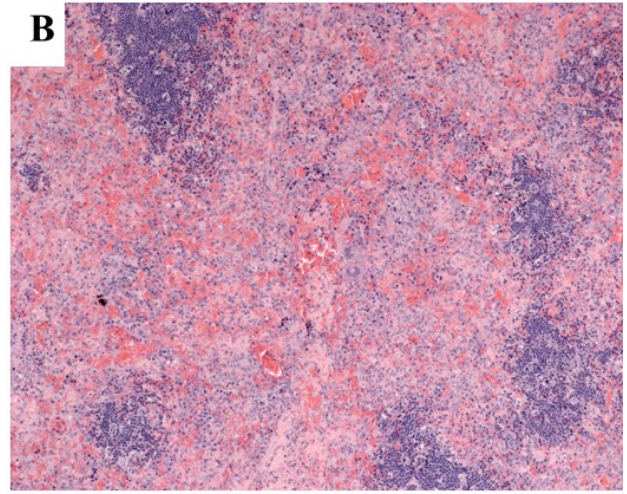
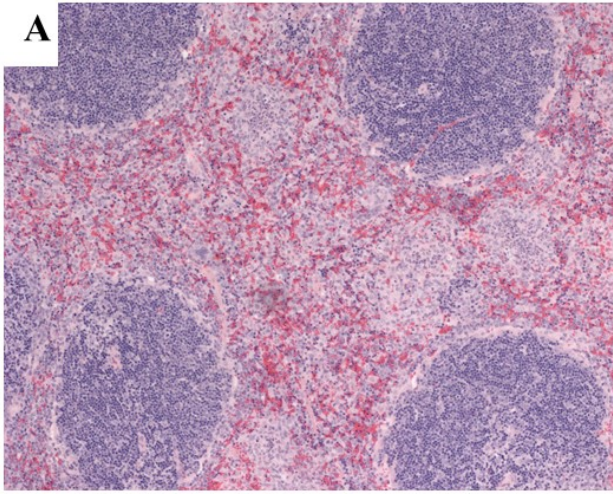
A**B****C**

SUPPLEMENTAL FIGURE 3: *ITy15^{M/M}* MICE DISPLAY SEVERE HISTOPATHOLOGICAL
CHANGES DURING INFECTION

Hematoxylin and eosin staining of spleen **(A, B)** and liver **(C, D)** of wild-type and *Ity15^{m/m}* mice shows marked spleen lymphocytolysis and more liver necrosis with the presence of frequent fibrin thrombi in the microvasculature at day 5 post infection.

Wild-type

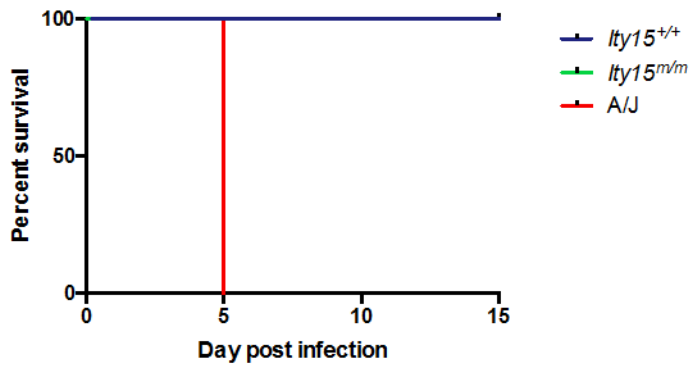
Ity15^{m/m}



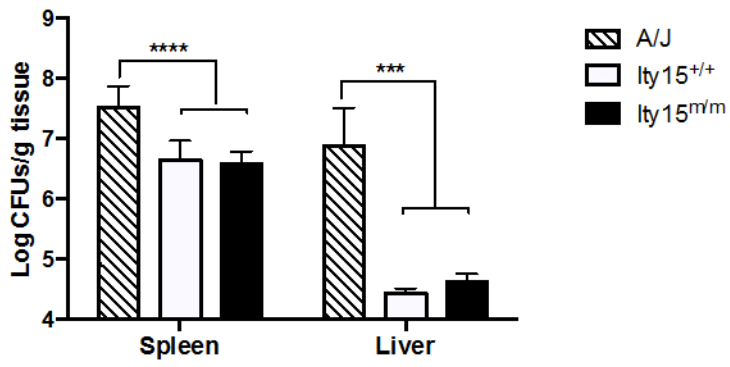
SUPPLEMENTAL FIGURE 4: *ITY15* MUTANT MICE ARE RESISTANT TO INFECTION WITH *LISTERIA MONOCYTOGENES*.

Mice were infected with 1000 CFUs *Listeria monocytogenes*. A/J mice were used as positive controls. **A)** All A/J mice (n=7) succumbed to infection by day 5 while all *Ity15* mice (n=4 per genotype) survived the 15 day period. **B)** Bacterial load was evaluated in spleen and liver at day 3 post infection (n=4 per group). *** p<0.001 **** p<0.0001

A

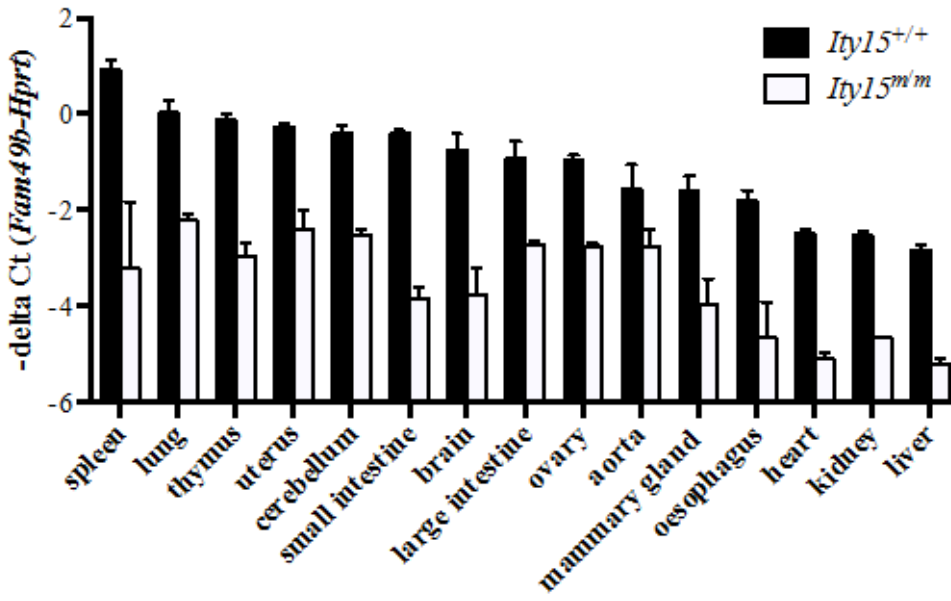


B



SUPPLEMENTAL FIGURE 5: *FAM49B* MRNA EXPRESSION IN *ITY15^{+/+}* AND *ITY15^{M/M}* MICE.

Fifteen different tissues were collected from three mice per genotype. RNA was extracted for further qPCR analysis. The spleen is the tissue showing the highest expression. For all tissues, levels of *Fam49b* mRNA are lower in *Ity15^{m/m}* mice. p<0.05 (large intestine, ovary) p<0.01 (lung, uterus, cerebellum, kidney) p<0.001 (mammary gland, heart, liver) p<0.0001 (spleen, thymus, small intestine, brain, oesophagus).



CHAPTER 5: GENERAL DISCUSSION

The study of the host response to *Salmonella* has come a long way since the discovery of *Bacillus typhosus* in 1880. Advances in our understanding of bacterial pathogenesis have led to the development of vaccinations and antibiotic treatment for enteric fever. In particular, the use of inbred strains of mice carrying natural variants responsible for susceptibility to infection has given us extensive insight into the pathogenesis of *Salmonella*. The overall aim of this thesis was to build upon the knowledge gained from inbred strains of mice. We used a forward genetics approach to identify genes in order to get a better understanding of the complex genetic and biochemical etiology underlying *Salmonella* susceptibility. Chemical mutagenesis has discovered nine additional loci controlling *Salmonella* susceptibility (*Ity9*, *Ity14* - *Ity21*). I have characterized two of these loci: *Ity15* and *Ity16*, which control two different aspects of infection.

CHAPTER 2: DISCOVERY OF NOVEL GENES IN SALMONELLA SUSCEPTIBILITY

In Chapter 2, we used a forward genetics and chemical mutagenesis approach to identify genes involved in susceptibility to *Salmonella* infection. I present data from an ENU screen that was part of a larger *Salmonella* initiative in our laboratory that took place from 2009 to 2012. Using the highly resistant 129S1 and genetically related 129X1 mouse strains, I successfully identified four deviant pedigrees with increased susceptibility to infection: *Ity14*, *Ity15*, *Ity19*, and *Ity21*. For two of the deviant pedigrees, we have identified and validated genes underlying the susceptibility phenotype: *Stat4* for *Ity14* [230] and *Fam49b* for *Ity15* (Chapter 4). Work still needs to be done for the characterization of the *Ity19* and *Ity21* deviant pedigrees including primary phenotyping (bacterial load in target tissues, serum cytokines, serum biochemistry, hematology and histopathological) and immunophenotyping. We have identified potential candidate genes underlying these susceptibility phenotypes but they will need to be validated. Additional methods to further refine the list of candidates can be achieved using whole genome sequencing of additional samples from affected individuals to identify IBD regions. *Cnp*, a strong candidate gene for the *Ity19* pedigree based on segregation

analysis, is an enzyme whose function in oligodendrocyte differentiation has been well studied. CNP may have a role in tubulin polymerization as well as having a role in regulating ROS and NO production following LPS treatment [331, 332]. The regulation of the cytoskeleton and reactive intermediates are important aspects of controlling *Salmonella* infection. Several questions still need to be answered for the *Ity19* pedigree. The first step will be to validate the candidacy of *Cnp* by allelic complementation. If validated, important questions will include: Which immune cell types have the highest CNP expression? Is tubulin polymerization affected? Does the mutation affect ROS or NO production following LPS stimulation? CNP has been shown to localize to both the cytoplasm and the membrane. Is localization affected during infection? Although our larger *Salmonella* ENU initiative was able to identify 9 deviant pedigrees (*Ity9*, *Ity14* – *Ity21*) and successfully identify the causative mutation in most of our pedigrees, there were some limitations to our ENU screen. Some of these limitations are inherent to the use of ENU as a chemical mutagen; others are due to our phenotyping protocol.

Limitations to ENU:

There are a number of limitations to using ENU chemical mutagenesis. First, due to the use of male G1 animals we are unable to probe for genes involved in susceptibility to *Salmonella* infection located on the X chromosome. The X chromosome has been recognized to contain a large number of immune genes within the human genome [333, 334]. It is also well known that females are more resistant to infection and it has been shown that they produce more antibodies and serum IgM [335-337]. A breeding scheme using two G1s to generate G2 offspring would allow for screening of genes on the X chromosome.

Second, there are limitations to the types of mutations that can be identified due to a number of biases inherent to ENU. ENU tends to induce mutations in genes with a high G/C nucleotide content or in sites flanked by G/C sites, in addition most of the reported mutations are A to T transversions or A to G transitions leading to an underrepresentation of GC to CG transversions and GC to TA transitions [208]. This can restrict the type of amino acid changes that are possible thereby limiting the generation of allelic series. However if the aim is gene discovery for a given phenotype or pathway, as it was for our ENU screen, this amino acid bias may be

less of a problem. In addition, we used exome sequencing to identify ENU induced mutations which biases the detection of mutations towards coding and splice variants. It may be difficult to identify a causative mutation in pedigrees in which the ENU induced mutation is within non-coding regions or miRNAs.

ENU also has a tendency to induce mutations in genes consisting of over 10 exons or a coding sequence over 1,000 base pairs thereby limiting the identification of smaller genes [206, 208]. We made the same observation, even the “smallest” genes we identified satisfied these conditions. *Fam49b*, *Usp18* and *Cnp* has 12, 11 and 4 exons respectively corresponding to coding sequences of 324, 368 and 420 amino acids respectively. The other 3 genes identified have coding sequences over 700 amino acids. This is also evidenced by the fact that 3 separate ENU screens have identified mutations in *Ank1* a gene encoding a large protein consisting of nearly 1900 amino acids [228, 245, 246].

Lastly, injection of ENU results in infertility of the G0 male for a period of 8-10 weeks while most G0 males will recover fertility approximately 4% of G0 males will stay infertile [218, 338]. In addition, it has been estimated that approximately 14-19% of G3 animals will not be viable due to embryonic lethality making it difficult to propagate and study these genes [338, 339].

Limitations to our phenotyping protocol:

One major limitation to our phenotyping protocol is the use of death as an endpoint. This phenotype is time consuming, taking 15 days from start to finish, and hinders our ability to study the mutation within the context of the original affected G3 animals. It necessitates the use of additional litters to further characterize the phenotype and identify the causative mutation. Our phenotype also makes the study of pedigrees difficult if the parental G1 and G2 mice are poor breeders. The pathogenesis of *Salmonella* leading to death is a result of a complex interplay between numerous pathways and cell types. This complexity of *Salmonella* infection means that we may miss mutations if there are any redundancies within different pathways that could compensate for the ENU induced mutation. One work around to this problem would be to look at simpler pathways such as TLR signaling, macrophage or DC

phagocytosis and hematopoietic cell development which could be a more effective starting point for identifying genes involved in susceptibility to *Salmonella* infection.

Despite the limitations outlined above, the ENU *Salmonella* susceptibility initiative in our lab identified a total of nine deviant pedigrees out of which six have confirmed causative mutations. Although I have laid out some reasons why death as a phenotype may not be optimal, it permits the identification of truly important regulators of immune response since the altered function of the gene results in death. The genes we have identified in our initiative have not overlapped or previously been identified to be implicated in acute *Salmonella* infections such as *Slc11a1* or *Tlr4*. This suggests that we have not saturated the genes involved in *Salmonella* susceptibility and there are still many genes involved that are left to be discovered. Unlike screens identifying genes involved in viral or malaria infection which were biased towards genes affecting T cell function none of the genes identified in our *Salmonella* screen were biased towards a specific pathway or even cell type [227, 252, 253, 255]. ENU was an excellent method to identify additional genes impacting survival as we were able to discover numerous deviant pedigrees in a relatively short period of time.

CHAPTER 3: IMPORTANCE OF IRON METABOLISM IN SALMONELLA INFECTION

In Chapter 3, I describe the impact of the *Ank1* mutation carried by the *Ity16* pedigree on *Salmonella* susceptibility. Previous work in other laboratories using *Ank1* mutant mice have shown that mutations in *Ank1* result in increased resistance to malaria. Our work was the first to show an impact with bacterial infection. The *Ank1* mutation impacts RBC morphology leading to increased erythrophagocytosis. This leads to increased RBC turnover and subsequent iron loading in liver and kidneys. We show that the increased susceptibility of the *Ity16* pedigree was a result of dampened hepcidin expression.

We demonstrated that hepcidin deficiency results in increased susceptibility and that administration of hepcidin improved survival of *Ank1*^{*Ity16/+*} mice to *Salmonella* infection. However recent studies looking at the impact of hepcidin expression and subsequent effects on iron during *Salmonella* infection have given contradictory results [340]. The difference in our findings can be explained by a number of factors such as the route of infection (i.v. vs *per os*),

iron status prior to infection (iron loaded vs normal), background strain effect (mixed 129S1/DBA2 vs homozygous B6 or DBA/2), levels of iron in the diet, or the number of hepcidin treatments given (once before infection vs six times given over the first three days of infection). But it also highlights the importance of balance and the goldilocks effect where both too little and too much iron can be detrimental to the host.

Recent work in the field of hemolytic anemia has discovered ERFE, a new regulator of iron metabolism. ERFE is upregulated in conditions of stress erythropoiesis in response to EPO and directly regulates *Hamp* expression [148]. In a mouse model of β -thalassemia, ablation of ERFE restored *Hamp* levels to those of control mice and restored iron content [148]. Although we have not investigated the levels of ERFE in our *Ity16* pedigree, we would expect ERFE to be upregulated in the *Ank1^{Ity16/Ity16}* mice due to the extensive hemolytic anemia. Taken together, these findings demonstrate that erythroid signals can override inflammatory signals and iron storage signals to regulate *Hamp* expression.

Susceptibility to infection in hemolytic anemias due to β -thalassemia or *Ank1* deficiency has been suggested to be secondary to hemolysis rather than to the anemia itself. Mice with anemia induced by phlebotomy did not show increased susceptibility to *Salmonella* infection whereas mice with increased hemolysis due to phenylhydrazine treatment were more susceptible [341]. The increased expression of *Hmox1* we observed in the *Ank1^{Ity16/Ity16}* mice suggests extensive hemolysis in these mice. Recent studies suggest that oxidative burst function in neutrophils is negatively affected by hemolysis [295, 342]. Additional work in the *Ity16* pedigree could look at the impact of the mutation on neutrophil oxidative burst function as well as macrophage function *in vivo* to see if this is a mechanism of susceptibility.

Unpublished *in vitro* work done in our laboratory suggests that BMDMs from *Ity16* mutant mice have defects in proliferation as well as increased bacterial load suggesting a defect in macrophage functions. It will be interesting to elucidate the mechanism by which an RBC structural protein could affect BMDM function, especially removed from the context of the iron loading found in these mice.

CHAPTER 4: PHENOTYPIC CHARACTERIZATION OF FAM49B

In chapter 4, I describe the functional characterization of the *Fam49b* mutation carried by the *Ity15* pedigree. We show that loss of FAM49B results in increased dissemination of *Salmonella* to target organs coinciding with increased pro-inflammatory cytokines IL-6 and TNF α and increased anti-inflammatory cytokine IL-10. Through the use of the BioID assay, we identified AHNAK and members of the cytoskeleton, such as actin, vimentin and tubulins, acting in close proximity to FAM49B.

Working with a protein with no known function and an uncharacterized domain was challenging and work still remains to elucidate the mechanism of action of FAM49B during infection. There are a number of avenues that could be explored.

Which cell types are important for conferring susceptibility?

We have shown that FAM49B is ubiquitously expressed within many tissues and cells and the importance of the hematopoietic compartment in conferring susceptibility to *Salmonella* infection. In order to determine if there is one particular cell type that confers susceptibility to *Salmonella* infection, survival analysis and phenotyping of conditional KO mice for either the lymphoid or myeloid compartments could be done to begin to answer this question. We are currently in the process of generating conditional KO mice. We have generated *Fam49b^{tm1d}* KO mice from *Fam49b^{tm1a}* KO mice following Flp recombination. We will be crossing them to either the Lysm-Cre mouse (which contains a myeloid specific promoter) or the Lck-Cre mouse (which contains a lymphoid specific promoter).

Fam49b interaction partners:

Prior to the BioID assay to identify proximity partners, we had undertaken a yeast-2-hybrid (Y2H) to identify interaction partners. Results from this Y2H identified 7 potential FAM49B interaction partners, of which 6 (CAD, DCTN2, ENAH, HOMER3, PRMT1, and UBQLN1) are present in the ExoCarta database, a database of exosome associated proteins. Attempts to validate these partners by co-immunoprecipitation were unsuccessful. There are several explanations for our inability to validate these results. Firstly, Y2H is an artificial system which

may produce interactions that are not physiologically possible. To go along with this idea, it is possible that the conditions of the co-IP were not optimal for detecting the interaction. The interaction with FAM49B may need the presence of infection or bacterial DNA to occur. Lastly, without a proper positive control of FAM49B interaction, it was difficult to say whether there was actually no interaction or if there was a problem with the FAM49B plasmid that would interfere with any potential interactions.

Our findings have highlighted a potential role for Fam49b in exosomes during the pathogenesis of infection in the *Ity15* mice. Exosomes have been shown to be released from many different cell types such as T cells, B cells, mast cells, DCs, platelets, macrophages, neurons and epithelial cells. In addition, exosomes have been shown to be an evolutionarily conserved mechanism of cell to cell communication [343, 344]. Exosomes have been well studied in the context of cancer, cardiovascular and autoimmune diseases. However recent work has looked at the role of exosomes during infection. In particular, exosomes released from *Salmonella* infected macrophages have been shown to carry LPS and have pro-inflammatory properties [345]. Perhaps Fam49b has a role in the biogenesis or regulation of exosome release.

The proximity partners identified by BioID, in particular AHNAK and Anxa2, will need to be validated. This could be done by immunoprecipitation or confocal microscopy to show co-localization. In addition, many of the proteins identified in our BioID assay have been shown to be expressed in exosomes following a search in ExoCarta. We could investigate these associations by looking at markers of exosomes by confocal or by isolating exosomes by differential centrifugation and look for FAM49B expression under naïve, LPS stimulated or *Salmonella* infected conditions.

The role of FAM49B in other infectious models:

Very little is known about the role of FAM49B during infection. We have already determined that FAM49B is important during *Salmonella* infection. Is this a *Salmonella* specific effect or does the loss of FAM49B affect survival to other pathogens? We have already determined that the loss of FAM49B was not important for survival to cerebral malaria, *Listeria monocytogenes* or CVB3 infections, but what about other intracellular pathogens such as BCG or

Mycobacterium tuberculosis or other Gram negative bacteria such as *Citrobacter rodentium*, a natural pathogen of mice that shares important pathogenic features with the human-specific pathogens EHEC and EPEC? The global transcriptional profile of naïve *Ity15* mutant mice displayed increased expression of genes found in neutrophil secretory granules, which are especially important for controlling *Candida albicans* infection. It is possible that the upregulation of these genes could impact survival to *Candida* infection in the *Ity15* pedigree. In addition, it was shown that in the context of endoplasmic reticulum aminopeptidase associated with antigen processing (ERAAP) deficiency, an enzyme involved in the cleavage of peptides for antigenic presentation to T cells, FAM49B is cleaved as an alternate peptide and presented by cytotoxic CD8+ T cells [346]. Does the loss of this FAM49B peptide affect susceptibility to viruses that decrease the expression of host ERAAP such as MCMV?

PERSPECTIVE:

Globally, deaths due to non-communicable disease have overtaken infectious disease as the most common cause of mortality around the world. However, rapid urbanization can lead to the increase of the spread of infectious disease. In 2014, the United Nations reported that 54% of the world population lived in urban centers [347]. Africa and Asia, the least urbanized of the continents had 48% and 40% of their population living in urban centers respectively [347]. In low income countries, 5 of the top 10 causes of death are due to infectious disease [1]. Urbanization without proper urban planning can result in poor waste management and sanitation as well as inadequate water supplies which can lead to the easy spread of diarrheal diseases like non-typhoidal *Salmonella*. In addition, the increase in population density of city centers can lead to the rapid spread of emerging infectious diseases as seen recently by SARS (Severe Acute Respiratory Syndrome) and avian flu [348]. The ability to identify at risk populations and develop therapies is important for the treatment and prevention of *Salmonella* disease.

Broadly, the work presented in this thesis has increased our understanding of *Salmonella* pathogenesis during acute infection and testifies to the complexity of *Salmonella* disease.

Through the use of ENU mutagenesis we have contributed new genes to pathways already known to regulate the outcome to infection including *Stat4* in the IL-12/IFN γ signaling axis, *Ank1* in iron metabolism, *Usp18* in type I IFN signaling and *Cnp* in the cytoskeleton. More interestingly, we have also identified genes with poorly studied or no known function: *Ncoa7* and *Fam49b*.

In humans, the genes we have identified in our ENU screen have also been shown to contribute to disease. Mutations in *ANK1* have been shown to be a major cause of hereditary spherocytosis, the most common cause of hereditary hemolytic anemia in people of northern European descent. In the United States and Europe, it is estimated that this disease affects 1 in 5000 people [287, 288]. Although the function of FAM49B has not been studied in humans, it has been associated with diseases such as multiple sclerosis and endometriosis [323, 349].

REFERENCES:

1. Organization, W.H., *Mortality and Global Health Estimates*. 2013, World Health Organization: Geneva, Switzerland.
2. Lozano, R., et al., *Global and regional mortality from 235 causes of death for 20 age groups in 1990 and 2010: a systematic analysis for the Global Burden of Disease Study 2010*. *Lancet*, 2012. **380**(9859): p. 2095-128.
3. Eberth, *Oranismen in den organen bei typhus abdominalis*. *Virchows Arch Path Anal*, 1880(81): p. 16-58.
4. Budd, W., *Typhoid fever : its nature, mode of spreading, and prevention*. 1873, London: Longmans, Green. xii, 193 p.
5. Budd, W., *ON INTESTINAL FEVER*. *The Lancet*, 1859. **74**(1878): p. 207-210.
6. Pegues, D.A. and S.I. Miller, *Salmonella Species*, in *Mandell, Douglas, and Bennett's principles and practice of infectious diseases*, J.E. Bennett, R. Dolin, and M.J. Blaser, Editors. 2015, Elsevier/Saunders: Philadelphia, PA. p. 2 volumes.
7. Brenner, F.W., et al., *Salmonella nomenclature*. *J Clin Microbiol*, 2000. **38**(7): p. 2465-7.
8. Buckle, G.C., C.L. Walker, and R.E. Black, *Typhoid fever and paratyphoid fever: Systematic review to estimate global morbidity and mortality for 2010*. *J Glob Health*, 2012. **2**(1): p. 010401.
9. Crump, J.A. and E.D. Mintz, *Global trends in typhoid and paratyphoid Fever*. *Clin Infect Dis*, 2010. **50**(2): p. 241-6.
10. Parry, C.M., et al., *Typhoid fever*. *N Engl J Med*, 2002. **347**(22): p. 1770-82.
11. Bhan, M.K., R. Bahl, and S. Bhatnagar, *Typhoid and paratyphoid fever*. *Lancet*, 2005. **366**(9487): p. 749-62.
12. Butler, T., *Treatment of typhoid fever in the 21st century: promises and shortcomings*. *Clin Microbiol Infect*, 2011. **17**(7): p. 959-63.
13. Thomas, H.L., S. Addiman, and A. Mellanby, *Evaluation of the effectiveness and efficiency of the public health management of cases of infection due to Salmonella typhi/paratyphi in North East London*. *Public Health*, 2006. **120**(12): p. 1188-93.
14. Ko, D.C. and T.J. Urban, *Understanding human variation in infectious disease susceptibility through clinical and cellular GWAS*. *PLoS Pathog*, 2013. **9**(8): p. e1003424.
15. Dunstan, S.J., et al., *Variation at HLA-DRB1 is associated with resistance to enteric fever*. *Nat Genet*, 2014. **46**(12): p. 1333-6.
16. Dunstan, S.J., et al., *Genes of the class II and class III major histocompatibility complex are associated with typhoid fever in Vietnam*. *J Infect Dis*, 2001. **183**(2): p. 261-268.
17. Dharmana, E., et al., *HLA-DRB1*12 is associated with protection against complicated typhoid fever, independent of tumour necrosis factor alpha*. *Eur J Immunogenet*, 2002. **29**(4): p. 297-300.
18. Dunstan, S.J., et al., *A TNF region haplotype offers protection from typhoid fever in Vietnamese patients*. *Hum Genet*, 2007. **122**(1): p. 51-61.
19. Ali, S., et al., *PARK2/PACRG polymorphisms and susceptibility to typhoid and paratyphoid fever*. *Clin Exp Immunol*, 2006. **144**(3): p. 425-31.
20. Levine, M.M., R.E. Black, and C. Lanata, *Precise estimation of the numbers of chronic carriers of Salmonella typhi in Santiago, Chile, an endemic area*. *J Infect Dis*, 1982. **146**(6): p. 724-6.
21. Merselis, J.G., Jr., et al., *Quantitative Bacteriology of the Typhoid Carrier State*. *Am J Trop Med Hyg*, 1964. **13**: p. 425-9.

22. Monack, D.M., D.M. Bouley, and S. Falkow, *Salmonella typhimurium* persists within macrophages in the mesenteric lymph nodes of chronically infected *Nramp1*^{+/+} mice and can be reactivated by IFN γ neutralization. *J Exp Med*, 2004. **199**(2): p. 231-41.
23. Crawford, R.W., et al., Gallstones play a significant role in *Salmonella* spp. gallbladder colonization and carriage. *Proc Natl Acad Sci U S A*, 2010. **107**(9): p. 4353-8.
24. Chart, H., *Salmonella*, in *Medical microbiology : a guide to microbial infections : pathogenesis, immunity, laboratory diagnosis and control*, D. Greenwood, Editor. 2012, Churchill Livingstone: Edinburgh ; New York. p. xvi, 778 p.
25. Majowicz, S.E., et al., *The global burden of nontyphoidal Salmonella gastroenteritis*. *Clin Infect Dis*, 2010. **50**(6): p. 882-9.
26. Mermin, J., et al., *Reptiles, amphibians, and human Salmonella infection: a population-based, case-control study*. *Clin Infect Dis*, 2004. **38 Suppl 3**: p. S253-61.
27. MacLennan, C., et al., *Interleukin (IL)-12 and IL-23 are key cytokines for immunity against Salmonella in humans*. *J Infect Dis*, 2004. **190**(10): p. 1755-7.
28. van de Vosse, E. and T.H. Ottenhoff, *Human host genetic factors in mycobacterial and Salmonella infection: lessons from single gene disorders in IL-12/IL-23-dependent signaling that affect innate and adaptive immunity*. *Microbes Infect*, 2006. **8**(4): p. 1167-73.
29. Kariuki, S., et al., *Antimicrobial resistance and management of invasive Salmonella disease*. *Vaccine*, 2015. **33 Suppl 3**: p. C21-C29.
30. Ao, T.T., et al., *Global burden of invasive nontyphoidal Salmonella disease, 2010(1)*. *Emerg Infect Dis*, 2015. **21**(6).
31. Reddy, E.A., A.V. Shaw, and J.A. Crump, *Community-acquired bloodstream infections in Africa: a systematic review and meta-analysis*. *Lancet Infect Dis*, 2010. **10**(6): p. 417-32.
32. Gordon, M.A., et al., *Epidemics of invasive Salmonella enterica serovar enteritidis and S. enterica Serovar typhimurium infection associated with multidrug resistance among adults and children in Malawi*. *Clin Infect Dis*, 2008. **46**(7): p. 963-9.
33. MacLennan, C.A. and M.M. Levine, *Invasive nontyphoidal Salmonella disease in Africa: current status*. *Expert Rev Anti Infect Ther*, 2013. **11**(5): p. 443-6.
34. Brent, A.J., et al., *Salmonella bacteremia in Kenyan children*. *Pediatr Infect Dis J*, 2006. **25**(3): p. 230-6.
35. Feasey, N.A., et al., *Invasive non-typhoidal salmonella disease: an emerging and neglected tropical disease in Africa*. *Lancet*, 2012. **379**(9835): p. 2489-99.
36. Fraenkel, E., *Ueber spezifische Behandlung des Abdominaltyphus1*. *Dtsch med Wochenschr*, 1893. **19**(41): p. 985-987.
37. Wright, A.E. and W.B. Leishman, *Remarks on the Results which have been Obtained by the Antityphoid Inoculations and on the Methods which have been Employed in the Preparation of the Vaccine*. *Br Med J*, 1900. **1**(2038): p. 122-9.
38. Carter, P.B. and F.M. Collins, *The route of enteric infection in normal mice*. *J Exp Med*, 1974. **139**(5): p. 1189-203.
39. Garcia-del Portillo, F., J.W. Foster, and B.B. Finlay, *Role of acid tolerance response genes in Salmonella typhimurium virulence*. *Infect Immun*, 1993. **61**(10): p. 4489-92.
40. Mastroeni, P. and A.J. Grant, *Spread of Salmonella enterica in the body during systemic infection: unravelling host and pathogen determinants*. *Expert Rev Mol Med*, 2011. **13**: p. e12.
41. House, D., et al., *Serology of typhoid fever in an area of endemicity and its relevance to diagnosis*. *J Clin Microbiol*, 2001. **39**(3): p. 1002-7.
42. Nguyen, Q.C., et al., *A clinical, microbiological, and pathological study of intestinal perforation associated with typhoid fever*. *Clin Infect Dis*, 2004. **39**(1): p. 61-7.

43. McCormick, B.A., et al., *Transepithelial signaling to neutrophils by salmonellae: a novel virulence mechanism for gastroenteritis*. *Infect Immun*, 1995. **63**(6): p. 2302-9.
44. Desai, P.T., et al., *Evolutionary Genomics of Salmonella enterica Subspecies*. *MBio*, 2013. **4**(2).
45. McClelland, M., et al., *Complete genome sequence of Salmonella enterica serovar Typhimurium LT2*. *Nature*, 2001. **413**(6858): p. 852-6.
46. Wisner, A., et al., *The Salmonella Pathogenicity Island-1 and-2 Encoded Type III Secretion Systems*. 2012: INTECH Open Access Publisher.
47. Mueller, C.A., P. Broz, and G.R. Cornelis, *The type III secretion system tip complex and translocon*. *Mol Microbiol*, 2008. **68**(5): p. 1085-95.
48. Patel, J.C. and J.E. Galan, *Manipulation of the host actin cytoskeleton by Salmonella--all in the name of entry*. *Curr Opin Microbiol*, 2005. **8**(1): p. 10-5.
49. Kuhle, V. and M. Hensel, *Cellular microbiology of intracellular Salmonella enterica: functions of the type III secretion system encoded by Salmonella pathogenicity island 2*. *Cellular and Molecular Life Sciences CMLS*, 2004. **61**(22): p. 2812-2826.
50. Brawn, L.C., R.D. Hayward, and V. Koronakis, *Salmonella SPI1 effector SipA persists after entry and cooperates with a SPI2 effector to regulate phagosome maturation and intracellular replication*. *Cell Host Microbe*, 2007. **1**(1): p. 63-75.
51. Wasylnka, J.A., et al., *Role for myosin II in regulating positioning of Salmonella-containing vacuoles and intracellular replication*. *Infect Immun*, 2008. **76**(6): p. 2722-35.
52. Brown, N.F., et al., *Salmonella pathogenicity island 2 is expressed prior to penetrating the intestine*. *PLoS Pathog*, 2005. **1**(3): p. e32.
53. Hayward, R.D. and V. Koronakis, *Direct nucleation and bundling of actin by the SipC protein of invasive Salmonella*. *EMBO J*, 1999. **18**(18): p. 4926-34.
54. Zhou, D., M.S. Mooseker, and J.E. Galan, *Role of the S. typhimurium actin-binding protein SipA in bacterial internalization*. *Science*, 1999. **283**(5410): p. 2092-5.
55. Patel, J.C. and J.E. Galan, *Differential activation and function of Rho GTPases during Salmonella-host cell interactions*. *J Cell Biol*, 2006. **175**(3): p. 453-63.
56. Jolly, C., et al., *The Annexin A2/p11 complex is required for efficient invasion of Salmonella Typhimurium in epithelial cells*. *Cell Microbiol*, 2014. **16**(1): p. 64-77.
57. Fu, Y. and J.E. Galan, *A salmonella protein antagonizes Rac-1 and Cdc42 to mediate host-cell recovery after bacterial invasion*. *Nature*, 1999. **401**(6750): p. 293-7.
58. Galan, J.E. and R. Curtiss, 3rd, *Cloning and molecular characterization of genes whose products allow Salmonella typhimurium to penetrate tissue culture cells*. *Proc Natl Acad Sci U S A*, 1989. **86**(16): p. 6383-7.
59. Godinez, I., et al., *T cells help to amplify inflammatory responses induced by Salmonella enterica serotype Typhimurium in the intestinal mucosa*. *Infect Immun*, 2008. **76**(5): p. 2008-17.
60. McCormick, B.A., et al., *Surface attachment of Salmonella typhimurium to intestinal epithelia imprints the subepithelial matrix with gradients chemotactic for neutrophils*. *J Cell Biol*, 1995. **131**(6 Pt 1): p. 1599-608.
61. Looney, R.J. and R.T. Steigbigel, *Role of the Vi antigen of Salmonella typhi in resistance to host defense in vitro*. *J Lab Clin Med*, 1986. **108**(5): p. 506-16.
62. Wilson, R.P., et al., *The Vi capsular polysaccharide prevents complement receptor 3-mediated clearance of Salmonella enterica serotype Typhi*. *Infect Immun*, 2011. **79**(2): p. 830-7.
63. Wangdi, T., et al., *The Vi capsular polysaccharide enables Salmonella enterica serovar typhi to evade microbe-guided neutrophil chemotaxis*. *PLoS Pathog*, 2014. **10**(8): p. e1004306.
64. Winter, S.E., et al., *The TviA auxiliary protein renders the Salmonella enterica serotype Typhi RcsB regulon responsive to changes in osmolarity*. *Mol Microbiol*, 2009. **74**(1): p. 175-93.

65. Winter, S.E., et al., *A rapid change in virulence gene expression during the transition from the intestinal lumen into tissue promotes systemic dissemination of Salmonella*. PLoS Pathog, 2010. **6**(8): p. e1001060.
66. Atif, S.M., et al., *Salmonella enterica serovar Typhi impairs CD4 T cell responses by reducing antigen availability*. Infect Immun, 2014. **82**(6): p. 2247-54.
67. Winter, S.E., et al., *Salmonella enterica Serovar Typhi conceals the invasion-associated type three secretion system from the innate immune system by gene regulation*. PLoS Pathog, 2014. **10**(7): p. e1004207.
68. Brumell, J.H. and S. Grinstein, *Salmonella redirects phagosomal maturation*. Curr Opin Microbiol, 2004. **7**(1): p. 78-84.
69. Meresse, S., et al., *Remodelling of the actin cytoskeleton is essential for replication of intravacuolar Salmonella*. Cell Microbiol, 2001. **3**(8): p. 567-77.
70. Hensel, M., T. Nikolaus, and C. Egelseer, *Molecular and functional analysis indicates a mosaic structure of Salmonella pathogenicity island 2*. Mol Microbiol, 1999. **31**(2): p. 489-98.
71. Beuzon, C.R., et al., *pH-dependent secretion of SseB, a product of the SPI-2 type III secretion system of Salmonella typhimurium*. Mol Microbiol, 1999. **33**(4): p. 806-16.
72. Cirillo, D.M., et al., *Macrophage-dependent induction of the Salmonella pathogenicity island 2 type III secretion system and its role in intracellular survival*. Mol Microbiol, 1998. **30**(1): p. 175-88.
73. Beuzon, C.R., et al., *Salmonella maintains the integrity of its intracellular vacuole through the action of SifA*. EMBO J, 2000. **19**(13): p. 3235-49.
74. Ruiz-Albert, J., et al., *Complementary activities of SseJ and SifA regulate dynamics of the Salmonella typhimurium vacuolar membrane*. Mol Microbiol, 2002. **44**(3): p. 645-61.
75. Abrahams, G.L., P. Muller, and M. Hensel, *Functional dissection of SseF, a type III effector protein involved in positioning the salmonella-containing vacuole*. Traffic, 2006. **7**(8): p. 950-65.
76. Vazquez-Torres, A., et al., *Salmonella pathogenicity island 2-dependent evasion of the phagocyte NADPH oxidase*. Science, 2000. **287**(5458): p. 1655-8.
77. Chakravorty, D., I. Hansen-Wester, and M. Hensel, *Salmonella pathogenicity island 2 mediates protection of intracellular Salmonella from reactive nitrogen intermediates*. J Exp Med, 2002. **195**(9): p. 1155-66.
78. Maskell, D., *Salmonella infections: clinical, immunological and molecular aspects*. Vol. 9. 2006: Cambridge University Press.
79. Vazquez-Torres, A., et al., *Extraintestinal dissemination of Salmonella by CD18-expressing phagocytes*. Nature, 1999. **401**(6755): p. 804-8.
80. Densen, P., L.A. MacKeen, and R.A. Clark, *Dissemination of gonococcal infection is associated with delayed stimulation of complement-dependent neutrophil chemotaxis in vitro*. Infect Immun, 1982. **38**(2): p. 563-72.
81. Montz, H., et al., *The role of C5a in interleukin-6 production induced by lipopolysaccharide or interleukin-1*. Immunology, 1991. **74**(3): p. 373-9.
82. Podack, E.R., W.P. Kolb, and H.J. Muller-Eberhard, *The C5b-9 complex: subunit composition of the classical and alternative pathway-generated complex*. J Immunol, 1976. **116**(5): p. 1431-4.
83. Vidal, S.M., et al., *Natural resistance to infection with intracellular parasites: isolation of a candidate for Bcg*. Cell, 1993. **73**(3): p. 469-85.
84. Forbes, J.R. and P. Gros, *Divalent-metal transport by NRAMP proteins at the interface of host-pathogen interactions*. Trends Microbiol, 2001. **9**(8): p. 397-403.
85. Blackwell, J.M., et al., *Understanding the multiple functions of Nramp1*. Microbes Infect, 2000. **2**(3): p. 317-21.

86. Canonne-Hergaux, F., et al., *Expression and subcellular localization of NRAMP1 in human neutrophil granules*. Blood, 2002. **100**(1): p. 268-75.
87. Cellier, M.F., P. Courville, and C. Campion, *Nramp1 phagocyte intracellular metal withdrawal defense*. Microbes Infect, 2007. **9**(14-15): p. 1662-70.
88. Forbes, J.R. and P. Gros, *Iron, manganese, and cobalt transport by Nramp1 (Slc11a1) and Nramp2 (Slc11a2) expressed at the plasma membrane*. Blood, 2003. **102**(5): p. 1884-92.
89. Barton, C.H., S.H. Whitehead, and J.M. Blackwell, *Nramp transfection transfers Ity/Lsh/Bcg-related pleiotropic effects on macrophage activation: influence on oxidative burst and nitric oxide pathways*. Mol Med, 1995. **1**(3): p. 267-79.
90. Barrera, L.F., et al., *Nitrite production by macrophages derived from BCG-resistant and -susceptible congenic mouse strains in response to IFN-gamma and infection with BCG*. Immunology, 1994. **82**(3): p. 457-64.
91. Fritsche, G., et al., *Nramp1-functionality increases iNOS expression via repression of IL-10 formation*. Eur J Immunol, 2008. **38**(11): p. 3060-7.
92. Fritsche, G., et al., *Nramp1 functionality increases inducible nitric oxide synthase transcription via stimulation of IFN regulatory factor 1 expression*. J Immunol, 2003. **171**(4): p. 1994-8.
93. Cuellar-Mata, P., et al., *Nramp1 modifies the fusion of Salmonella typhimurium-containing vacuoles with cellular endomembranes in macrophages*. J Biol Chem, 2002. **277**(3): p. 2258-65.
94. Govoni, G., et al., *Functional expression of Nramp1 in vitro in the murine macrophage line RAW264.7*. Infect Immun, 1999. **67**(5): p. 2225-32.
95. Dunstan, S.J., et al., *Typhoid fever and genetic polymorphisms at the natural resistance-associated macrophage protein 1*. J Infect Dis, 2001. **183**(7): p. 1156-60.
96. Biggs, T.E., et al., *Nramp1 modulates iron homeostasis in vivo and in vitro: evidence for a role in cellular iron release involving de-acidification of intracellular vesicles*. Eur J Immunol, 2001. **31**(7): p. 2060-70.
97. Fritsche, G., et al., *Modulation of macrophage iron transport by Nramp1 (Slc11a1)*. Immunobiology, 2007. **212**(9-10): p. 751-7.
98. Nairz, M., et al., *Slc11a1 limits intracellular growth of Salmonella enterica sv. Typhimurium by promoting macrophage immune effector functions and impairing bacterial iron acquisition*. Cell Microbiol, 2009. **11**(9): p. 1365-81.
99. Soe-Lin, S., et al., *Nramp1 promotes efficient macrophage recycling of iron following erythrophagocytosis in vivo*. Proc Natl Acad Sci U S A, 2009. **106**(14): p. 5960-5.
100. Mastroeni, P., et al., *Antimicrobial actions of the NADPH phagocyte oxidase and inducible nitric oxide synthase in experimental salmonellosis. II. Effects on microbial proliferation and host survival in vivo*. J Exp Med, 2000. **192**(2): p. 237-48.
101. Paiva, C.N. and M.T. Bozza, *Are reactive oxygen species always detrimental to pathogens?* Antioxid Redox Signal, 2014. **20**(6): p. 1000-37.
102. Kobayashi, Y., *The regulatory role of nitric oxide in proinflammatory cytokine expression during the induction and resolution of inflammation*. J Leukoc Biol, 2010. **88**(6): p. 1157-62.
103. Pacelli, R., et al., *Nitric oxide potentiates hydrogen peroxide-induced killing of Escherichia coli*. J Exp Med, 1995. **182**(5): p. 1469-79.
104. Norbury, C.J. and I.D. Hickson, *Cellular responses to DNA damage*. Annu Rev Pharmacol Toxicol, 2001. **41**: p. 367-401.
105. Paesold, G., et al., *Genes in the Salmonella pathogenicity island 2 and the Salmonella virulence plasmid are essential for Salmonella-induced apoptosis in intestinal epithelial cells*. Cell Microbiol, 2002. **4**(11): p. 771-81.

106. Schauser, K., J.E. Olsen, and L.I. Larsson, *Salmonella typhimurium* infection in the porcine intestine: evidence for caspase-3-dependent and -independent programmed cell death. *Histochem Cell Biol*, 2005. **123**(1): p. 43-50.
107. Robinson, N., et al., *Type I interferon induces necroptosis in macrophages during infection with Salmonella enterica serovar Typhimurium*. *Nat Immunol*, 2012. **13**(10): p. 954-62.
108. Shi, J., et al., *Inflammatory caspases are innate immune receptors for intracellular LPS*. *Nature*, 2014. **514**(7521): p. 187-92.
109. Miao, E.A., et al., *Innate immune detection of the type III secretion apparatus through the NLRC4 inflammasome*. *Proc Natl Acad Sci U S A*, 2010. **107**(7): p. 3076-80.
110. Birmingham, C.L., et al., *Autophagy controls Salmonella infection in response to damage to the Salmonella-containing vacuole*. *J Biol Chem*, 2006. **281**(16): p. 11374-83.
111. Benjamin, J.L., et al., *Intestinal epithelial autophagy is essential for host defense against invasive bacteria*. *Cell Host Microbe*, 2013. **13**(6): p. 723-34.
112. Conway, K.L., et al., *Atg16l1 is required for autophagy in intestinal epithelial cells and protection of mice from Salmonella infection*. *Gastroenterology*, 2013. **145**(6): p. 1347-57.
113. Mastroeni, P., et al., *Effect of interleukin 12 neutralization on host resistance and gamma interferon production in mouse typhoid*. *Infect Immun*, 1996. **64**(1): p. 189-96.
114. Muotiala, A. and P.H. Makela, *The role of IFN-gamma in murine Salmonella typhimurium infection*. *Microb Pathog*, 1990. **8**(2): p. 135-41.
115. Mastroeni, P., et al., *Interleukin-12 is required for control of the growth of attenuated aromatic-compound-dependent salmonellae in BALB/c mice: role of gamma interferon and macrophage activation*. *Infect Immun*, 1998. **66**(10): p. 4767-76.
116. van de Vosse, E., J.T. van Dissel, and T.H. Ottenhoff, *Genetic deficiencies of innate immune signalling in human infectious disease*. *Lancet Infect Dis*, 2009. **9**(11): p. 688-98.
117. de Jong, R., et al., *Severe mycobacterial and Salmonella infections in interleukin-12 receptor-deficient patients*. *Science*, 1998. **280**(5368): p. 1435-8.
118. Jouanguy, E., et al., *In a novel form of IFN-gamma receptor 1 deficiency, cell surface receptors fail to bind IFN-gamma*. *J Clin Invest*, 2000. **105**(10): p. 1429-36.
119. Mastroeni, P., et al., *Serum TNF alpha in mouse typhoid and enhancement of a Salmonella infection by anti-TNF alpha antibodies*. *Microb Pathog*, 1991. **11**(1): p. 33-8.
120. Everest, P., M. Roberts, and G. Dougan, *Susceptibility to Salmonella typhimurium infection and effectiveness of vaccination in mice deficient in the tumor necrosis factor alpha p55 receptor*. *Infect Immun*, 1998. **66**(7): p. 3355-64.
121. Ohmori, Y., R.D. Schreiber, and T.A. Hamilton, *Synergy between interferon-gamma and tumor necrosis factor-alpha in transcriptional activation is mediated by cooperation between signal transducer and activator of transcription 1 and nuclear factor kappaB*. *J Biol Chem*, 1997. **272**(23): p. 14899-907.
122. Mihara, M., et al., *IL-6/IL-6 receptor system and its role in physiological and pathological conditions*. *Clin Sci (Lond)*, 2012. **122**(4): p. 143-59.
123. Saraiva, M. and A. O'Garra, *The regulation of IL-10 production by immune cells*. *Nat Rev Immunol*, 2010. **10**(3): p. 170-81.
124. Mittal, S.K., et al., *Interleukin 10 (IL-10)-mediated Immunosuppression: MARCH-I INDUCTION REGULATES ANTIGEN PRESENTATION BY MACROPHAGES BUT NOT DENDRITIC CELLS*. *J Biol Chem*, 2015. **290**(45): p. 27158-67.
125. Couper, K.N., D.G. Blount, and E.M. Riley, *IL-10: the master regulator of immunity to infection*. *J Immunol*, 2008. **180**(9): p. 5771-7.

126. Berg, D.J., et al., *Interleukin-10 is a central regulator of the response to LPS in murine models of endotoxic shock and the Shwartzman reaction but not endotoxin tolerance*. J Clin Invest, 1995. **96**(5): p. 2339-47.
127. Latifi, S.Q., M.A. O'Riordan, and A.D. Levine, *Interleukin-10 controls the onset of irreversible septic shock*. Infect Immun, 2002. **70**(8): p. 4441-6.
128. Lokken, K.L., et al., *Malaria parasite infection compromises control of concurrent systemic non-typhoidal Salmonella infection via IL-10-mediated alteration of myeloid cell function*. PLoS Pathog, 2014. **10**(5): p. e1004049.
129. Sultzer, B.M., *Genetic control of leucocyte responses to endotoxin*. Nature, 1968. **219**(5160): p. 1253-4.
130. Qureshi, S.T., et al., *A high-resolution map in the chromosomal region surrounding the Lps locus*. Genomics, 1996. **31**(3): p. 283-94.
131. Qureshi, S.T., P. Gros, and D. Malo, *The Lps locus: genetic regulation of host responses to bacterial lipopolysaccharide*. Inflamm Res, 1999. **48**(12): p. 613-20.
132. Poltorak, A., et al., *Defective LPS signaling in C3H/HeJ and C57BL/10ScCr mice: mutations in Tlr4 gene*. Science, 1998. **282**(5396): p. 2085-8.
133. Hoshino, K., et al., *Cutting edge: Toll-like receptor 4 (TLR4)-deficient mice are hyporesponsive to lipopolysaccharide: evidence for TLR4 as the Lps gene product*. J Immunol, 1999. **162**(7): p. 3749-52.
134. Agnese, D.M., et al., *Human toll-like receptor 4 mutations but not CD14 polymorphisms are associated with an increased risk of gram-negative infections*. J Infect Dis, 2002. **186**(10): p. 1522-5.
135. Lorenz, E., et al., *Relevance of mutations in the TLR4 receptor in patients with gram-negative septic shock*. Arch Intern Med, 2002. **162**(9): p. 1028-32.
136. Ciacci-Woolwine, F., et al., *Salmonella flagellin induces tumor necrosis factor alpha in a human promonocytic cell line*. Infect Immun, 1998. **66**(3): p. 1127-34.
137. Wyant, T.L., M.K. Tanner, and M.B. Sztein, *Salmonella typhi flagella are potent inducers of proinflammatory cytokine secretion by human monocytes*. Infect Immun, 1999. **67**(7): p. 3619-24.
138. Wyant, T.L., M.K. Tanner, and M.B. Sztein, *Potent immunoregulatory effects of Salmonella typhi flagella on antigenic stimulation of human peripheral blood mononuclear cells*. Infect Immun, 1999. **67**(3): p. 1338-46.
139. Hayashi, F., et al., *The innate immune response to bacterial flagellin is mediated by Toll-like receptor 5*. Nature, 2001. **410**(6832): p. 1099-103.
140. Uematsu, S., et al., *Detection of pathogenic intestinal bacteria by Toll-like receptor 5 on intestinal CD11c+ lamina propria cells*. Nat Immunol, 2006. **7**(8): p. 868-74.
141. Hormaeche, C.E., K.A. Harrington, and H.S. Joysey, *Natural resistance to salmonellae in mice: control by genes within the major histocompatibility complex*. J Infect Dis, 1985. **152**(5): p. 1050-6.
142. Sinha, K., et al., *Salmonella typhimurium aroA, htrA, and aroD htrA mutants cause progressive infections in athymic (nu/nu) BALB/c mice*. Infect Immun, 1997. **65**(4): p. 1566-9.
143. Hess, J., et al., *Salmonella typhimurium aroA- infection in gene-targeted immunodeficient mice: major role of CD4+ TCR-alpha beta cells and IFN-gamma in bacterial clearance independent of intracellular location*. J Immunol, 1996. **156**(9): p. 3321-6.
144. Lee, S.J., S. Dunmire, and S.J. McSorley, *MHC class-I-restricted CD8 T cells play a protective role during primary Salmonella infection*. Immunol Lett, 2012. **148**(2): p. 138-43.
145. Mastroeni, P., et al., *Igh-6(-/-) (B-cell-deficient) mice fail to mount solid acquired resistance to oral challenge with virulent Salmonella enterica serovar typhimurium and show impaired Th1 T-cell responses to Salmonella antigens*. Infect Immun, 2000. **68**(1): p. 46-53.

146. Nemeth, E., et al., *Hepcidin regulates cellular iron efflux by binding to ferroportin and inducing its internalization*. *Science*, 2004. **306**(5704): p. 2090-3.
147. Ganz, T. and E. Nemeth, *Iron homeostasis in host defence and inflammation*. *Nat Rev Immunol*, 2015. **15**(8): p. 500-10.
148. Kautz, L., et al., *Identification of erythroferrone as an erythroid regulator of iron metabolism*. *Nat Genet*, 2014. **46**(7): p. 678-84.
149. Delaby, C., et al., *Presence of the iron exporter ferroportin at the plasma membrane of macrophages is enhanced by iron loading and down-regulated by hepcidin*. *Blood*, 2005. **106**(12): p. 3979-84.
150. Delaby, C., et al., *Sequential regulation of ferroportin expression after erythrophagocytosis in murine macrophages: early mRNA induction by haem, followed by iron-dependent protein expression*. *Biochem J*, 2008. **411**(1): p. 123-31.
151. Cartwright, G.E. and G.R. Lee, *The anaemia of chronic disorders*. *Br J Haematol*, 1971. **21**(2): p. 147-52.
152. Cartwright, G.E., et al., *The Anemia of Infection. I. Hypoferremia, Hypercupremia, and Alterations in Porphyrin Metabolism in Patients*. *J Clin Invest*, 1946. **25**(1): p. 65-80.
153. Freireich, E.J., et al., *Radioactive iron metabolism and erythrocyte survival studies of the mechanism of the anemia associated with rheumatoid arthritis*. *J Clin Invest*, 1957. **36**(7): p. 1043-58.
154. Libregts, S.F., et al., *Chronic IFN-gamma production in mice induces anemia by reducing erythrocyte life span and inhibiting erythropoiesis through an IRF-1/PU.1 axis*. *Blood*, 2011. **118**(9): p. 2578-88.
155. Cartwright, G.E., *The anemia of chronic disorders*. *Semin Hematol*, 1966. **3**(4): p. 351-75.
156. Roy, M.F., et al., *Pyruvate kinase deficiency confers susceptibility to Salmonella typhimurium infection in mice*. *J Exp Med*, 2007. **204**(12): p. 2949-61.
157. Sawatzki, G., F.A. Hoffmann, and B. Kubanek, *Acute iron overload in mice: pathogenesis of Salmonella typhimurium infection*. *Infect Immun*, 1983. **39**(2): p. 659-65.
158. Ampel, N.M., et al., *Resistance to infection in murine beta-thalassemia*. *Infect Immun*, 1989. **57**(4): p. 1011-7.
159. Puschmann, M. and A.M. Ganzoni, *Increased resistance of iron-deficient mice to salmonella infection*. *Infect Immun*, 1977. **17**(3): p. 663-4.
160. Min-Oo, G., et al., *Phenotypic expression of pyruvate kinase deficiency and protection against malaria in a mouse model*. *Genes Immun*, 2004. **5**(3): p. 168-75.
161. Kortman, G.A., et al., *Iron availability increases the pathogenic potential of Salmonella typhimurium and other enteric pathogens at the intestinal epithelial interface*. *PLoS One*, 2012. **7**(1): p. e29968.
162. Leong, J. and J. Neilands, *Mechanisms of siderophore iron transport in enteric bacteria*. *Journal of bacteriology*, 1976. **126**(2): p. 823-830.
163. Goetz, D.H., et al., *The neutrophil lipocalin NGAL is a bacteriostatic agent that interferes with siderophore-mediated iron acquisition*. *Mol Cell*, 2002. **10**(5): p. 1033-43.
164. Kingsley, R., et al., *Iron supplying systems of Salmonella in diagnostics, epidemiology and infection*. *FEMS Immunol Med Microbiol*, 1995. **11**(4): p. 257-64.
165. Nagy, T.A., S.M. Moreland, and C.S. Detweiler, *Salmonella acquires ferrous iron from haemophagocytic macrophages*. *Mol Microbiol*, 2014. **93**(6): p. 1314-26.
166. Ferguson, A.D. and J. Deisenhofer, *Metal import through microbial membranes*. *Cell*, 2004. **116**(1): p. 15-24.
167. Kammler, M., C. Schon, and K. Hantke, *Characterization of the ferrous iron uptake system of Escherichia coli*. *J Bacteriol*, 1993. **175**(19): p. 6212-9.

168. Postle, K., *TonB system, in vivo assays and characterization*. Methods Enzymol, 2007. **422**: p. 245-69.
169. Vidal, S., et al., *The Ity/Lsh/Bcg locus: natural resistance to infection with intracellular parasites is abrogated by disruption of the Nramp1 gene*. J Exp Med, 1995. **182**(3): p. 655-66.
170. Qureshi, S.T., et al., *Endotoxin-tolerant mice have mutations in Toll-like receptor 4 (Tlr4)*. J Exp Med, 1999. **189**(4): p. 615-25.
171. Church, D.M., et al., *Lineage-specific biology revealed by a finished genome assembly of the mouse*. PLoS Biol, 2009. **7**(5): p. e1000112.
172. Edwards, P. and D. Bruner, *The occurrence and distribution of Salmonella types in the United States*. Journal of Infectious Diseases, 1943. **72**(1): p. 58-67.
173. Hormaeche, C.E., *Natural resistance to Salmonella typhimurium in different inbred mouse strains*. Immunology, 1979. **37**(2): p. 311-8.
174. Roy, M.F. and D. Malo, *Genetic regulation of host responses to Salmonella infection in mice*. Genes Immun, 2002. **3**(7): p. 381-93.
175. Mian, M.F., et al., *Humanized mice for Salmonella typhi infection: new tools for an old problem*. Virulence, 2011. **2**(3): p. 248-52.
176. Libby, S.J., et al., *Humanized nonobese diabetic-scid IL2rgammanull mice are susceptible to lethal Salmonella Typhi infection*. Proc Natl Acad Sci U S A, 2010. **107**(35): p. 15589-94.
177. Miller, C.P. and M. Bohnhoff, *Changes in the Mouse's Enteric Microflora Associated with Enhanced Susceptibility to Salmonella Infection Following Streptomycin Treatment*. J Infect Dis, 1963. **113**: p. 59-66.
178. Que, J.U. and D.J. Hentges, *Effect of streptomycin administration on colonization resistance to Salmonella typhimurium in mice*. Infect Immun, 1985. **48**(1): p. 169-74.
179. Barthel, M., et al., *Pretreatment of mice with streptomycin provides a Salmonella enterica serovar Typhimurium colitis model that allows analysis of both pathogen and host*. Infect Immun, 2003. **71**(5): p. 2839-58.
180. Carpenter, H.A. and N.J. Talley, *The importance of clinicopathological correlation in the diagnosis of inflammatory conditions of the colon: histological patterns with clinical implications*. Am J Gastroenterol, 2000. **95**(4): p. 878-96.
181. Richer, E., et al., *Impact of Usp18 and IFN signaling in Salmonella-induced typhlitis*. Genes Immun, 2011. **12**(7): p. 531-43.
182. Coombes, B.K., et al., *Analysis of the contribution of Salmonella pathogenicity islands 1 and 2 to enteric disease progression using a novel bovine ileal loop model and a murine model of infectious enterocolitis*. Infect Immun, 2005. **73**(11): p. 7161-9.
183. Vijay-Kumar, M., et al., *Toll-like receptor 5-deficient mice have dysregulated intestinal gene expression and nonspecific resistance to Salmonella-induced typhoid-like disease*. Infect Immun, 2008. **76**(3): p. 1276-81.
184. Hapfelmeier, S., et al., *The Salmonella pathogenicity island (SPI)-2 and SPI-1 type III secretion systems allow Salmonella serovar typhimurium to trigger colitis via MyD88-dependent and MyD88-independent mechanisms*. J Immunol, 2005. **174**(3): p. 1675-85.
185. Sukupolvi, S., et al., *Development of a murine model of chronic Salmonella infection*. Infect Immun, 1997. **65**(2): p. 838-42.
186. Gonzalez-Escobedo, G. and J.S. Gunn, *Gallbladder epithelium as a niche for chronic Salmonella carriage*. Infect Immun, 2013. **81**(8): p. 2920-30.
187. Caron, J., et al., *Influence of Slc11a1 on the outcome of Salmonella enterica serovar Enteritidis infection in mice is associated with Th polarization*. Infect Immun, 2006. **74**(5): p. 2787-802.
188. International Mouse Knockout, C., et al., *A mouse for all reasons*. Cell, 2007. **128**(1): p. 9-13.

189. Collins, F.S., et al., *A new partner for the international knockout mouse consortium*. Cell, 2007. **129**(2): p. 235.
190. Ringwald, M., et al., *The IKMC web portal: a central point of entry to data and resources from the International Knockout Mouse Consortium*. Nucleic Acids Res, 2011. **39**(Database issue): p. D849-55.
191. Blake, J.A., et al., *The Mouse Genome Database: integration of and access to knowledge about the laboratory mouse*. Nucleic Acids Res, 2014. **42**(Database issue): p. D810-7.
192. Eppig, J.T., et al., *The Mouse Genome Database (MGD): facilitating mouse as a model for human biology and disease*. Nucleic Acids Res, 2015. **43**(Database issue): p. D726-36.
193. Smith, C.M., et al., *The mouse Gene Expression Database (GXD): 2014 update*. Nucleic Acids Res, 2014. **42**(Database issue): p. D818-24.
194. Mackay, T.F., E.A. Stone, and J.F. Ayroles, *The genetics of quantitative traits: challenges and prospects*. Nat Rev Genet, 2009. **10**(8): p. 565-77.
195. Roy, M.F., et al., *Complexity in the host response to Salmonella Typhimurium infection in AcB and BcA recombinant congenic strains*. Genes Immun, 2006. **7**(8): p. 655-66.
196. Beatty, S.C., et al., *Survival analysis and microarray profiling identify Cd40 as a candidate for the Salmonella susceptibility locus, Ity5*. Genes Immun, 2015.
197. Collaborative Cross, C., *The genome architecture of the Collaborative Cross mouse genetic reference population*. Genetics, 2012. **190**(2): p. 389-401.
198. Aylor, D.L., et al., *Genetic analysis of complex traits in the emerging Collaborative Cross*. Genome Res, 2011. **21**(8): p. 1213-22.
199. Rasmussen, A.L., et al., *Host genetic diversity enables Ebola hemorrhagic fever pathogenesis and resistance*. Science, 2014. **346**(6212): p. 987-91.
200. Vered, K., et al., *Susceptibility to Klebsiella pneumoniae infection in collaborative cross mice is a complex trait controlled by at least three loci acting at different time points*. BMC Genomics, 2014. **15**: p. 865.
201. Durrant, C., et al., *Collaborative Cross mice and their power to map host susceptibility to Aspergillus fumigatus infection*. Genome Res, 2011. **21**(8): p. 1239-48.
202. Ferris, M.T., et al., *Modeling host genetic regulation of influenza pathogenesis in the collaborative cross*. PLoS Pathog, 2013. **9**(2): p. e1003196.
203. Muller, H.J., *Artificial Transmutation of the Gene*. Science, 1927. **66**(1699): p. 84-7.
204. Ehling, U.H. and A. Neuhauser, *Procarbazine-induced specific-locus mutations in male mice*. Mutat Res, 1979. **59**(2): p. 245-56.
205. Russell, W.L., et al., *Specific-locus test shows ethylnitrosourea to be the most potent mutagen in the mouse*. Proc Natl Acad Sci U S A, 1979. **76**(11): p. 5818-9.
206. Noveroske, J.K., J.S. Weber, and M.J. Justice, *The mutagenic action of N-ethyl-N-nitrosourea in the mouse*. Mamm Genome, 2000. **11**(7): p. 478-83.
207. Nguyen, N., et al., *Random mutagenesis of the mouse genome: a strategy for discovering gene function and the molecular basis of disease*. Am J Physiol Gastrointest Liver Physiol, 2011. **300**(1): p. G1-11.
208. Barbaric, I., et al., *Spectrum of ENU-induced mutations in phenotype-driven and gene-driven screens in the mouse*. Environ Mol Mutagen, 2007. **48**(2): p. 124-42.
209. Hitotsumachi, S., D.A. Carpenter, and W.L. Russell, *Dose-repetition increases the mutagenic effectiveness of N-ethyl-N-nitrosourea in mouse spermatogonia*. Proc Natl Acad Sci U S A, 1985. **82**(19): p. 6619-21.
210. Kile, B.T. and D.J. Hilton, *The art and design of genetic screens: mouse*. Nat Rev Genet, 2005. **6**(7): p. 557-67.

211. Gondo, Y., *Trends in large-scale mouse mutagenesis: from genetics to functional genomics*. Nat Rev Genet, 2008. **9**(10): p. 803-10.
212. Hoebe, K., et al., *CD36 is a sensor of diacylglycerides*. Nature, 2005. **433**(7025): p. 523-7.
213. Xiao, N., et al., *The Tpl2 mutation Sluggish impairs type I IFN production and increases susceptibility to group B streptococcal disease*. J Immunol, 2009. **183**(12): p. 7975-83.
214. Sauer, J.D., et al., *The N-ethyl-N-nitrosourea-induced Goldenticket mouse mutant reveals an essential function of Sting in the in vivo interferon response to Listeria monocytogenes and cyclic dinucleotides*. Infect Immun, 2011. **79**(2): p. 688-94.
215. Rutschmann, S., et al., *PanR1, a dominant negative missense allele of the gene encoding TNF-alpha (Tnf), does not impair lymphoid development*. J Immunol, 2006. **176**(12): p. 7525-32.
216. Berger, M., et al., *An Sfn2 mutation causes lymphoid and myeloid immunodeficiency due to loss of immune cell quiescence*. Nat Immunol, 2010. **11**(4): p. 335-43.
217. Ordonez-Rueda, D., et al., *A hypomorphic mutation in the Gfi1 transcriptional repressor results in a novel form of neutropenia*. Eur J Immunol, 2012. **42**(9): p. 2395-408.
218. Justice, M.J., et al., *Mouse ENU mutagenesis*. Hum Mol Genet, 1999. **8**(10): p. 1955-63.
219. Arnold, C.N., et al., *ENU-induced phenovariance in mice: inferences from 587 mutations*. BMC Res Notes, 2012. **5**: p. 577.
220. Bull, K.R., et al., *Unlocking the bottleneck in forward genetics using whole-genome sequencing and identity by descent to isolate causative mutations*. PLoS Genet, 2013. **9**(1): p. e1003219.
221. Richer, E., et al., *Chemical mutagenesis: a new strategy against the global threat of infectious diseases*. Mamm Genome, 2008. **19**(5): p. 309-17.
222. Richer, E., et al., *N-ethyl-N-nitrosourea-induced mutation in ubiquitin-specific peptidase 18 causes hyperactivation of IFN-alpha signaling and suppresses STAT4-induced IFN-gamma production, resulting in increased susceptibility to Salmonella typhimurium*. J Immunol, 2010. **185**(6): p. 3593-601.
223. World Health Organization., *World health statistics 2015*. 2015, Geneva: World Health Organization. 161 p.
224. International HapMap, C., *The International HapMap Project*. Nature, 2003. **426**(6968): p. 789-96.
225. Raney, B.J., et al., *ENCODE whole-genome data in the UCSC genome browser (2011 update)*. Nucleic Acids Res, 2011. **39**(Database issue): p. D871-5.
226. Harrow, J., et al., *GENCODE: the reference human genome annotation for The ENCODE Project*. Genome Res, 2012. **22**(9): p. 1760-74.
227. Caignard, G., et al., *Mouse ENU Mutagenesis to Understand Immunity to Infection: Methods, Selected Examples, and Perspectives*. Genes (Basel), 2014. **5**(4): p. 887-925.
228. Yuki, K.E., et al., *Suppression of hepcidin expression and iron overload mediate Salmonella susceptibility in ankyrin 1 ENU-induced mutant*. PLoS One, 2013. **8**(2): p. e55331.
229. Torre, S., et al., *Susceptibility to lethal cerebral malaria is regulated by epistatic interaction between chromosome 4 (Berr6) and chromosome 1 (Berr7) loci in mice*. Genes Immun, 2013. **14**(4): p. 249-57.
230. Eva, M.M., et al., *Altered IFN-gamma-mediated immunity and transcriptional expression patterns in N-Ethyl-N-nitrosourea-induced STAT4 mutants confer susceptibility to acute typhoid-like disease*. J Immunol, 2014. **192**(1): p. 259-70.
231. Li, H. and R. Durbin, *Fast and accurate short read alignment with Burrows-Wheeler transform*. Bioinformatics, 2009. **25**(14): p. 1754-60.
232. McKenna, A., et al., *The Genome Analysis Toolkit: a MapReduce framework for analyzing next-generation DNA sequencing data*. Genome Res, 2010. **20**(9): p. 1297-303.

233. DePristo, M.A., et al., *A framework for variation discovery and genotyping using next-generation DNA sequencing data*. Nat Genet, 2011. **43**(5): p. 491-8.
234. Li, H., et al., *The Sequence Alignment/Map format and SAMtools*. Bioinformatics, 2009. **25**(16): p. 2078-9.
235. Kaplan, M.H., *STAT4: a critical regulator of inflammation in vivo*. Immunol Res, 2005. **31**(3): p. 231-42.
236. Andrews, T.D., et al., *Massively parallel sequencing of the mouse exome to accurately identify rare, induced mutations: an immediate source for thousands of new mouse models*. Open Biol, 2012. **2**(5): p. 120061.
237. Sakamoto, Y., et al., *Crystal structure of the catalytic fragment of human brain 2',3'-cyclic-nucleotide 3'-phosphodiesterase*. J Mol Biol, 2005. **346**(3): p. 789-800.
238. Jackson, E.K., et al., *Role of 2',3'-cyclic nucleotide 3'-phosphodiesterase in the renal 2',3'-cAMP-adenosine pathway*. Am J Physiol Renal Physiol, 2014. **307**(1): p. F14-24.
239. Wilson, S.J., et al., *Inhibition of HIV-1 particle assembly by 2',3'-cyclic-nucleotide 3'-phosphodiesterase*. Cell Host Microbe, 2012. **12**(4): p. 585-97.
240. Dauphinee, S.M., et al., *Contribution of increased ISG15, ISGylation and deregulated type I IFN signaling in Usp18 mutant mice during the course of bacterial infections*. Genes Immun, 2014. **15**(5): p. 282-92.
241. Chen, L., S. Li, and I. McGilvray, *The ISG15/USP18 ubiquitin-like pathway (ISGylation system) in hepatitis C virus infection and resistance to interferon therapy*. Int J Biochem Cell Biol, 2011. **43**(10): p. 1427-31.
242. Ketscher, L., et al., *Selective inactivation of USP18 isopeptidase activity in vivo enhances ISG15 conjugation and viral resistance*. Proc Natl Acad Sci U S A, 2015. **112**(5): p. 1577-82.
243. Ritchie, K.J., et al., *Role of ISG15 protease UBP43 (USP18) in innate immunity to viral infection*. Nat Med, 2004. **10**(12): p. 1374-8.
244. Goldmann, T., et al., *USP18 lack in microglia causes destructive interferonopathy of the mouse brain*. EMBO J, 2015. **34**(12): p. 1612-29.
245. Rank, G., et al., *Novel roles for erythroid Ankyrin-1 revealed through an ENU-induced null mouse mutant*. Blood, 2009. **113**(14): p. 3352-62.
246. Greth, A., et al., *A novel ENU-mutation in ankyrin-1 disrupts malaria parasite maturation in red blood cells of mice*. PLoS One, 2012. **7**(6): p. e38999.
247. Shear, H.L., et al., *Resistance to malaria in ankyrin and spectrin deficient mice*. Br J Haematol, 1991. **78**(4): p. 555-60.
248. Sabri, A., et al., *Association study of genes controlling IL-12-dependent IFN-gamma immunity: STAT4 alleles increase risk of pulmonary tuberculosis in Morocco*. J Infect Dis, 2014. **210**(4): p. 611-8.
249. Ma, H., et al., *2',3'-cyclic nucleotide 3'-phosphodiesterases inhibit hepatitis B virus replication*. PLoS One, 2013. **8**(11): p. e80769.
250. Gilchrist, J.J., et al., *Genetic variants associated with non-typhoidal *Salmonella* bacteraemia in African children*. The Lancet. **385**: p. S13.
251. Bongfen, S.E., et al., *An N-ethyl-N-nitrosourea (ENU)-induced dominant negative mutation in the JAK3 kinase protects against cerebral malaria*. PLoS One, 2012. **7**(2): p. e31012.
252. Kennedy, J.M., et al., *CCDC88B is a novel regulator of maturation and effector functions of T cells during pathological inflammation*. J Exp Med, 2014. **211**(13): p. 2519-35.
253. Torre, S., et al., *THEMIS is required for pathogenesis of cerebral malaria and protection against pulmonary tuberculosis*. Infect Immun, 2015. **83**(2): p. 759-68.
254. Caignard, G., et al., *Genome-wide mouse mutagenesis reveals CD45-mediated T cell function as critical in protective immunity to HSV-1*. PLoS Pathog, 2013. **9**(9): p. e1003637.

255. Moresco, E.M. and B. Beutler, *Resisting viral infection: the gene by gene approach*. *Curr Opin Virol*, 2011. **1**(6): p. 513-8.
256. Lafferty, E.I., et al., *An ENU-induced splicing mutation reveals a role for Unc93b1 in early immune cell activation following influenza A H1N1 infection*. *Genes Immun*, 2014. **15**(5): p. 320-32.
257. Tabeta, K., et al., *The Unc93b1 mutation 3d disrupts exogenous antigen presentation and signaling via Toll-like receptors 3, 7 and 9*. *Nat Immunol*, 2006. **7**(2): p. 156-64.
258. Croker, B.A., et al., *Inflammation and autoimmunity caused by a SHP1 mutation depend on IL-1, MyD88, and a microbial trigger*. *Proc Natl Acad Sci U S A*, 2008. **105**(39): p. 15028-33.
259. Tabeta, K., et al., *Toll-like receptors 9 and 3 as essential components of innate immune defense against mouse cytomegalovirus infection*. *Proc Natl Acad Sci U S A*, 2004. **101**(10): p. 3516-21.
260. Hoebe, K., et al., *Identification of Lps2 as a key transducer of MyD88-independent TIR signalling*. *Nature*, 2003. **424**(6950): p. 743-8.
261. Jaeger, B.N., et al., *Neutrophil depletion impairs natural killer cell maturation, function, and homeostasis*. *J Exp Med*, 2012. **209**(3): p. 565-80.
262. Barquero-Calvo, E., et al., *Neutrophils exert a suppressive effect on Th1 responses to intracellular pathogen *Brucella abortus**. *PLoS Pathog*, 2013. **9**(2): p. e1003167.
263. Mastroeni, P. and D. Maskell, *Salmonella infections : clinical, immunological, and molecular aspects*. *Advances in molecular and cellular microbiology*. 2006, Cambridge, UK ; New York: Cambridge University Press.
264. Casanova, J.L., et al., *Revisiting human primary immunodeficiencies*. *J Intern Med*, 2008. **264**(2): p. 115-27.
265. Gordon, M.A., *Salmonella infections in immunocompromised adults*. *J Infect*, 2008. **56**(6): p. 413-22.
266. Bustamante, J., et al., *From infectious diseases to primary immunodeficiencies*. *Immunol Allergy Clin North Am*, 2008. **28**(2): p. 235-58, vii.
267. Schaible, U.E. and S.H. Kaufmann, *Iron and microbial infection*. *Nat Rev Microbiol*, 2004. **2**(12): p. 946-53.
268. Vento, S., F. Cainelli, and F. Cesario, *Infections and thalassaemia*. *Lancet Infect Dis*, 2006. **6**(4): p. 226-33.
269. Vidal, S., P. Gros, and E. Skamene, *Natural resistance to infection with intracellular parasites: molecular genetics identifies Nramp1 as the Bcg/Ity/Lsh locus*. *J Leukoc Biol*, 1995. **58**(4): p. 382-90.
270. Rubtsov, A.M. and O.D. Lopina, *Ankyrins*. *FEBS Lett*, 2000. **482**(1-2): p. 1-5.
271. Perrotta, S., P.G. Gallagher, and N. Mohandas, *Hereditary spherocytosis*. *Lancet*, 2008. **372**(9647): p. 1411-26.
272. Birkenmeier, C.S., E.J. Gifford, and J.E. Barker, *Normoblastosis, a murine model for ankyrin-deficient hemolytic anemia, is caused by a hypomorphic mutation in the erythroid ankyrin gene Ank1*. *Hematol J*, 2003. **4**(6): p. 445-9.
273. Hughes, M.R., et al., *A novel ENU-generated truncation mutation lacking the spectrin-binding and C-terminal regulatory domains of Ank1 models severe hemolytic hereditary spherocytosis*. *Exp Hematol*, 2011. **39**(3): p. 305-320 e2.
274. Harris, B.S.W.-B.P.F.J., K.R.; Bronson, R.T.; Reinholdt, L.G.; Karst, S.Y.; Davisson-Fahey, M., *A new pale lethal mouse mutation (pale) has been identified on Chromosome 8*. MGI Direct Data Submission, 2009.
275. Gallagher, P.G., *Hematologically important mutations: ankyrin variants in hereditary spherocytosis*. *Blood Cells Mol Dis*, 2005. **35**(3): p. 345-7.
276. Eber, S.W., et al., *Ankyrin-1 mutations are a major cause of dominant and recessive hereditary spherocytosis*. *Nat Genet*, 1996. **13**(2): p. 214-8.

277. Delaunay, J., *Molecular basis of red cell membrane disorders*. Acta Haematol, 2002. **108**(4): p. 210-8.
278. Lesbordes-Brion, J.C., et al., *Targeted disruption of the hepcidin 1 gene results in severe hemochromatosis*. Blood, 2006. **108**(4): p. 1402-5.
279. Boyer, E., et al., *Acquisition of Mn(II) in addition to Fe(II) is required for full virulence of Salmonella enterica serovar Typhimurium*. Infect Immun, 2002. **70**(11): p. 6032-42.
280. Team, R.D.C. R: *A language and environment for statistical computing*. 2011; Available from: <http://www.R-project.org>.
281. Bennett, V. and J. Healy, *Organizing the fluid membrane bilayer: diseases linked to spectrin and ankyrin*. Trends Mol Med, 2008. **14**(1): p. 28-36.
282. Peters, L.L. and S.E. Lux, *Ankyrins: structure and function in normal cells and hereditary spherocytes*. Semin Hematol, 1993. **30**(2): p. 85-118.
283. Bennett, V., *Ankyrins. Adaptors between diverse plasma membrane proteins and the cytoplasm*. J Biol Chem, 1992. **267**(13): p. 8703-6.
284. Veuthey, T., M.C. D'Anna, and M.E. Roque, *Role of the kidney in iron homeostasis: renal expression of Prohepcidin, Ferroportin, and DMT1 in anemic mice*. Am J Physiol Renal Physiol, 2008. **295**(4): p. F1213-21.
285. Kulaksiz, H., et al., *The iron-regulatory peptide hormone hepcidin: expression and cellular localization in the mammalian kidney*. J Endocrinol, 2005. **184**(2): p. 361-70.
286. Smith, C.P. and F. Thevenod, *Iron transport and the kidney*. Biochim Biophys Acta, 2009. **1790**(7): p. 724-30.
287. Sanchez-Lopez, J.Y., et al., *Red cell membrane protein deficiencies in Mexican patients with hereditary spherocytosis*. Blood Cells Mol Dis, 2003. **31**(3): p. 357-9.
288. Boguslawska, D.M., et al., *Hereditary spherocytosis: identification of several HS families with ankyrin and band 3 deficiency in a population of southwestern Poland*. Ann Hematol, 2004. **83**(1): p. 28-33.
289. Gardenghi, S., R.W. Grady, and S. Rivella, *Anemia, ineffective erythropoiesis, and hepcidin: interacting factors in abnormal iron metabolism leading to iron overload in beta-thalassemia*. Hematol Oncol Clin North Am, 2010. **24**(6): p. 1089-107.
290. Jones, R.L., et al., *Effects of iron chelators and iron overload on Salmonella infection*. Nature, 1977. **267**(5606): p. 63-5.
291. Walker, E.M., Jr. and S.M. Walker, *Effects of iron overload on the immune system*. Ann Clin Lab Sci, 2000. **30**(4): p. 354-65.
292. Collins, H.L., S.H. Kaufmann, and U.E. Schaible, *Iron chelation via deferoxamine exacerbates experimental salmonellosis via inhibition of the nicotinamide adenine dinucleotide phosphate oxidase-dependent respiratory burst*. J Immunol, 2002. **168**(7): p. 3458-63.
293. Kovtunovych, G., et al., *Dysfunction of the heme recycling system in heme oxygenase 1-deficient mice: effects on macrophage viability and tissue iron distribution*. Blood, 2010. **116**(26): p. 6054-62.
294. Nix, R.N., et al., *Hemophagocytic macrophages harbor Salmonella enterica during persistent infection*. PLoS Pathog, 2007. **3**(12): p. e193.
295. Cunnington, A.J., et al., *Malaria impairs resistance to Salmonella through heme- and heme oxygenase-dependent dysfunctional granulocyte mobilization*. Nat Med, 2012. **18**(1): p. 120-7.
296. Wareing, M., et al., *In vivo characterization of renal iron transport in the anaesthetized rat*. J Physiol, 2000. **524 Pt 2**: p. 581-6.
297. Zhou, X.J., et al., *Association of renal injury with increased oxygen free radical activity and altered nitric oxide metabolism in chronic experimental hemosiderosis*. Lab Invest, 2000. **80**(12): p. 1905-14.

298. Hentze, M.W., et al., *Two to tango: regulation of Mammalian iron metabolism*. Cell, 2010. **142**(1): p. 24-38.
299. Ganz, T., *Hepcidin and iron regulation, 10 years later*. Blood, 2011. **117**(17): p. 4425-33.
300. Tanno, T., et al., *High levels of GDF15 in thalassemia suppress expression of the iron regulatory protein hepcidin*. Nat Med, 2007. **13**(9): p. 1096-101.
301. Tanno, T., P. Noel, and J.L. Miller, *Growth differentiation factor 15 in erythroid health and disease*. Curr Opin Hematol, 2010. **17**(3): p. 184-90.
302. Kattamis, A., et al., *The effects of erythropoetic activity and iron burden on hepcidin expression in patients with thalassemia major*. Haematologica, 2006. **91**(6): p. 809-12.
303. Bootcov, M.R., et al., *MIC-1, a novel macrophage inhibitory cytokine, is a divergent member of the TGF-beta superfamily*. Proc Natl Acad Sci U S A, 1997. **94**(21): p. 11514-9.
304. Lakhai, S., et al., *Regulation of growth differentiation factor 15 expression by intracellular iron*. Blood, 2009. **113**(7): p. 1555-63.
305. Nairz, M., et al., *Absence of functional Hfe protects mice from invasive Salmonella enterica serovar Typhimurium infection via induction of lipocalin-2*. Blood, 2009. **114**(17): p. 3642-51.
306. Ferguson, C.J., et al., *Cellular localization of divalent metal transporter DMT-1 in rat kidney*. Am J Physiol Renal Physiol, 2001. **280**(5): p. F803-14.
307. Gordeuk, V.R., et al., *Chuvash polycythemia VHLR200W mutation is associated with down-regulation of hepcidin expression*. Blood, 2011. **118**(19): p. 5278-82.
308. Viatte, L., et al., *Chronic hepcidin induction causes hyposideremia and alters the pattern of cellular iron accumulation in hemochromatotic mice*. Blood, 2006. **107**(7): p. 2952-8.
309. Gardenghi, S., et al., *Hepcidin as a therapeutic tool to limit iron overload and improve anemia in beta-thalassemic mice*. J Clin Invest, 2010. **120**(12): p. 4466-77.
310. Ramos, E., et al., *Minihepcidins prevent iron overload in a hepcidin-deficient mouse model of severe hemochromatosis*. Blood, 2012. **120**(18): p. 3829-36.
311. Sow, F.B., et al., *Expression and localization of hepcidin in macrophages: a role in host defense against tuberculosis*. J Leukoc Biol, 2007. **82**(4): p. 934-45.
312. Lux, S.E., K.M. John, and V. Bennett, *Analysis of cDNA for human erythrocyte ankyrin indicates a repeated structure with homology to tissue-differentiation and cell-cycle control proteins*. Nature, 1990. **344**(6261): p. 36-42.
313. Karaghiosoff, M., et al., *Central role for type I interferons and Tyk2 in lipopolysaccharide-induced endotoxin shock*. Nat Immunol, 2003. **4**(5): p. 471-7.
314. Chawla-Sarkar, M., et al., *Apoptosis and interferons: role of interferon-stimulated genes as mediators of apoptosis*. Apoptosis, 2003. **8**(3): p. 237-49.
315. Mendoza, J.A., et al., *Human papillomavirus type 5 E6 oncoprotein represses the transforming growth factor beta signaling pathway by binding to SMAD3*. J Virol, 2006. **80**(24): p. 12420-4.
316. Lambert, J.P., et al., *Proximity biotinylation and affinity purification are complementary approaches for the interactome mapping of chromatin-associated protein complexes*. J Proteomics, 2015. **118**: p. 81-94.
317. Huang da, W., B.T. Sherman, and R.A. Lempicki, *Systematic and integrative analysis of large gene lists using DAVID bioinformatics resources*. Nat Protoc, 2009. **4**(1): p. 44-57.
318. Huang da, W., B.T. Sherman, and R.A. Lempicki, *Bioinformatics enrichment tools: paths toward the comprehensive functional analysis of large gene lists*. Nucleic Acids Res, 2009. **37**(1): p. 1-13.
319. Doumas, S., A. Kolokotronis, and P. Stefanopoulos, *Anti-inflammatory and antimicrobial roles of secretory leukocyte protease inhibitor*. Infect Immun, 2005. **73**(3): p. 1271-4.
320. Davis, T.A., B. Loos, and A.M. Engelbrecht, *AHNAK: the giant jack of all trades*. Cell Signal, 2014. **26**(12): p. 2683-93.

321. De Rubeis, S., et al., *CYFIP1 coordinates mRNA translation and cytoskeleton remodeling to ensure proper dendritic spine formation*. *Neuron*, 2013. **79**(6): p. 1169-82.
322. Chen, Z., et al., *Structure and control of the actin regulatory WAVE complex*. *Nature*, 2010. **468**(7323): p. 533-8.
323. Gilli, F., et al., *Loss of braking signals during inflammation: a factor affecting the development and disease course of multiple sclerosis*. *Arch Neurol*, 2011. **68**(7): p. 879-88.
324. Hutchins, A.P., S. Poulain, and D. Miranda-Saavedra, *Genome-wide analysis of STAT3 binding in vivo predicts effectors of the anti-inflammatory response in macrophages*. *Blood*, 2012. **119**(13): p. e110-9.
325. Matza, D., et al., *A scaffold protein, AHNAK1, is required for calcium signaling during T cell activation*. *Immunity*, 2008. **28**(1): p. 64-74.
326. Merrifield, C.J., et al., *Endocytic vesicles move at the tips of actin tails in cultured mast cells*. *Nat Cell Biol*, 1999. **1**(1): p. 72-4.
327. Merrifield, C.J., et al., *Annexin 2 has an essential role in actin-based macropinocytic rocketing*. *Curr Biol*, 2001. **11**(14): p. 1136-41.
328. Zobiack, N., et al., *Cell-surface attachment of pedestal-forming enteropathogenic E. coli induces a clustering of raft components and a recruitment of annexin 2*. *J Cell Sci*, 2002. **115**(Pt 1): p. 91-8.
329. Skogberg, G., et al., *Characterization of human thymic exosomes*. *PLoS One*, 2013. **8**(7): p. e67554.
330. Moulding, D.A., et al., *Actin cytoskeletal defects in immunodeficiency*. *Immunol Rev*, 2013. **256**(1): p. 282-99.
331. Bifulco, M., et al., *2',3'-Cyclic nucleotide 3'-phosphodiesterase: a membrane-bound, microtubule-associated protein and membrane anchor for tubulin*. *Proc Natl Acad Sci U S A*, 2002. **99**(4): p. 1807-12.
332. Yang, L., et al., *Expression of 2',3'-cyclic nucleotide 3'-phosphodiesterase (CNPase) and its roles in activated microglia in vivo and in vitro*. *J Neuroinflammation*, 2014. **11**: p. 148.
333. Bianchi, I., et al., *The X chromosome and immune associated genes*. *J Autoimmun*, 2012. **38**(2-3): p. J187-92.
334. Libert, C., L. Dejager, and I. Pinheiro, *The X chromosome in immune functions: when a chromosome makes the difference*. *Nat Rev Immunol*, 2010. **10**(8): p. 594-604.
335. Choudhry, M.A., K.I. Bland, and I.H. Chaudry, *Gender and susceptibility to sepsis following trauma*. *Endocr Metab Immune Disord Drug Targets*, 2006. **6**(2): p. 127-35.
336. Butterworth, M., B. McClellan, and M. Allansmith, *Influence of sex in immunoglobulin levels*. *Nature*, 1967. **214**(5094): p. 1224-5.
337. Purtilo, D.T. and J.L. Sullivan, *Immunological bases for superior survival of females*. *Am J Dis Child*, 1979. **133**(12): p. 1251-3.
338. Kile, B.T., et al., *Functional genetic analysis of mouse chromosome 11*. *Nature*, 2003. **425**(6953): p. 81-6.
339. Wilson, L., et al., *Random mutagenesis of proximal mouse chromosome 5 uncovers predominantly embryonic lethal mutations*. *Genome Res*, 2005. **15**(8): p. 1095-105.
340. Kim, D.K., et al., *Inverse agonist of estrogen-related receptor gamma controls Salmonella typhimurium infection by modulating host iron homeostasis*. *Nat Med*, 2014. **20**(4): p. 419-24.
341. Kaye, D., F.A. Gill, and E.W. Hook, *Factors influencing host resistance to Salmonella infections: the effects of hemolysis and erythrophagocytosis*. *Am J Med Sci*, 1967. **254**(2): p. 205-15.
342. Cunnington, A.J., et al., *Prolonged neutrophil dysfunction after Plasmodium falciparum malaria is related to hemolysis and heme oxygenase-1 induction*. *J Immunol*, 2012. **189**(11): p. 5336-46.
343. Schorey, J.S., et al., *Exosomes and other extracellular vesicles in host-pathogen interactions*. *EMBO Rep*, 2015. **16**(1): p. 24-43.

344. van Niel, G., et al., *Exosomes: a common pathway for a specialized function*. J Biochem, 2006. **140**(1): p. 13-21.
345. Bhatnagar, S., et al., *Exosomes released from macrophages infected with intracellular pathogens stimulate a proinflammatory response in vitro and in vivo*. Blood, 2007. **110**(9): p. 3234-44.
346. Nagarajan, N.A., F. Gonzalez, and N. Shastri, *Nonclassical MHC class Ib-restricted cytotoxic T cells monitor antigen processing in the endoplasmic reticulum*. Nat Immunol, 2012. **13**(6): p. 579-86.
347. United Nations. Dept. of Economic and Social Affairs, P.D., *World Urbanization Prospects: The 2014 Revision, Highlights (ST/ESA/SER.A/352)*. 2014.
348. Neiderud, C.J., *How urbanization affects the epidemiology of emerging infectious diseases*. Infect Ecol Epidemiol, 2015. **5**: p. 27060.
349. Williams, K.E., et al., *Urine, peritoneal fluid and omental fat proteomes of reproductive age women: Endometriosis-related changes and associations with endocrine disrupting chemicals*. J Proteomics, 2015. **113**: p. 194-205.